An introduction to Radio-Loud AGN

Paola Grandi (INAF-OAS Bologna)

INAF
ISTITUTO NAZIONALE DI ASTROFISICA

Laboratorio alte energie
22-2-2021

High and very high energy observations

Spectrum of Electromagnetic Radiation			
Region	**Wavelength (Angstroms)**	**Wavelength (centimeters)**	**Frequency (Hz)**
Radio	$> 10^9$	> 10	$< 3 \times 10^9$
Microwave	$10^9 - 10^6$	$10 - 0.01$	$3 \times 10^9 - 3 \times 10^{12}$
Infrared	$10^6 - 7000$	$0.01 - 7 \times 10^{-5}$	$3 \times 10^{12} - 4.3 \times 10^{14}$
Visible	$7000 - 4000$	$7 \times 10^{-5} - 4 \times 10^{-5}$	$4.3 \times 10^{14} - 7.5 \times 10^{14}$
Ultraviolet	$4000 - 10$	$4 \times 10^{-5} - 10^{-7}$	$7.5 \times 10^{14} - 3 \times 10^{17}$
X-Rays	$10 - 0.1$	$10^{-7} - 10^{-9}$	$3 \times 10^{17} - 3 \times 10^{19}$
Gamma Rays	< 0.1	$< 10^{-9}$	$> 3 \times 10^{19}$

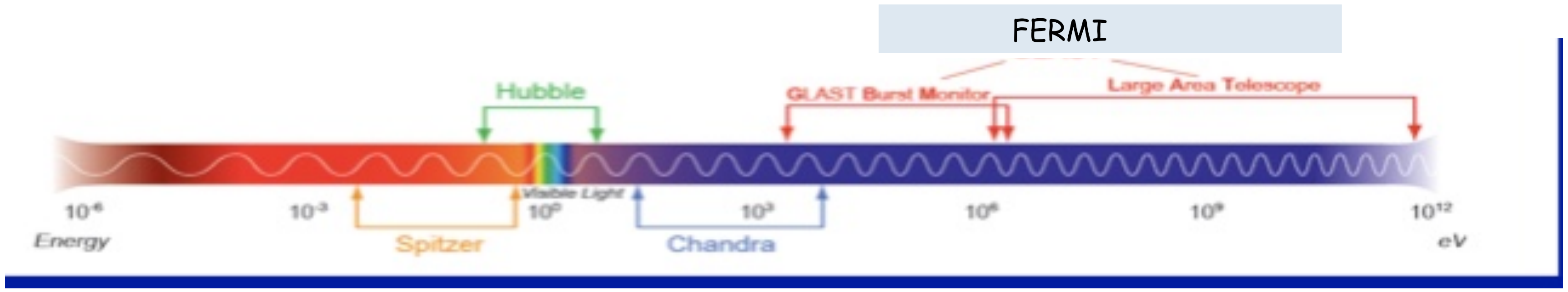

FERMI -LAT ~ 100 MeV - 2 TeV

Chandra ~0.5- 7 keV

Magic ~ 30 GeV- 100 TeV

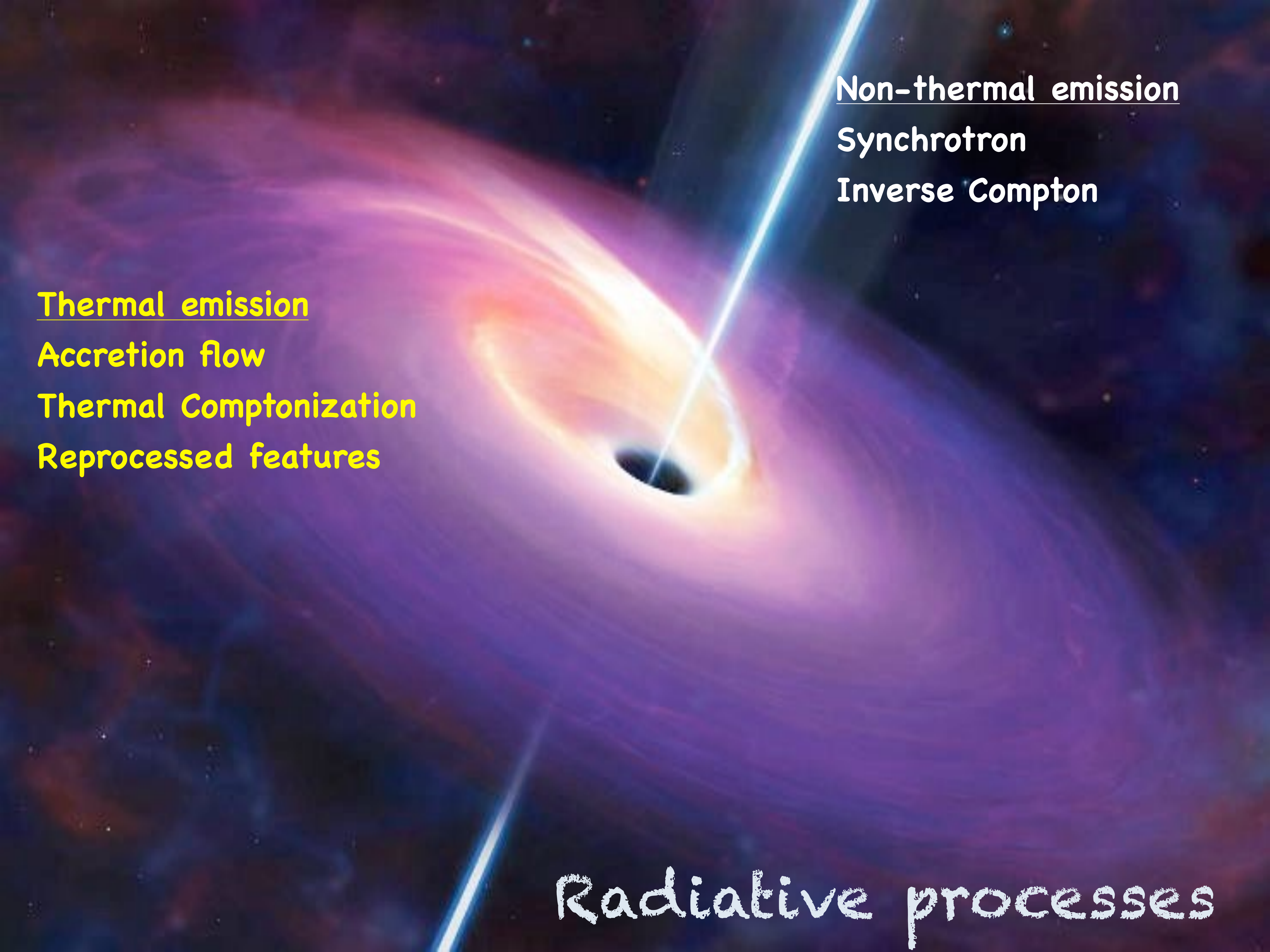

Non-thermal emission

Synchrotron

Inverse Compton

Thermal emission

Accretion flow

Thermal Comptonization

Reprocessed features

Radiative processes

Thermal: Particles have Maxwellian velocity distribution due to collisions

Non-Thermal: e.g. Synchrotron radiation with power-law energy distribution of particles $F(E) \propto E^{-\alpha}$

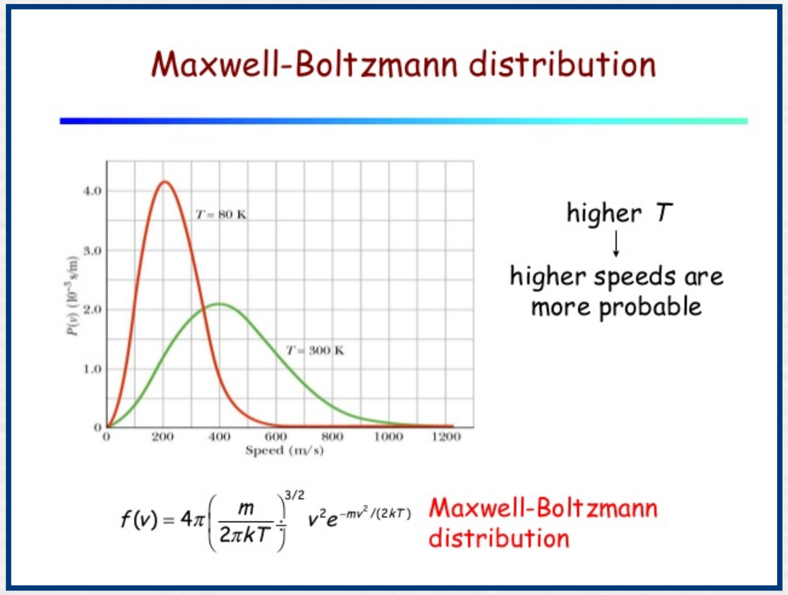

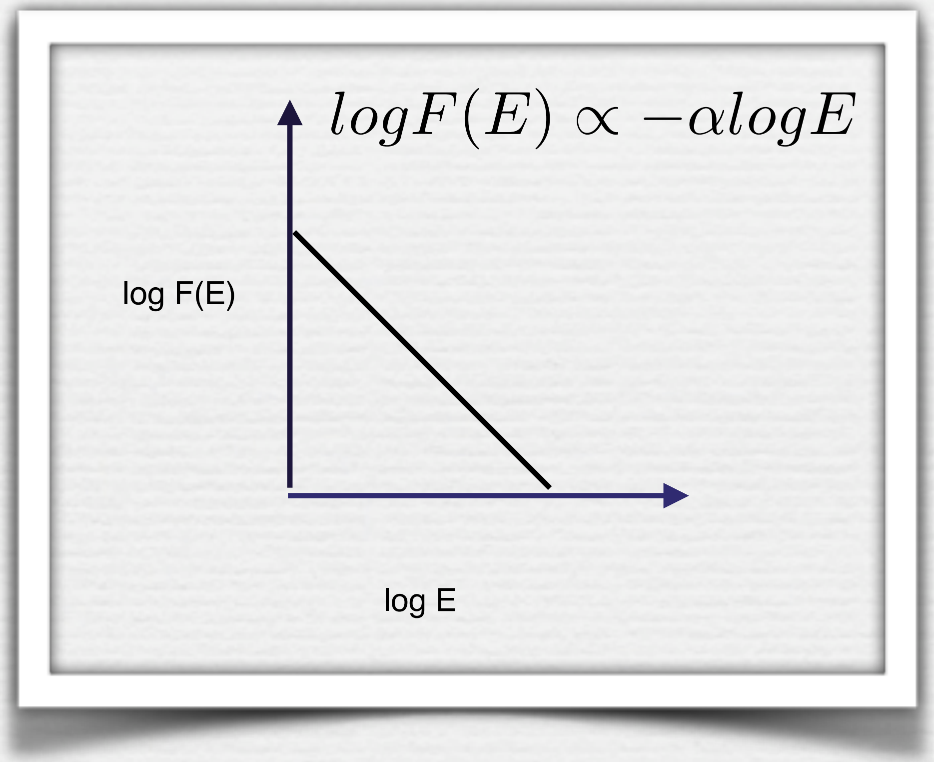

Thermal

Non-Thermal

Almost every galaxy hosts a black hole from millions to billions of solar masses

but...

1% active 99% silent

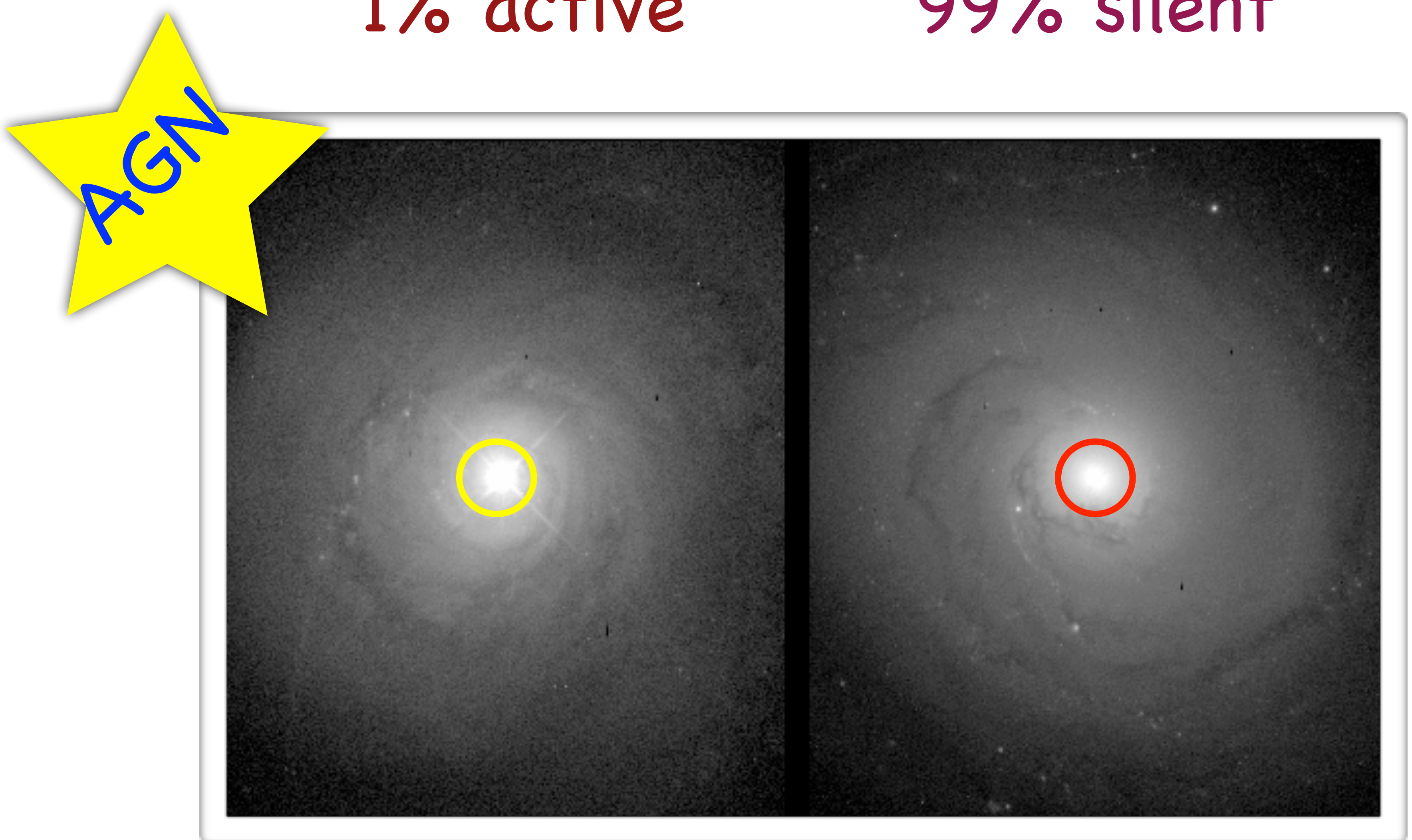

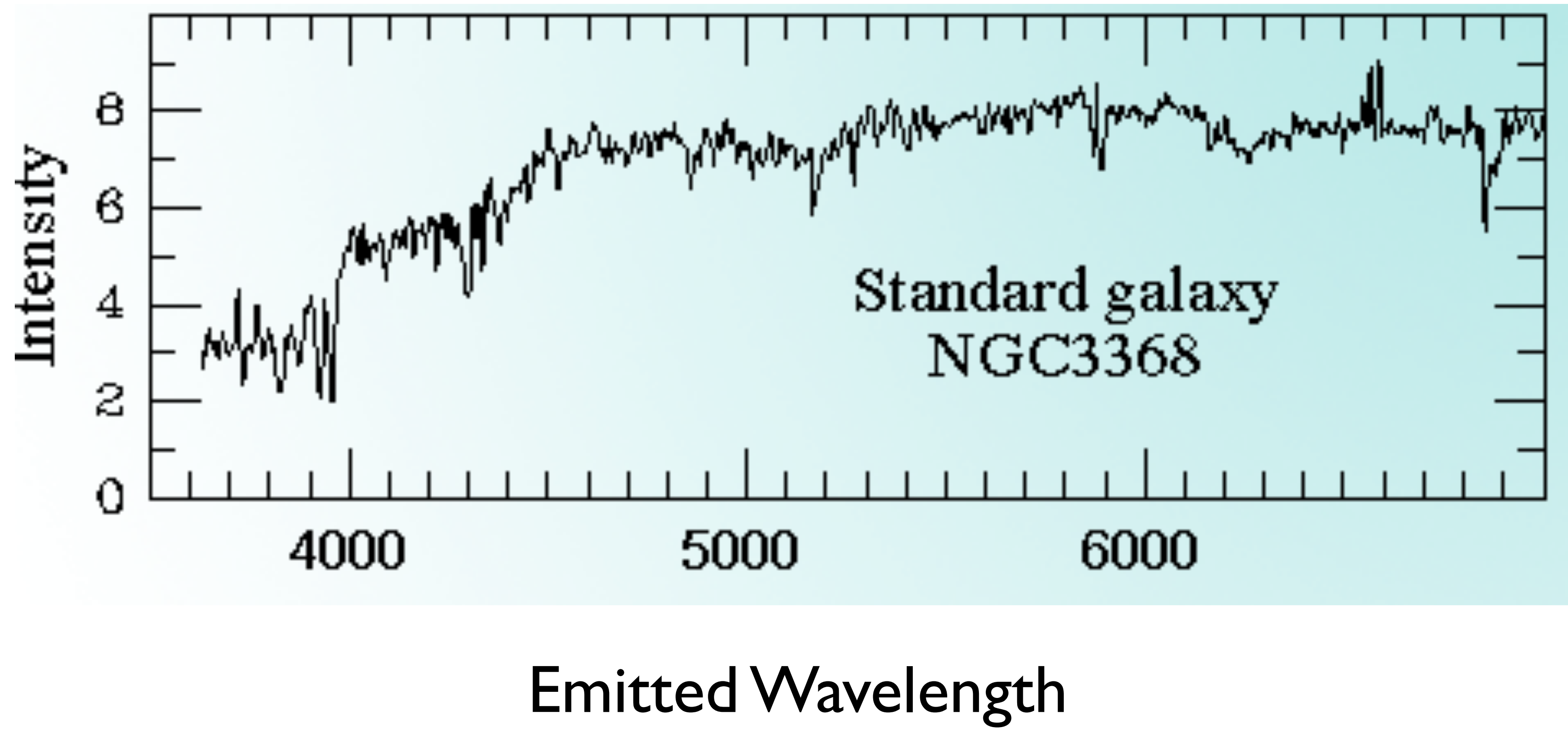

Intensity
0
2
4
6
8
4000
5000
6000
Standard galaxy
NGC3368
Emitted Wavelength

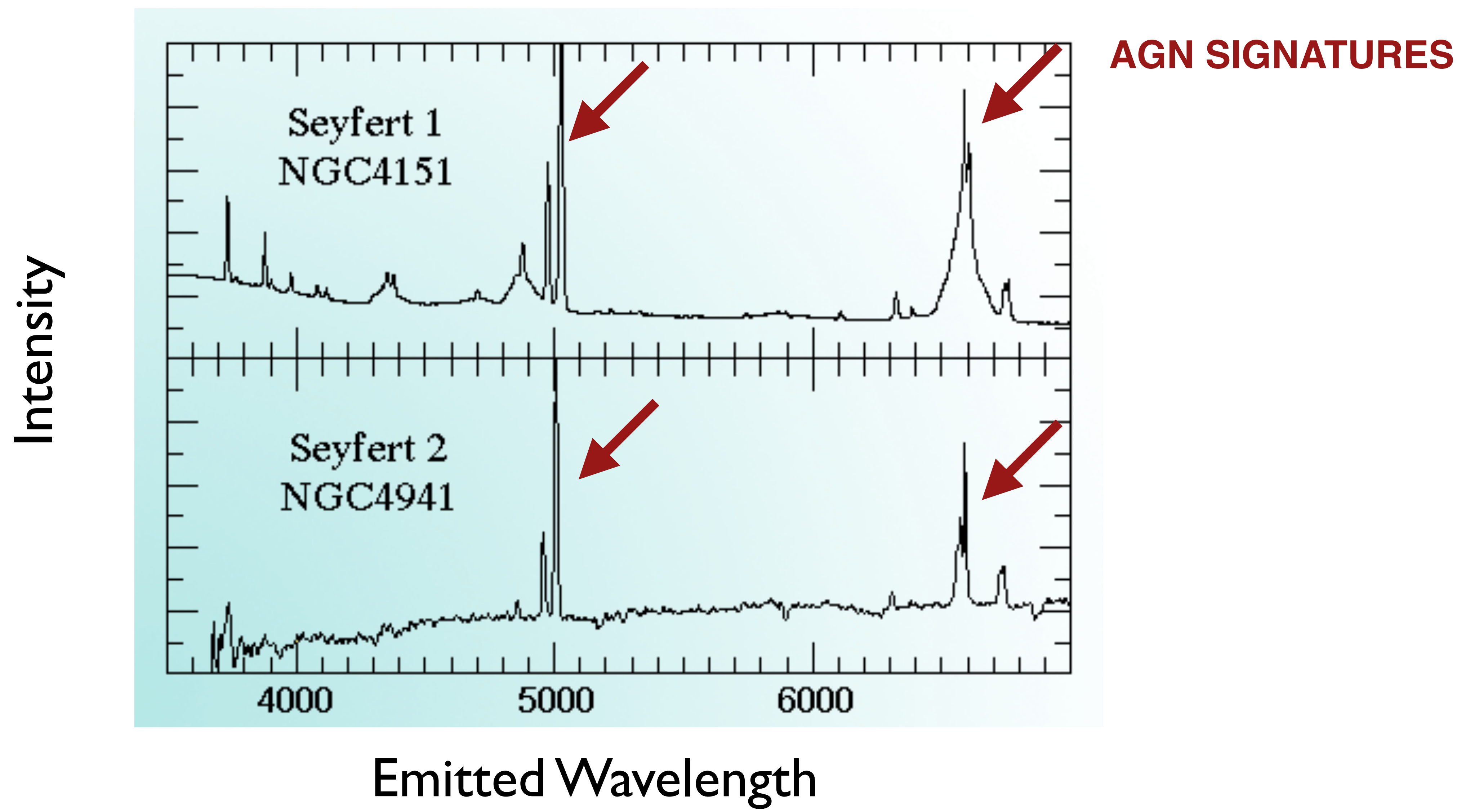

AGN SIGNATURES
Seyfert 1
NGC4151
Seyfert 2
NGC4941
Intensity
4000
5000
6000
Emitted Wavelength

AGN engine occupies a tiny region in the center of the galaxy

30 kpc

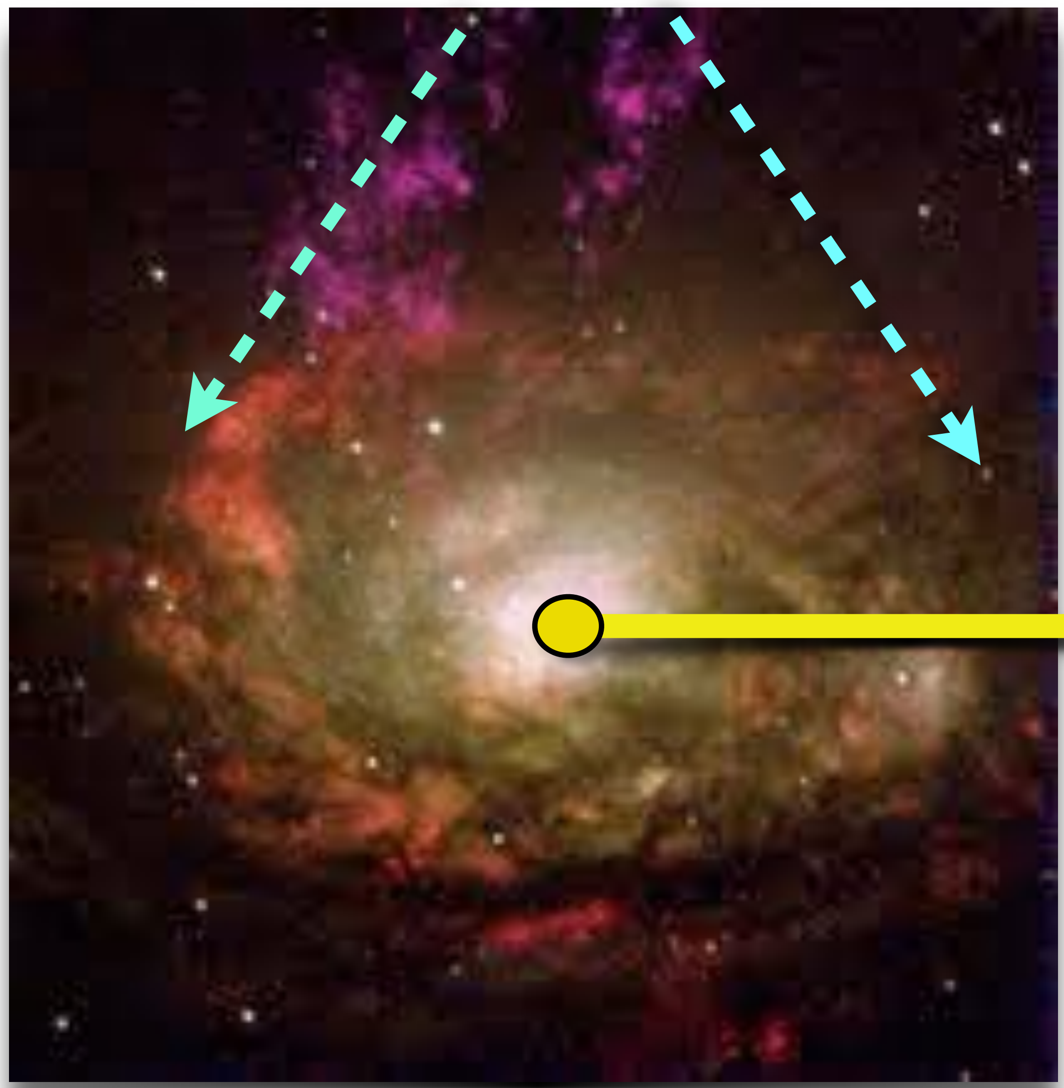

2-3 pc

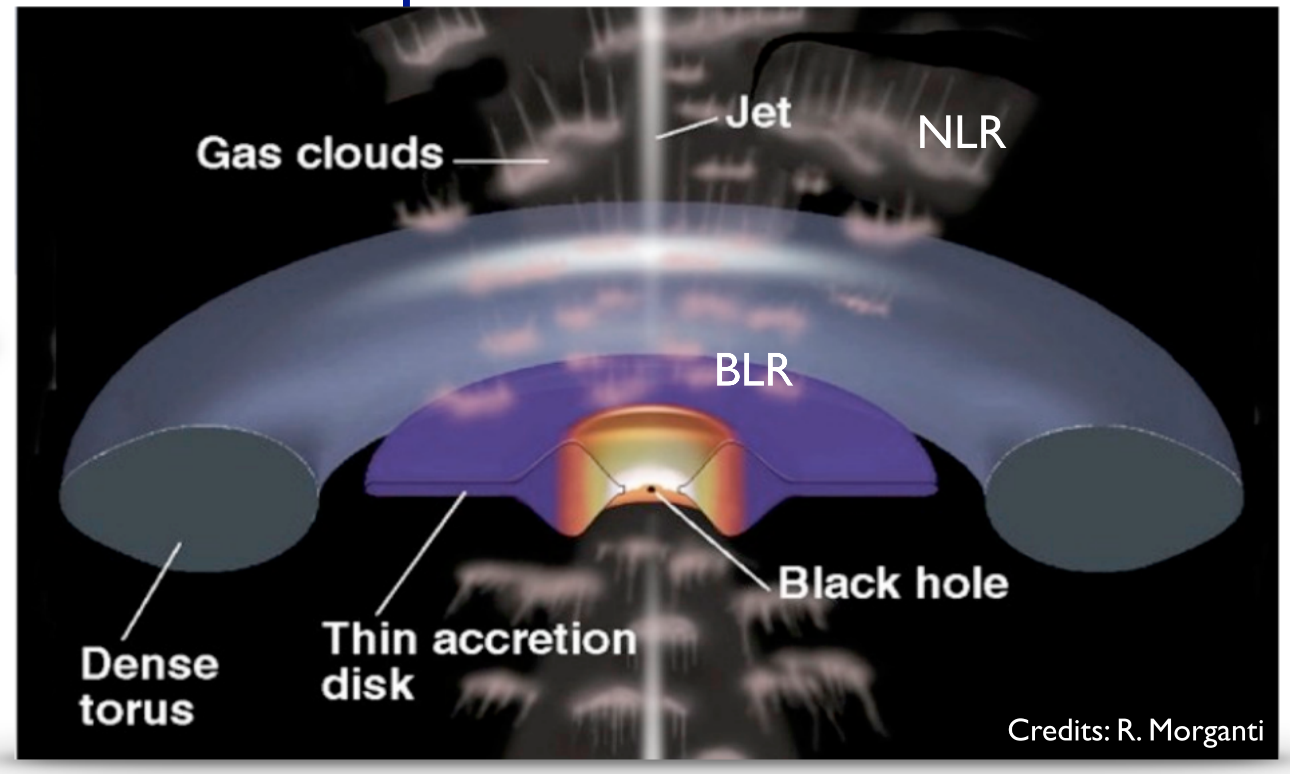

The extraordinary amount of energy is produced through accretion of gas close to a SMBH

About 10% of AGN are Radio-Loud, i.e. these systems can launch relativistic jets

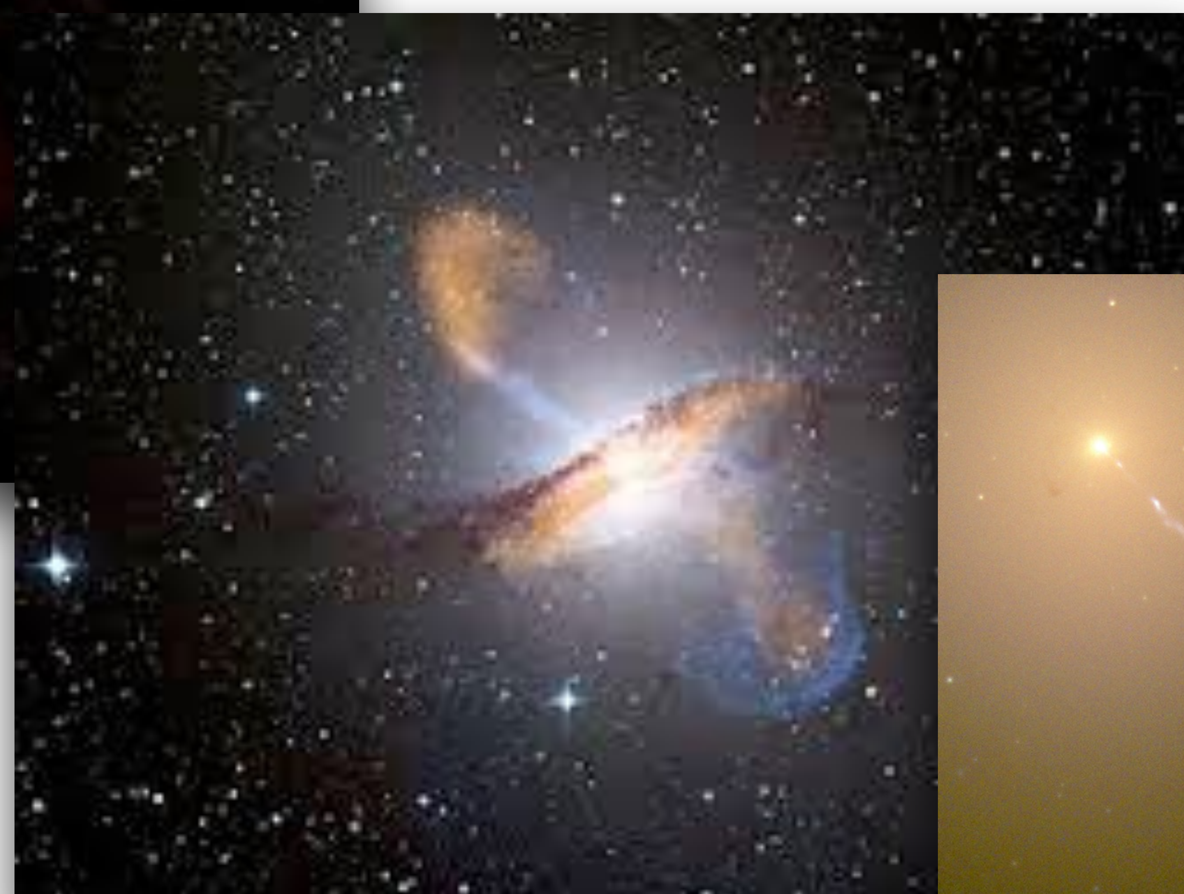

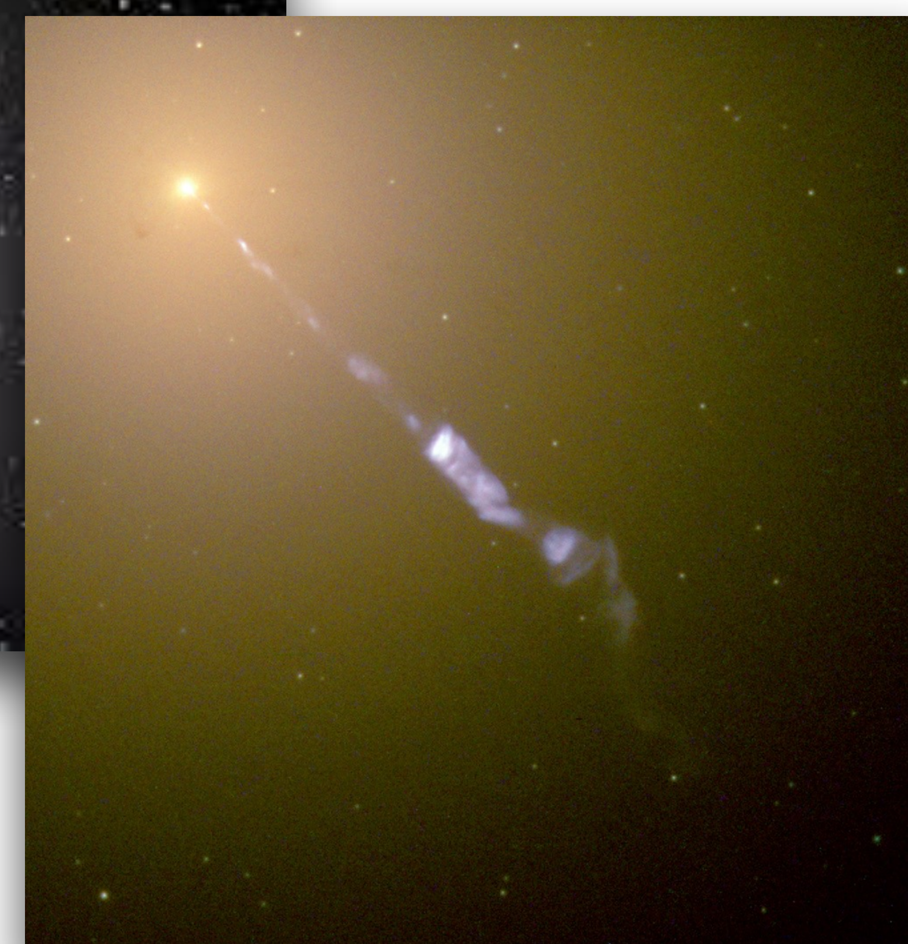

RL AGN lie in ellipticals
RQ AGN lie in spirals and ellipticals

RADIO LOUDNESS PARAMETER (R)

$$R = \frac{F_{5GHz}}{F_B} \geq 10$$

This "classical" definition is based on a study of quasars of the Palomar Bright Quasar Survey with VLA (Kellermann et al 1989).

More recent works based on deeper radio surveys show that the radio loudness is better described by two components. RL AGN are ~ 12% of the objects (see for example Balokovic et al. 2012). The evidence for a local minimum in the loudness distribution (bimodality) is not strong.

Some numbers for a typical AGN

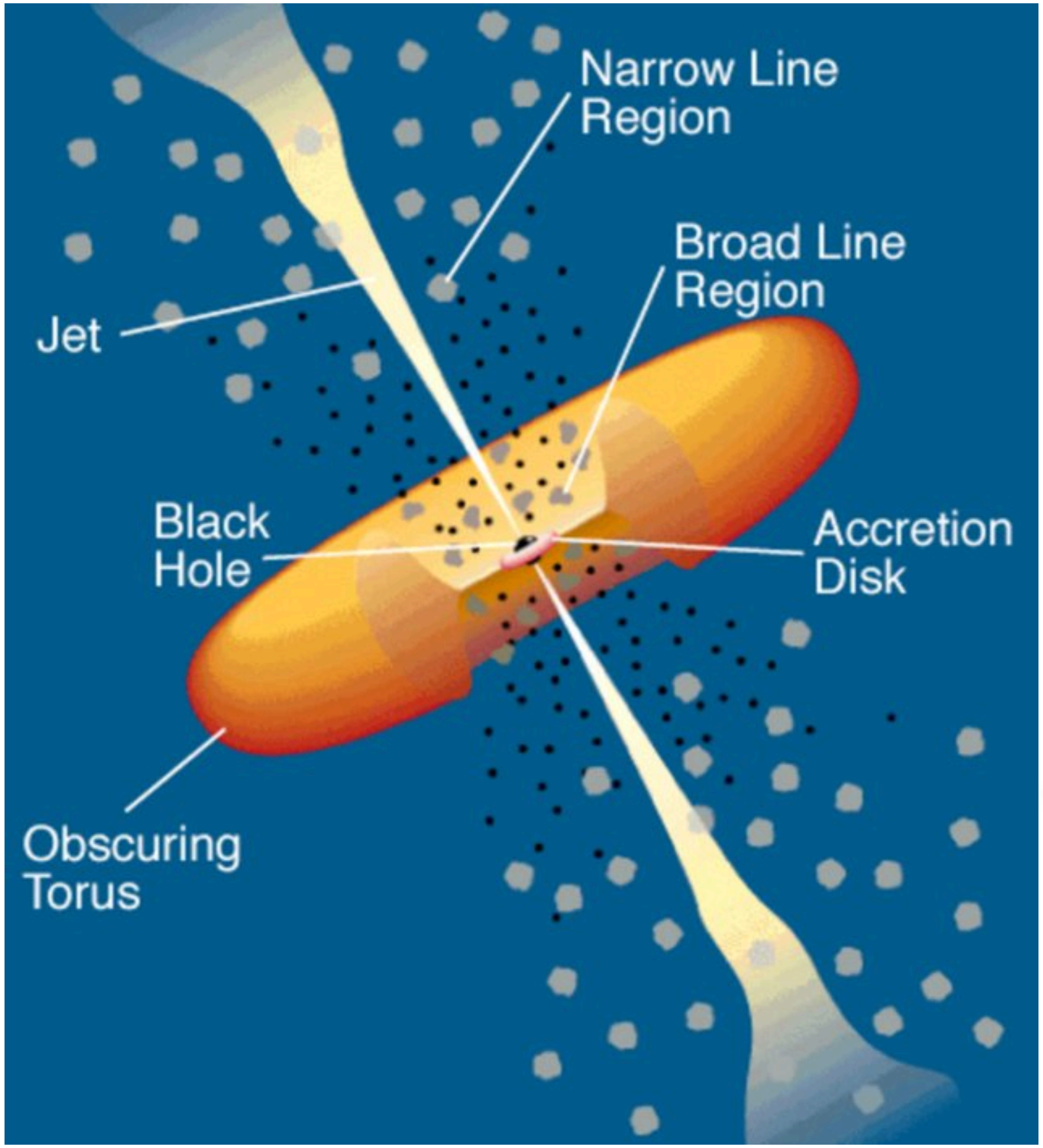

BH Mass	$\sim 10^8 M_\odot$
Luminosity	$\sim 10^{44}\ erg\ s^{-1}$
BH radius	$\sim 3 \times 10^{13}\ cm$
BLR radius	$\sim 2 - 20 \times 10^{16}\ cm$
NLR radius	$\sim 10^{18} - 10^{20}\ cm$

In RL AGN: Jets end at kpc distances forming radio lobes

Urry & Padovani 1995

Centaurus A

Colour composite image of Centaurus A, revealing the lobes and jets emanating from the active galaxy's central black hole. This is a composite of (mm, optical and X-ray) images

Credit: ESO/WFI (Optical); MPIfR/ESO/APEX/A.Weiss et al. (Submillimetre); NASA/CXC/CfA/R.Kraft et al. (X-ray)

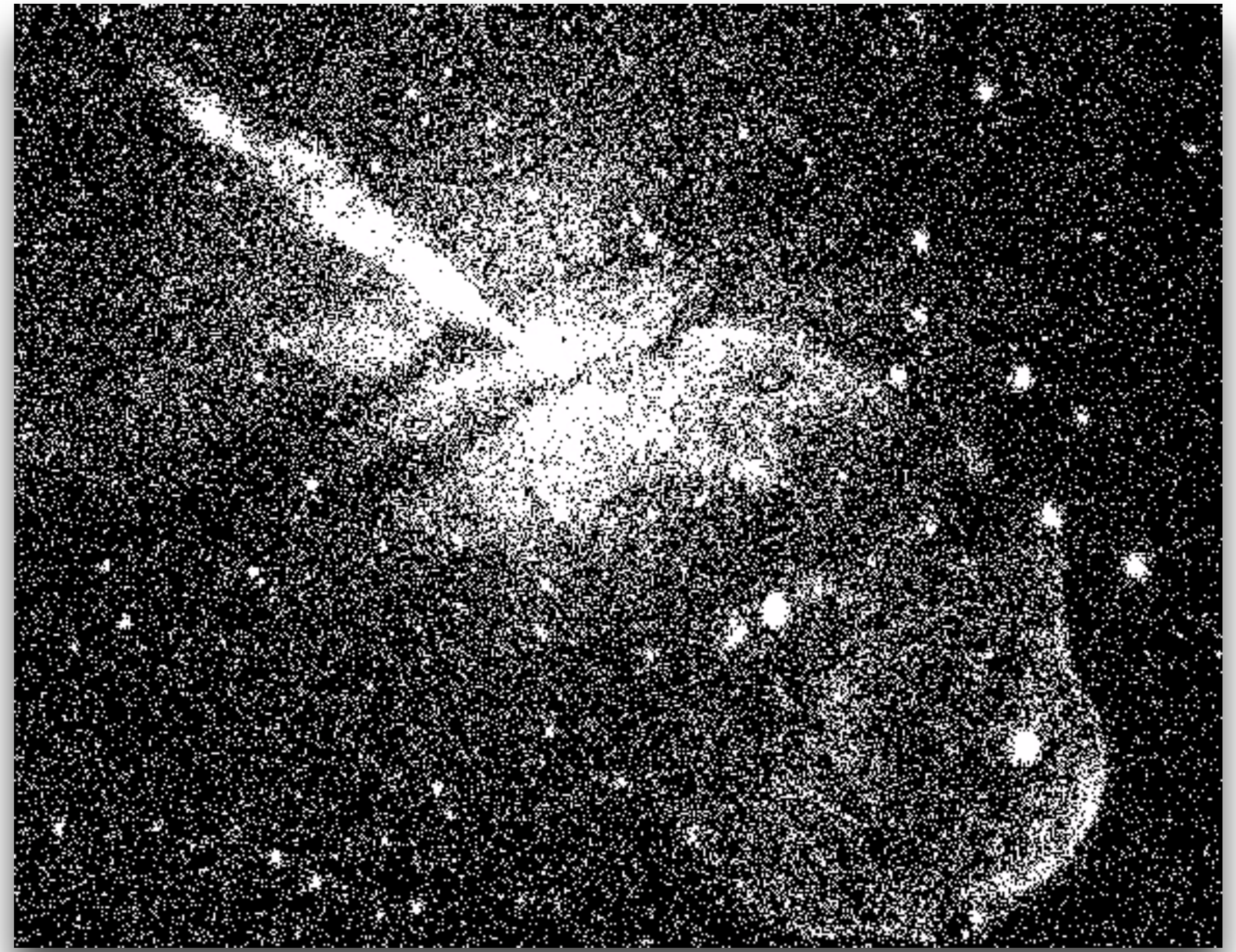

Chandra ACIS-I 0.3-7 keV mosaic (750 ks)
Linear extension ~ 500X 250 kpc

Credit: Prof. Vignali

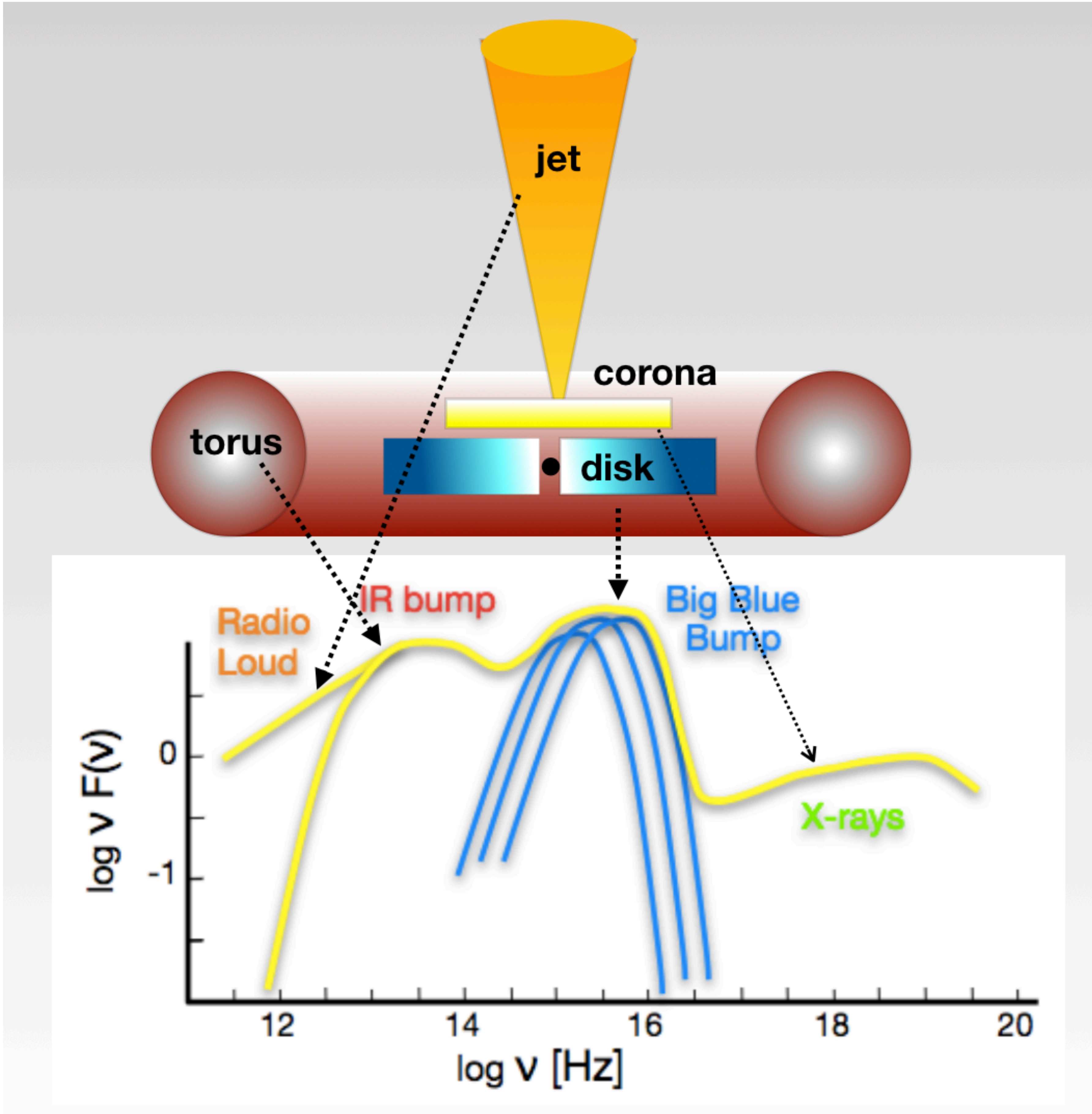

jet
corona
torus
disk
Radio
Loud
IR bump
Big Blue
Bump
X-rays
log ν F(ν)
0
-1
12
14
16
18
20
log ν [Hz]

AGN classification

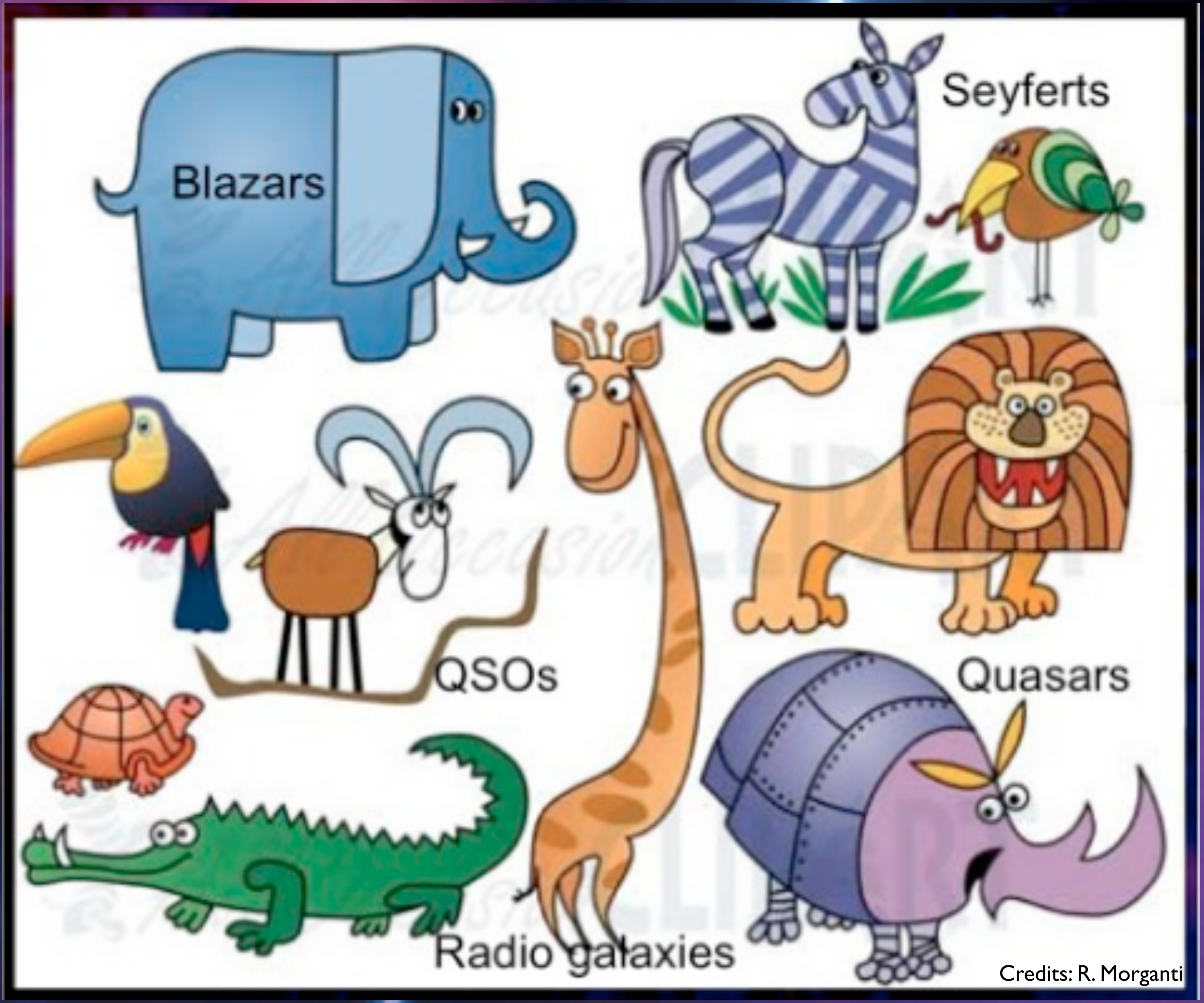

Radio Loud **OLD** Optical Classifications:

Brod Line Radio Galaxy (BLRG) Quasar	**bright continuum and BROAD emission lines from hot high velocity hot gas (FWHM~10^{3-4} km s^{-1})**	Radio Loud counterpart of Seyfert 1s QSO
Narrow line Radio Galaxy	weak continuum and only NARROW emission lines (FWHM~10^2 km s^{-1})	Radio Loud counterpart of Seyfert 2s
LINER (Low Ionization Emission-line region)	Spectra dominated by low ionisation emission lines such as OI OII NII . High excitation lines such as OIII and NeIII are weak	

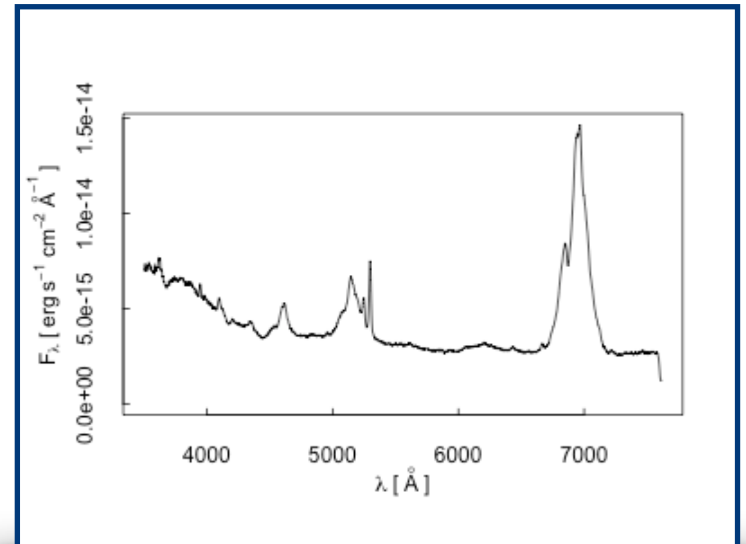

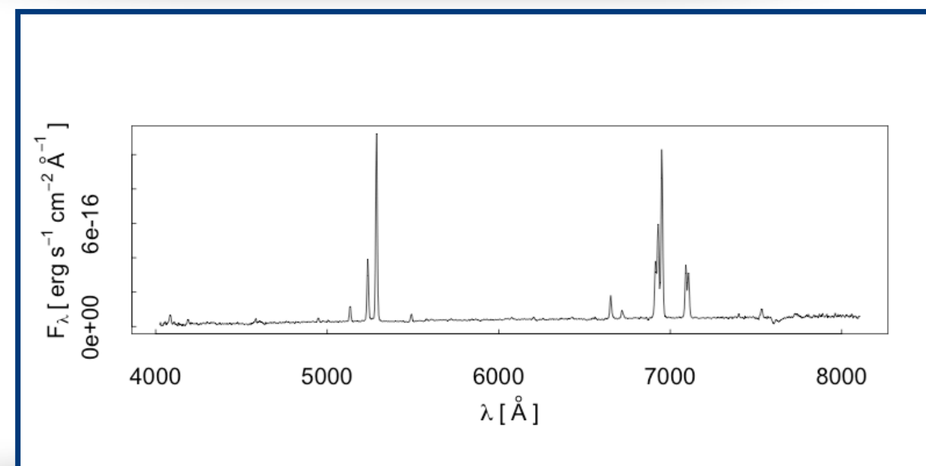

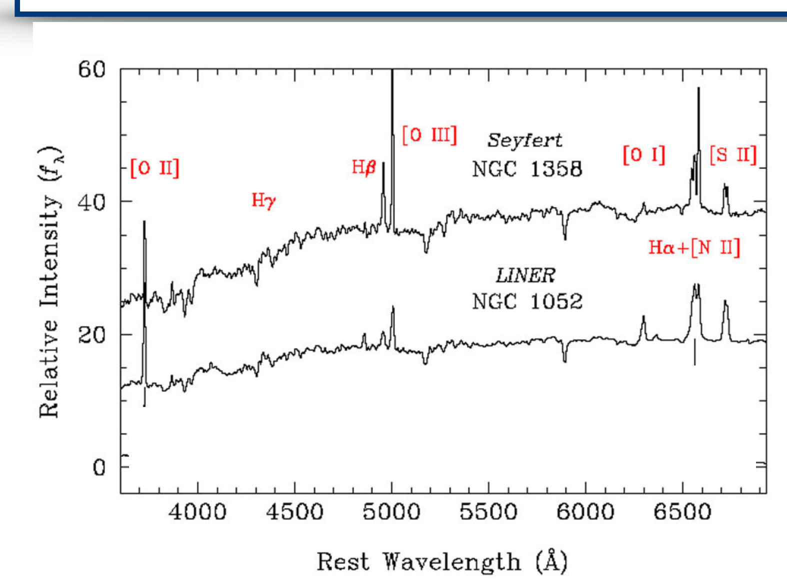

Buttiglione et al. 2011

New optical Radio Loud classification

BLRG +NLRG → High-Excitation Radio Galaxy (HERG)

Efficient engine

LINER → Low-Excitation Radio Galaxy (LERG)

Inefficient engine

in converting gravitational power into radiation

New optical classification
High-excitation (HERG) low-excitation (LERG) Radio Galaxy

This classification is related to the excitation modes of the gas in the Narrow Line Regions:

different excitation modes correspond to different accretion rates

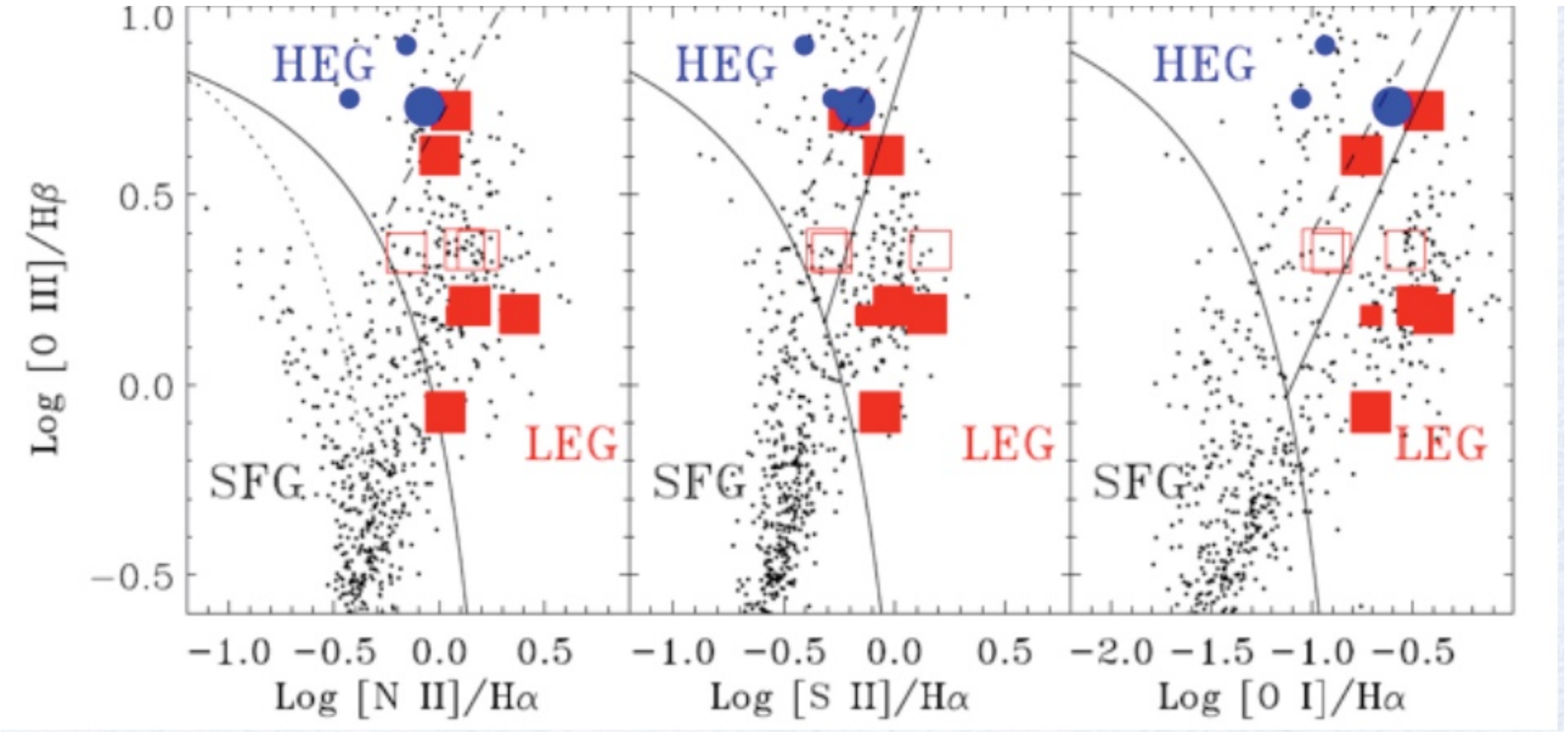

Radio

FRI/FRII classification (Fanaroff & Riley FR1974)

RADIO MORPHOLOGY

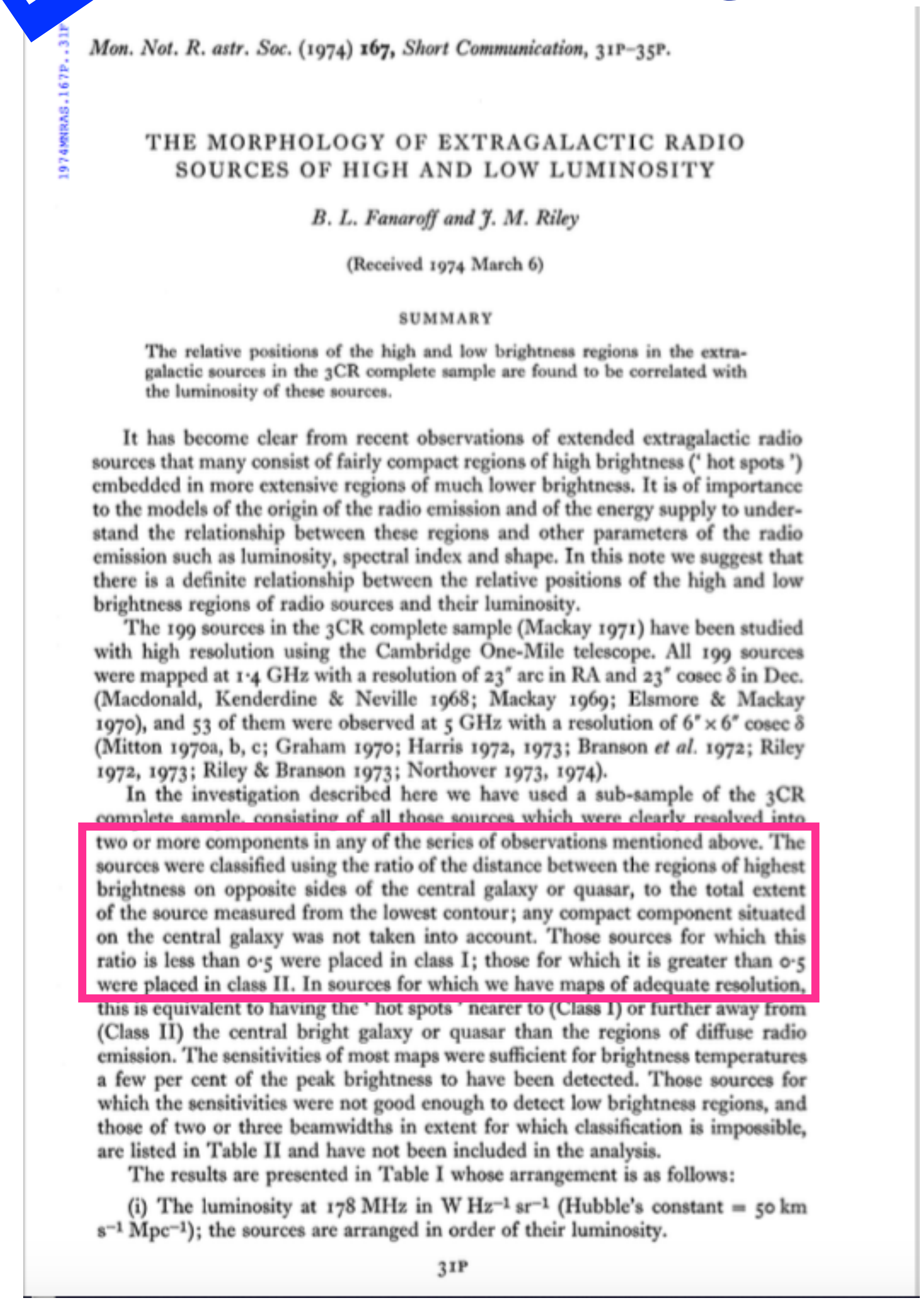

Mon. Not. R. astr. Soc. (1974) **167**, *Short Communication*, 31P–35P.

THE MORPHOLOGY OF EXTRAGALACTIC RADIO SOURCES OF HIGH AND LOW LUMINOSITY

B. L. Fanaroff and J. M. Riley

(Received 1974 March 6)

SUMMARY

The relative positions of the high and low brightness regions in the extragalactic sources in the 3CR complete sample are found to be correlated with the luminosity of these sources.

It has become clear from recent observations of extended extragalactic radio sources that many consist of fairly compact regions of high brightness (' hot spots ') embedded in more extensive regions of much lower brightness. It is of importance to the models of the origin of the radio emission and of the energy supply to understand the relationship between these regions and other parameters of the radio emission such as luminosity, spectral index and shape. In this note we suggest that there is a definite relationship between the relative positions of the high and low brightness regions of radio sources and their luminosity.

The 199 sources in the 3CR complete sample (Mackay 1971) have been studied with high resolution using the Cambridge One-Mile telescope. All 199 sources were mapped at 1·4 GHz with a resolution of 23" arc in RA and 23" cosec δ in Dec. (Macdonald, Kenderdine & Neville 1968; Mackay 1969; Elsmore & Mackay 1970), and 53 of them were observed at 5 GHz with a resolution of $6'' \times 6''$ cosec δ (Mitton 1970a, b, c; Graham 1970; Harris 1972, 1973; Branson *et al.* 1972; Riley 1972, 1973; Riley & Branson 1973; Northover 1973, 1974).

In the investigation described here we have used a sub-sample of the 3CR complete sample, consisting of all those sources which were clearly resolved into two or more components in any of the series of observations mentioned above. The sources were classified using the ratio of the distance between the regions of highest brightness on opposite sides of the central galaxy or quasar, to the total extent of the source measured from the lowest contour; any compact component situated on the central galaxy was not taken into account. Those sources for which this ratio is less than 0·5 were placed in class I; those for which it is greater than 0·5 were placed in class II. In sources for which we have maps of adequate resolution, this is equivalent to having the ' hot spots ' nearer to (Class I) or further away from (Class II) the central bright galaxy or quasar than the regions of diffuse radio emission. The sensitivities of most maps were sufficient for brightness temperatures a few per cent of the peak brightness to have been detected. Those sources for which the sensitivities were not good enough to detect low brightness regions, and those of two or three beamwidths in extent for which classification is impossible, are listed in Table II and have not been included in the analysis.

The results are presented in Table I whose arrangement is as follows:

(i) The luminosity at 178 MHz in W Hz^{-1} sr^{-1} (Hubble's constant = 50 km s^{-1} Mpc^{-1}); the sources are arranged in order of their luminosity.

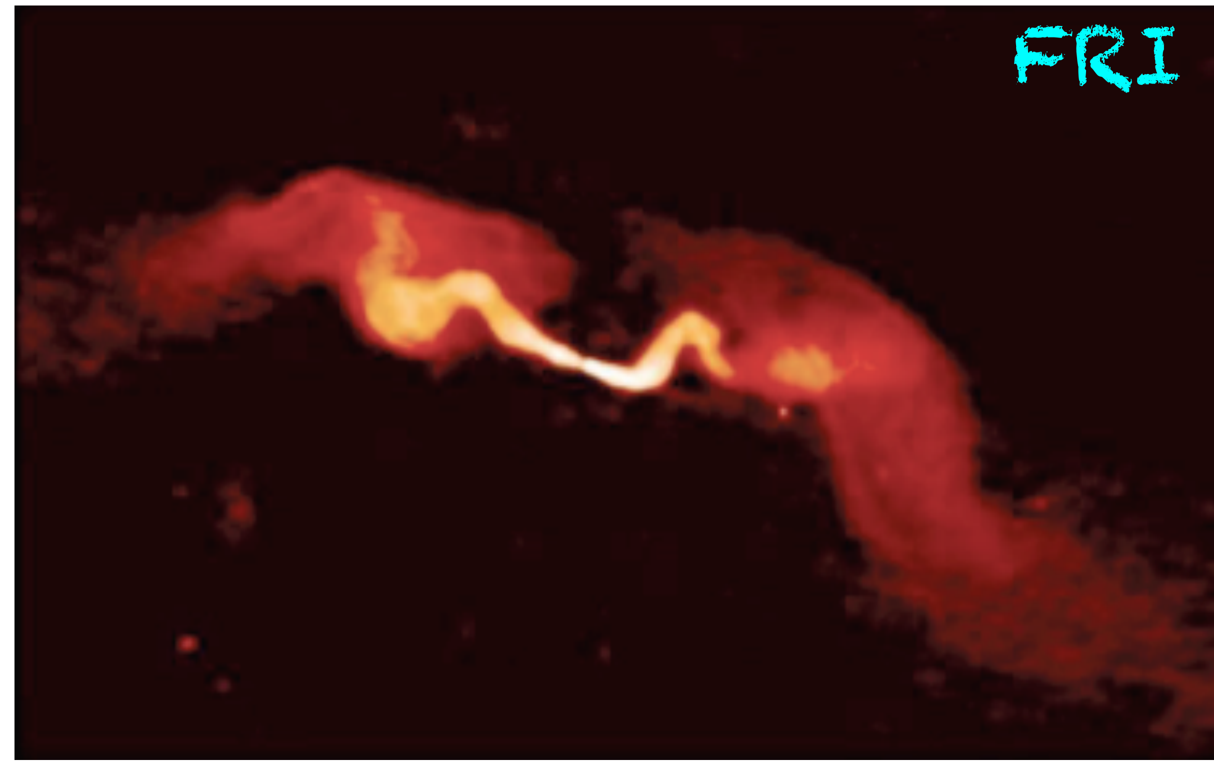

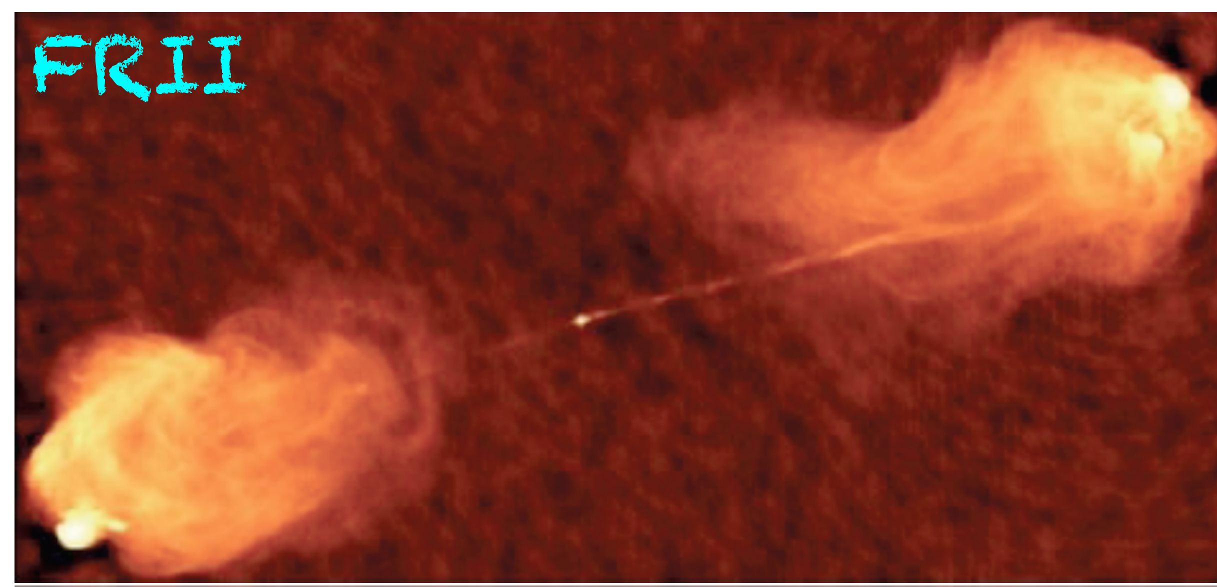

FRI - $L_{178MHz} < 2\times10^{25}$ W Hz^{-1} sr^{-1}

FRII - $L_{178MHz} > 2\times10^{25}$ W Hz^{-1} sr^{-1}

FRI/jet dominated

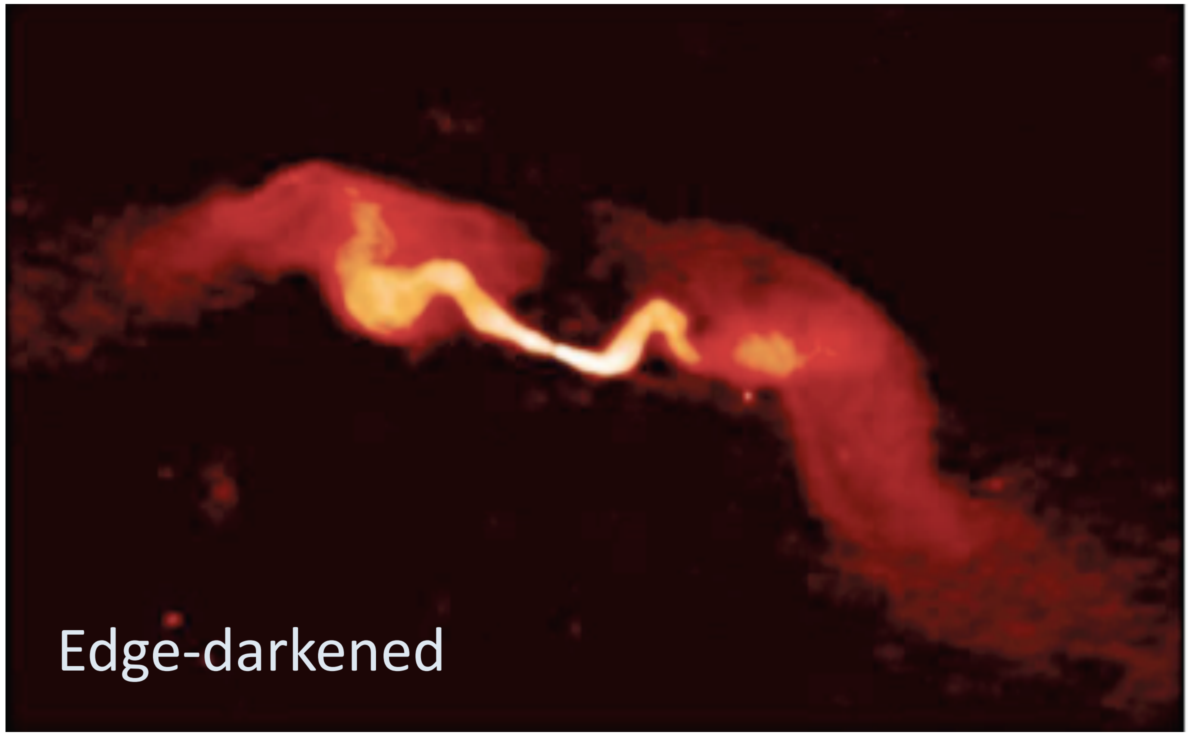

In FRI the jets are thought to decelerate and become sub-relativistic on scales of hundred of pc to kpc.

The nuclei of FRI are powered by inefficient engine

FRII/lobe dominated

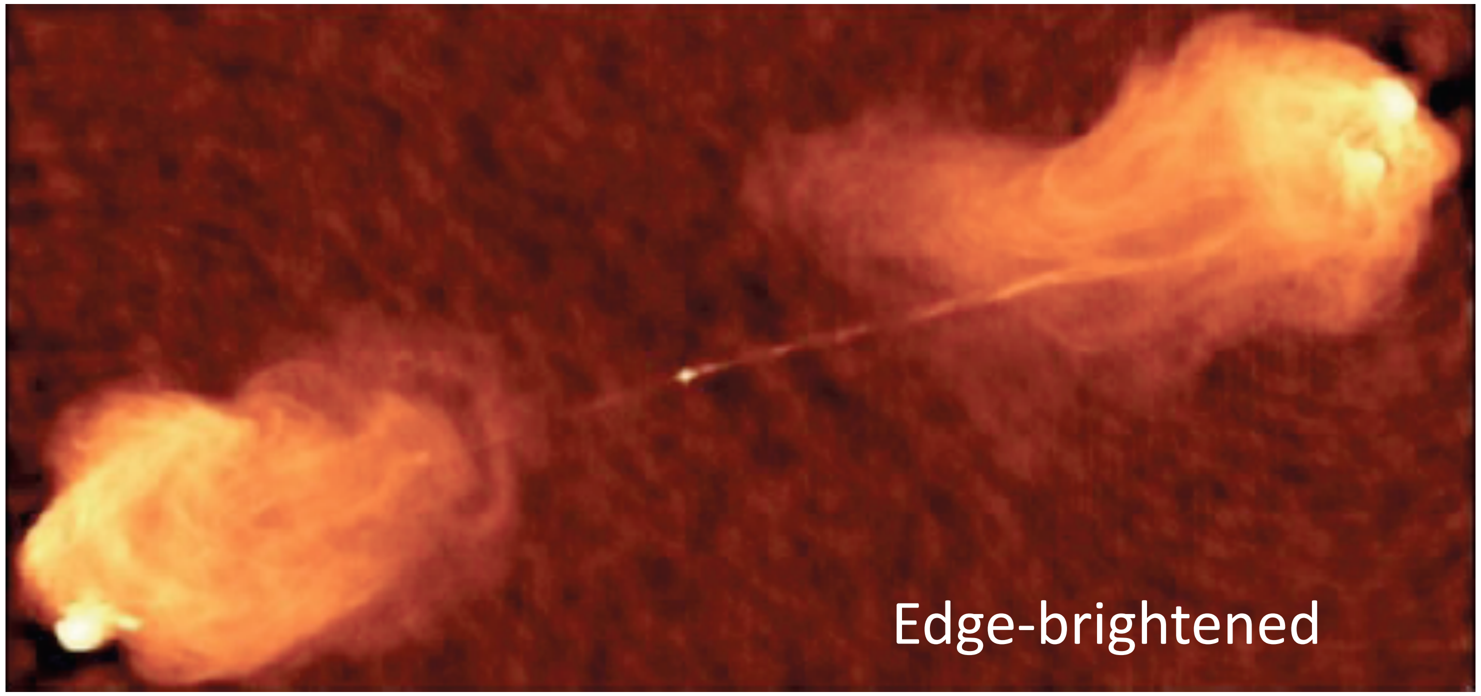

The jets in FRII are at least moderately relativistic and supersonic from the core to the hot spots.

Most FRII are **thought** to have an efficient engine

In general

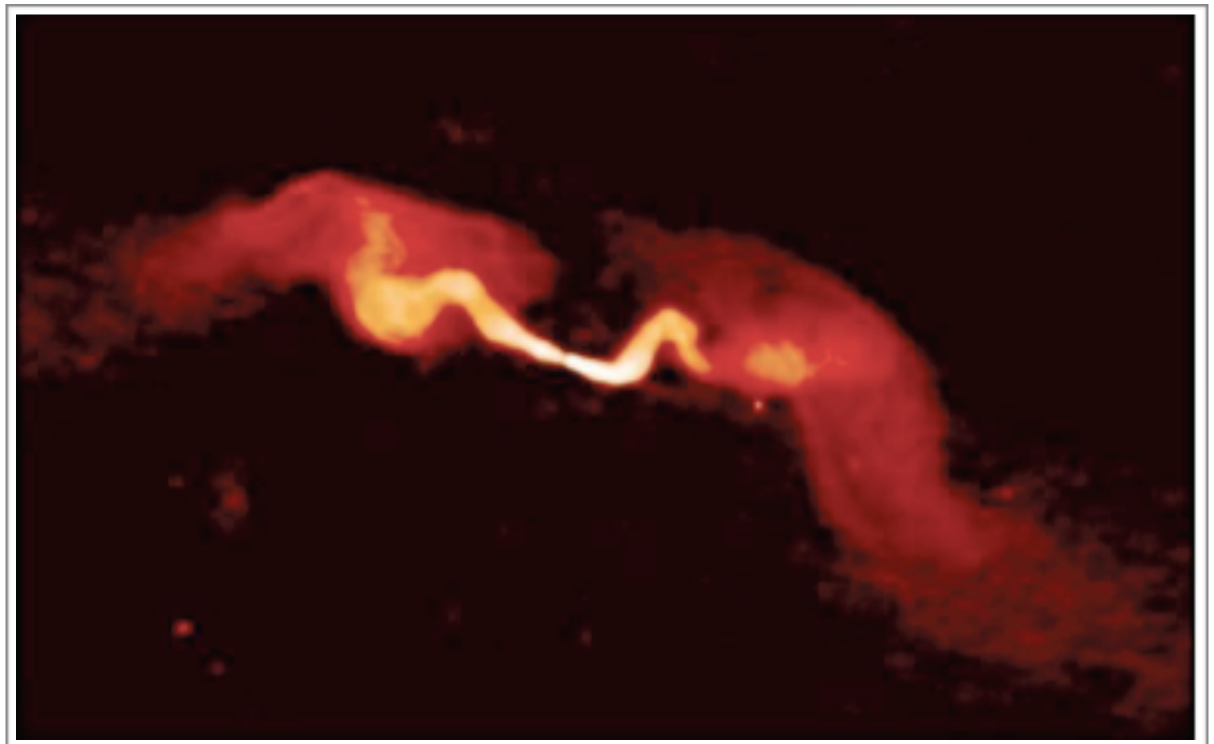

FRI/jet dominated

FRI LERG

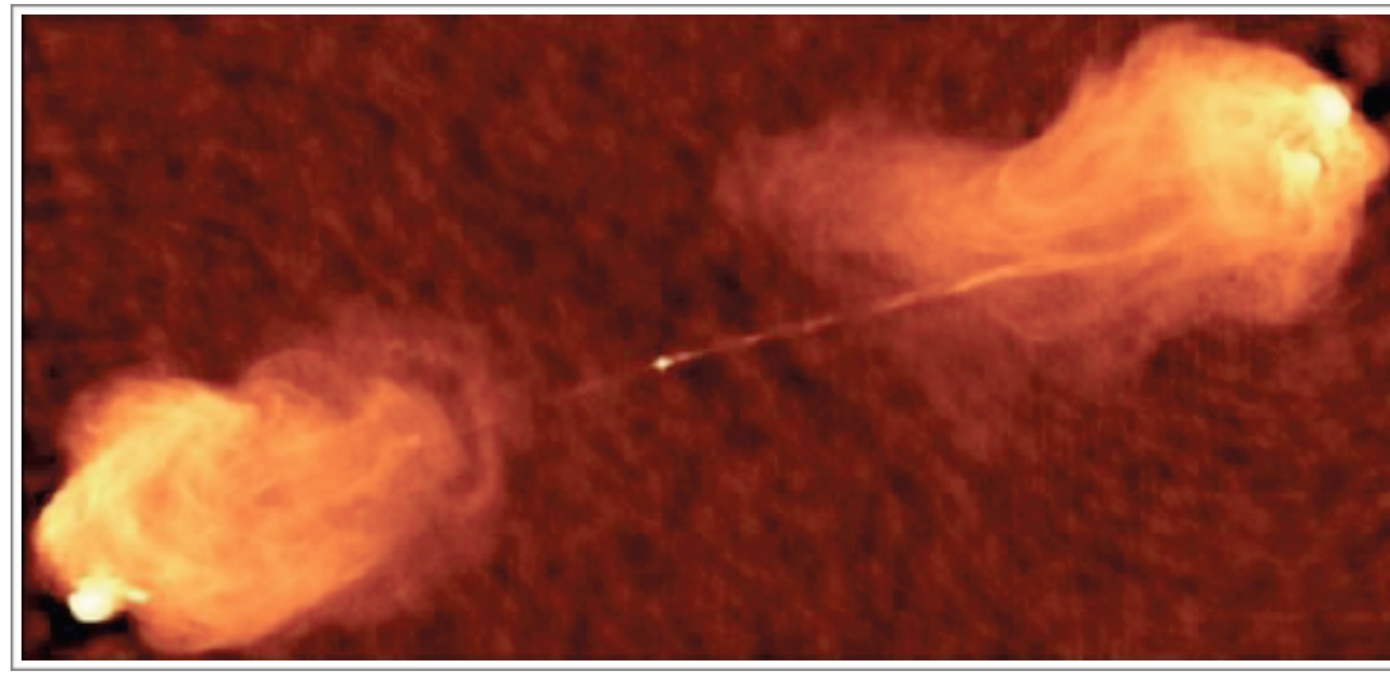

FRII/lobe dominated

FRII HERG

Different Engines

The central engine

Black Hole as engine of AGN

BH is a very efficient engine

The gravitational energy released on a star surface, assuming $M \sim M_{sun}$ and R=10 Km is

$$\Delta E_{acc} = \frac{GMm}{R} \sim 10^{20} \text{ erg/g}$$

The same mass m of H converted into He

$$\Delta E_{nuc} = 7 \times 10^{-2} mc^2 \sim 6 \times 10^{18} erg/g$$

Black Hole as engine of AGN

$$\Delta E_{acc} = \frac{GMm}{R}$$

- *M/R is the compactness of the accretor*
  - *The more compact, the more energy can be released*

$$L_{acc} = GM\boxed{\dot{M}}/R$$

The luminosity depends on the accretion rate

Eddington Luminosity L_E is the luminosity at which the outward force of the radiation pressure is balanced by the inward gravitational force

$$L_{Edd} = \frac{4\pi GMm_pc}{\sigma_T} \sim 1.3 \times 10^{38} \frac{M}{M_\odot} erg/s$$

Schwarzschild radius

Black hole radius can be derived by the escape velocity of the light

$$v_{escape} = c = \left(\frac{2GM}{R_S}\right)^{\frac{1}{2}}$$

$$R_S = \frac{2GM}{c^2}$$

$$\boxed{L_{acc} = GM\dot{M}/R}$$

Introducing the Schwarzschild radius

$$\boxed{R_S = \frac{2GM}{c^2}}$$

L_{acc} can be written as:

$$\boxed{L_{acc} = 2\eta GM\dot{M}/R = \eta\dot{M}c^2}$$

NOTE: In the case of a black hole, R would require a more complex discussion.
This complexity is absorbed by the term 2η

Accretion

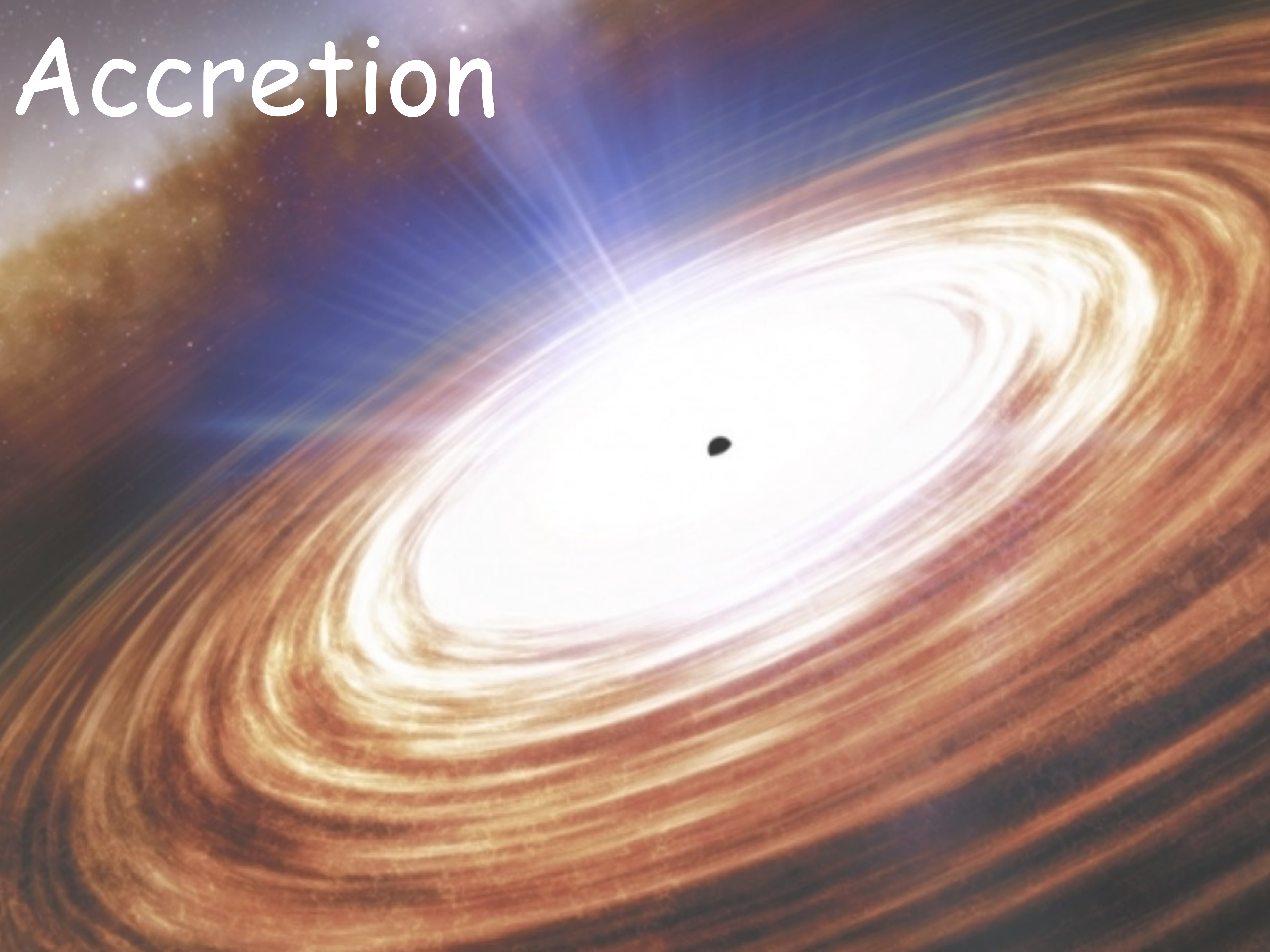

Accretion processes around black holes involve rotating gas flow. Therefore the accretion flow structure is determined by solving simultaneously four conservation equations:

conservation of vertical momentum
conservation of mass
conservation of energy
conservation of angular momentum

Four solutions are currently known. In these solutions viscosity transports angular momentum outward, allowing the accretion gas to spiral in toward the BH. Viscosity acts a source of heat that is radiated away.

The most famous solutions are:

i) Shakura & Sunyaev thin optically thick disk model (standard model)
ii) ii) Optically thick Advection-Dominated Accretion Flow (ADAF)

Efficient Engine

Shakura & Sunyaev thin optically thick disk model (standard model)

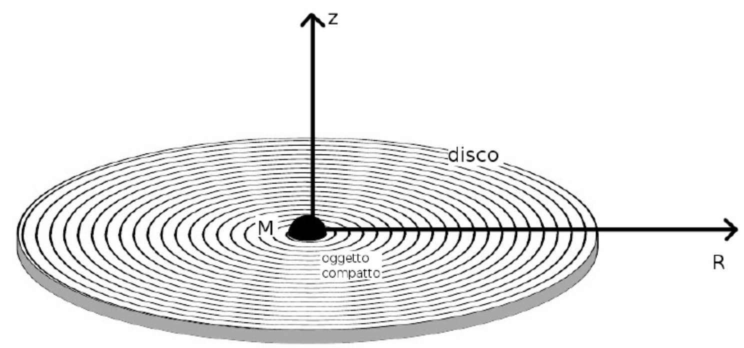

Thin   H/R<< 1

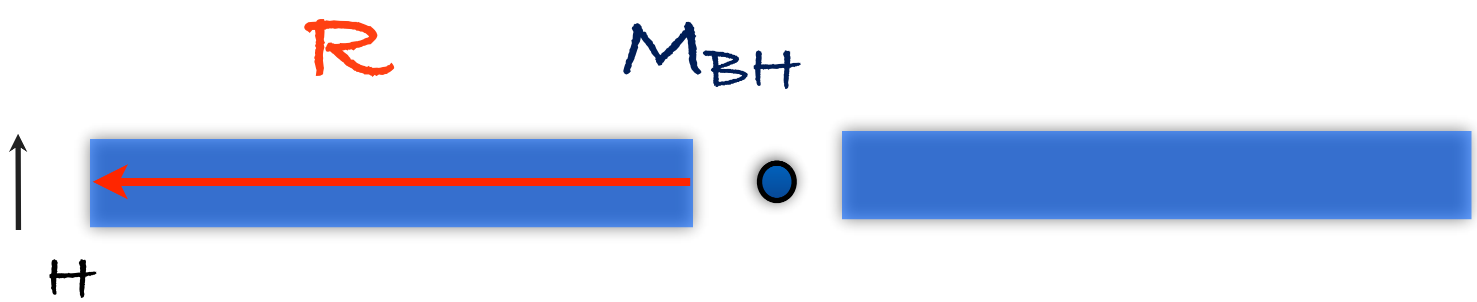

Thick, in the sense that each element of the disk radiates as a black body

UV-Optical Continuum

In reality, energy is dissipated locally in the disk through viscosity. This yields:

$$T(r)=\left[\frac{3GM\dot{M}}{8\pi\sigma r^3}\left\{1-(R_i/r)^{1/2}\right\}\right]^{1/4}$$

or

$$T(r)=\left[\frac{3GM\dot{M}}{8\pi\sigma R_s^3}\right]^{1/4}\left(\frac{r}{R_s}\right)^{-3/4}$$

when $r \gg R_i$ and $R_i \approx R_s$

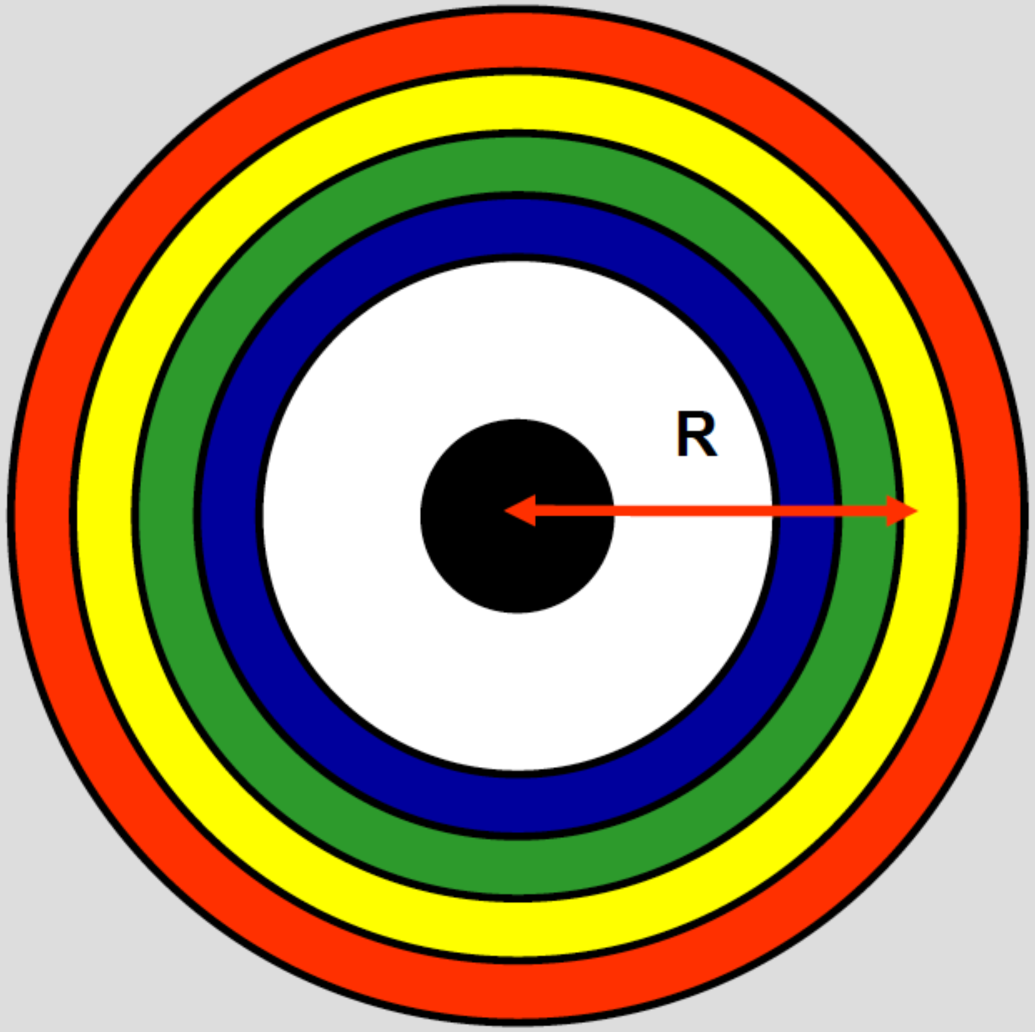

UV-Optical Continuum

The superposition of these BB spectra will thus look like:

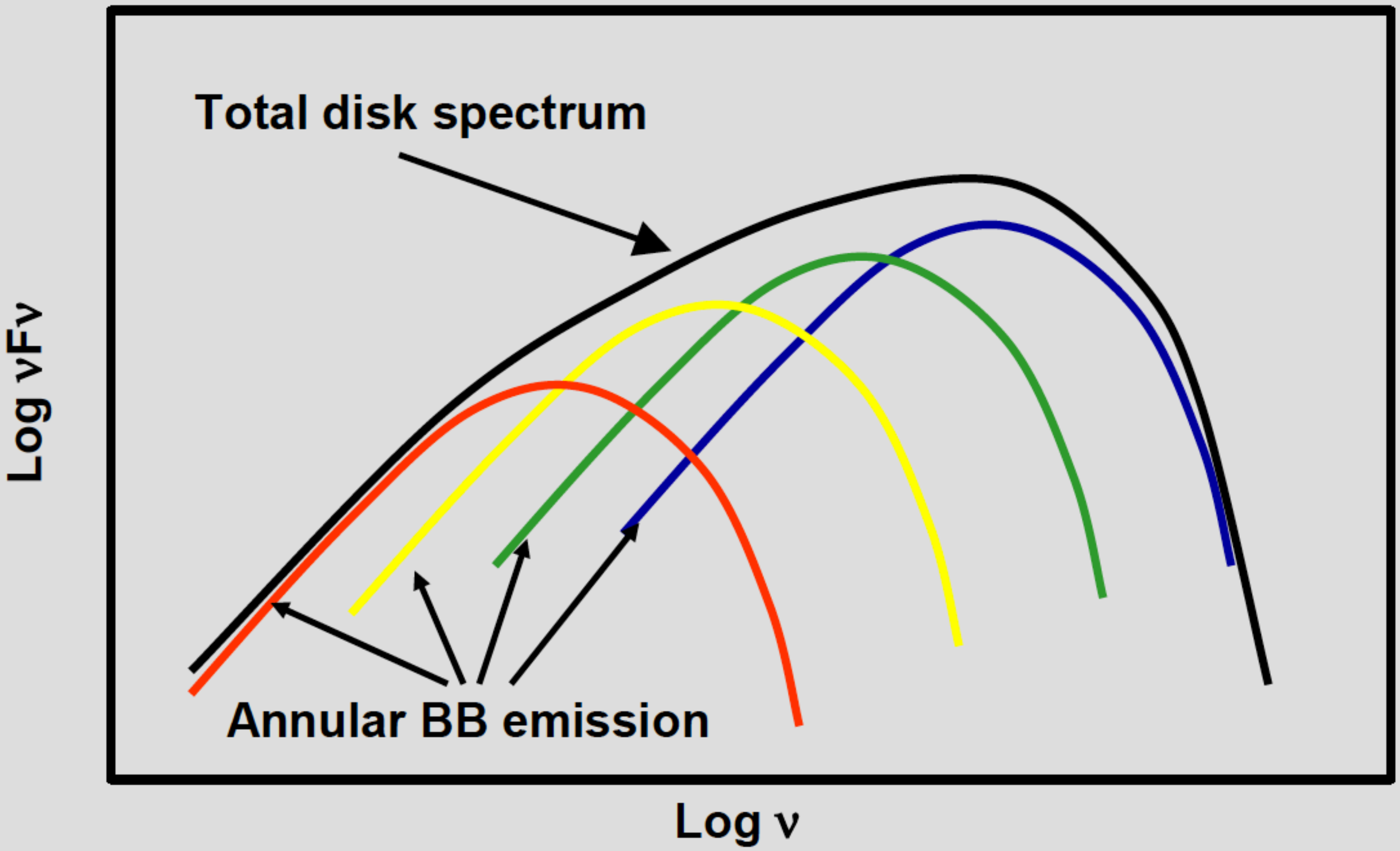

If the the disk is optically thick, we can approximate the local emission as blackbody and the effective temperature of the photosphere

$$T(r) \sim 6.3 \times 10^5 \left(\frac{\dot{M}}{\dot{M}_E}\right)^{1/4} M_8^{-1/4} \left(\frac{r}{R_s}\right)^{-3/4} \quad K$$

For AGN with $M_{BH} = 10_8 = 10^8 M_\odot$ $\quad \dot{M} \sim \dot{M}_E = \frac{L_E}{\eta c^2}$

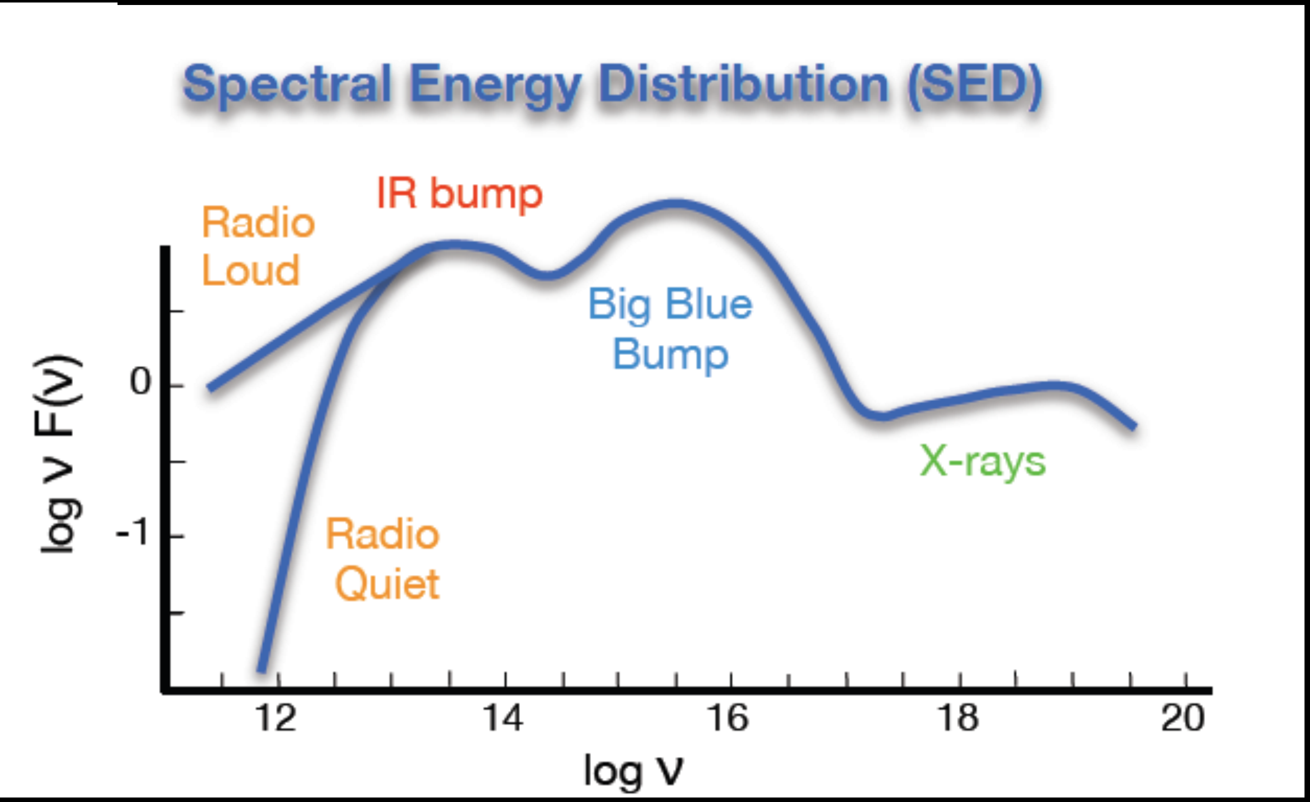

the peak occurs at UV-soft-X-ray region

$$\frac{\partial B}{\partial \nu} = 0 \qquad B(\nu) \propto \nu^3 [e^{\frac{h\nu}{kT}} - 1]^{-1}$$

$$\nu_{max} = 2.8kT/h \sim 10^{16} \quad Hz$$

$k = 1.38\times10^{-16}$ erg/K

$h = 6.6 \times 10^{-26}$ erg s

Nome	Massa del buco nero ($M_\odot$)	Massa del compagno stellare ($M_\odot$)	Periodo orbitale (giorni)	Distanza dalla Terra (anni luce)
A0620-00	9–13	2,6–2,8	0,33	~ 3500
GRO J1655-40	6–6,5	2,6–2,8	2,8	5000–10000
XTE J1118+480	6,4–7,2	6–6,5	0,17	6200
Cyg X-1	7–13	≥18	5,6	6000–8000
GRO J0422+32	3–5	1,1	0,21	~ 8500
GS 2000+25	7–8	4,9–5,1	0,35	~ 8800
V404 Cyg	10–14	6,0	6,5	~ 10000
GX 339-4		5–6	1,75	~ 15000
GRS 1124-683	6,5–8,2		0,43	~ 17000
LB-1 B	69–71	8–10	78,9	~ 13800
XTE J1550-564	10–11	6,0–7,5	1,5	~ 17000
XTE J1819-254	10–18	~3	2,8	< 25000
4U 1543-475	8–10	0,25	1,1	~ 24000
GRS 1915+105	>14	~1	33,5	~ 40000
XTE J1650-500	3,8 ± 0,5[6]	.	0.32[7]	.

What about X-rays?

Corona above the disk

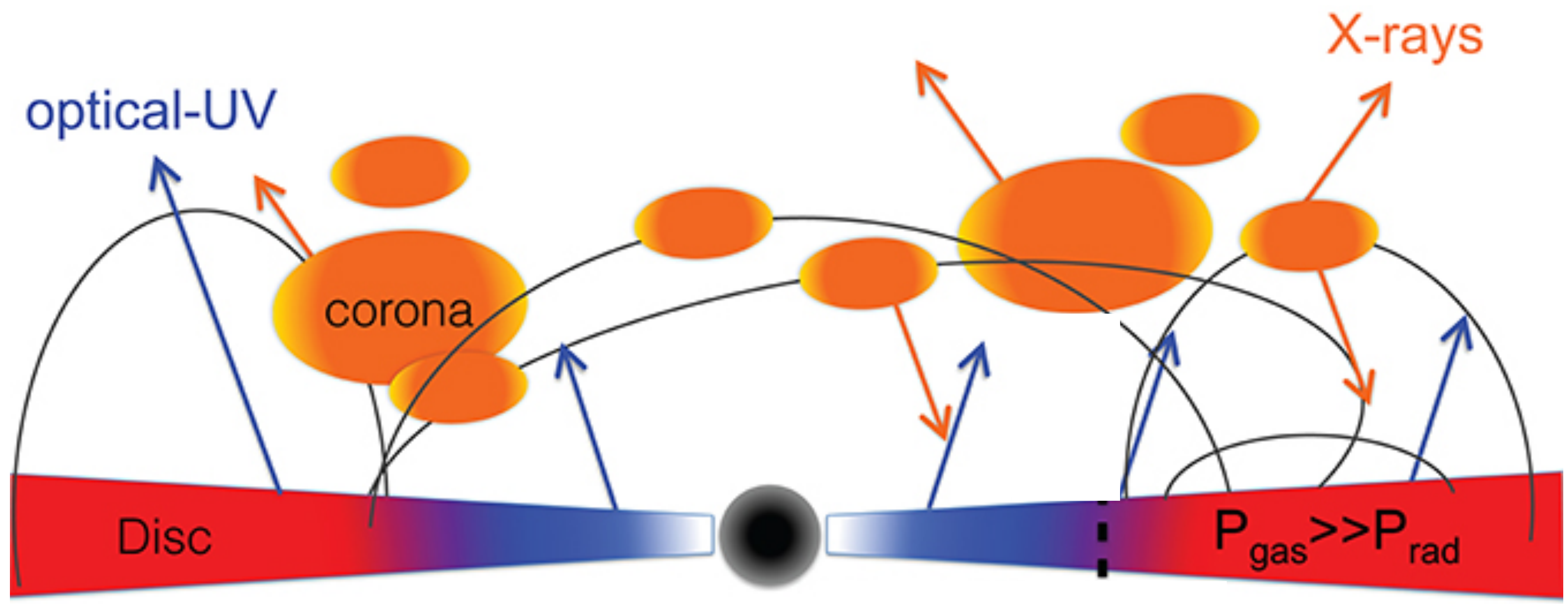

Thermal Comptonization

With this term we mean the process of multiple scattering of a photon due to a **thermal (Maxwellian)** distribution of electrons.

There is one fundamental parameter measuring the importance of the Inverse Compton process in general, and of multiple scatterings in particular: the Comptonization parameter, usually denoted with the letter **y**.

y = [average # of scatt.] x[average fractional energy gain for scatt.]

<u>Haardt & Maraschi 1991</u>

Thermal Comptonization

Comptonization on a thermal plasma of electrons characterized by a temp. T and optical depth τ

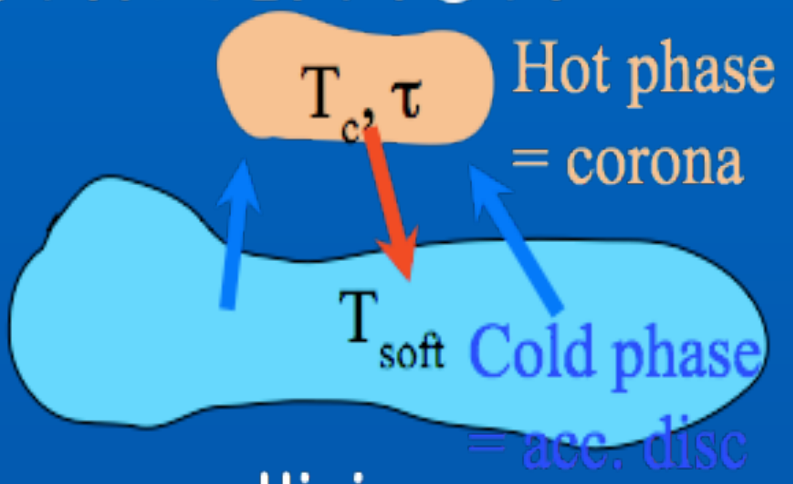

✓ mean relative energy gain per collision

$$\frac{\Delta E}{E} \simeq \left(\frac{4kT}{mc^2}\right) + 16\left(\frac{kT}{mc^2}\right)^2 \quad \text{for } E \ll kT$$

$$\leq \quad 0 \quad \text{for } E \gtrsim kT$$

✓ mean number of scatterings

$$N \simeq (\tau + \tau^2)$$

➡ Compton parameter $y = \frac{\Delta E}{E} N$

$$E_f = E_i\, e^y$$

Thermal Comptonization Spectrum: the continuum

$$F_E \propto E^{-\Gamma(kT,\tau)} \exp\left(-\frac{E}{E_c(kT,\tau)}\right)$$

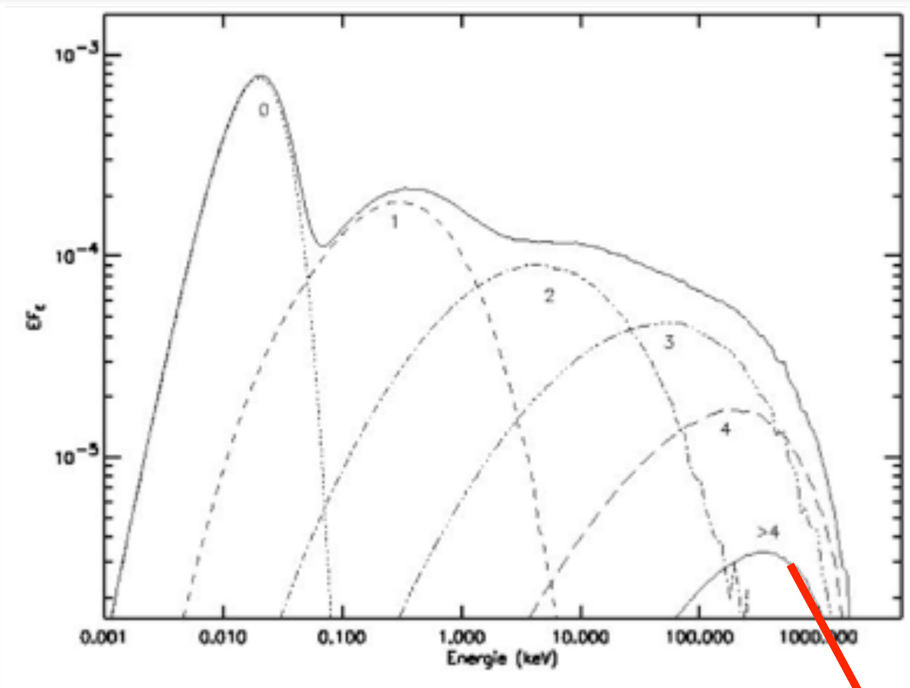

$$\Gamma(\tau, kT)$$

The exact relation between spectral index and optical depth depends on the geometry of the scattering region.

$$E_c \simeq kT$$

As photons approach the electron thermal energy, they no longer gain energy from scattering, and a sharp rollover is expected in the spectrum.

The observed high energy spectral cutoff yields information about the temperature of the underlying electron distribution.

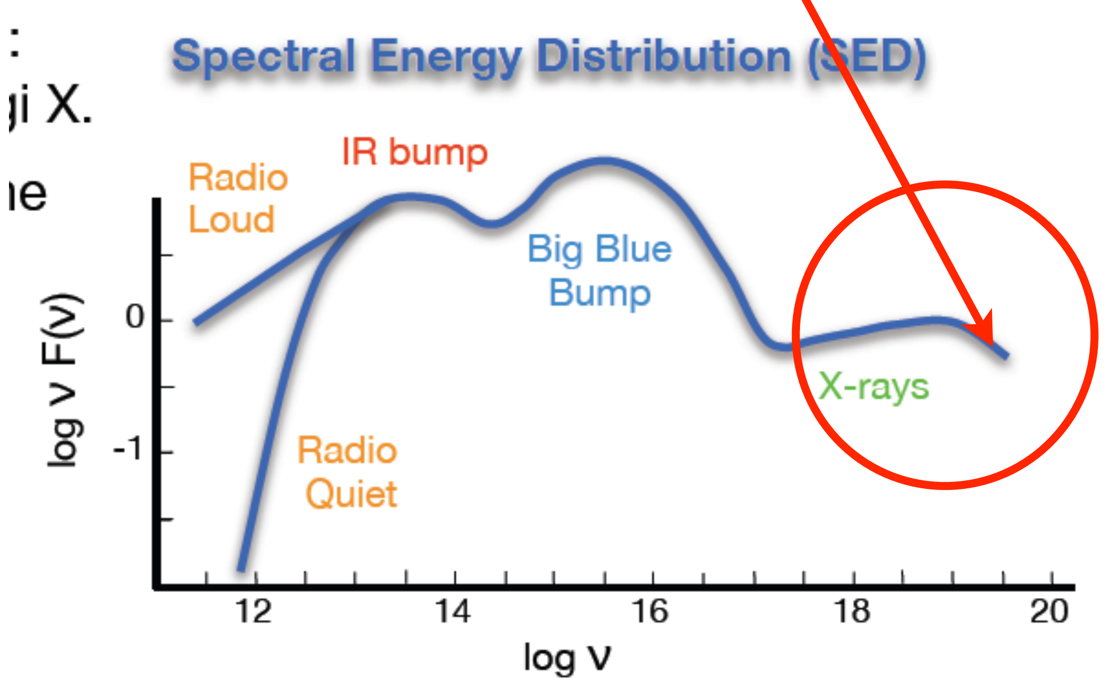

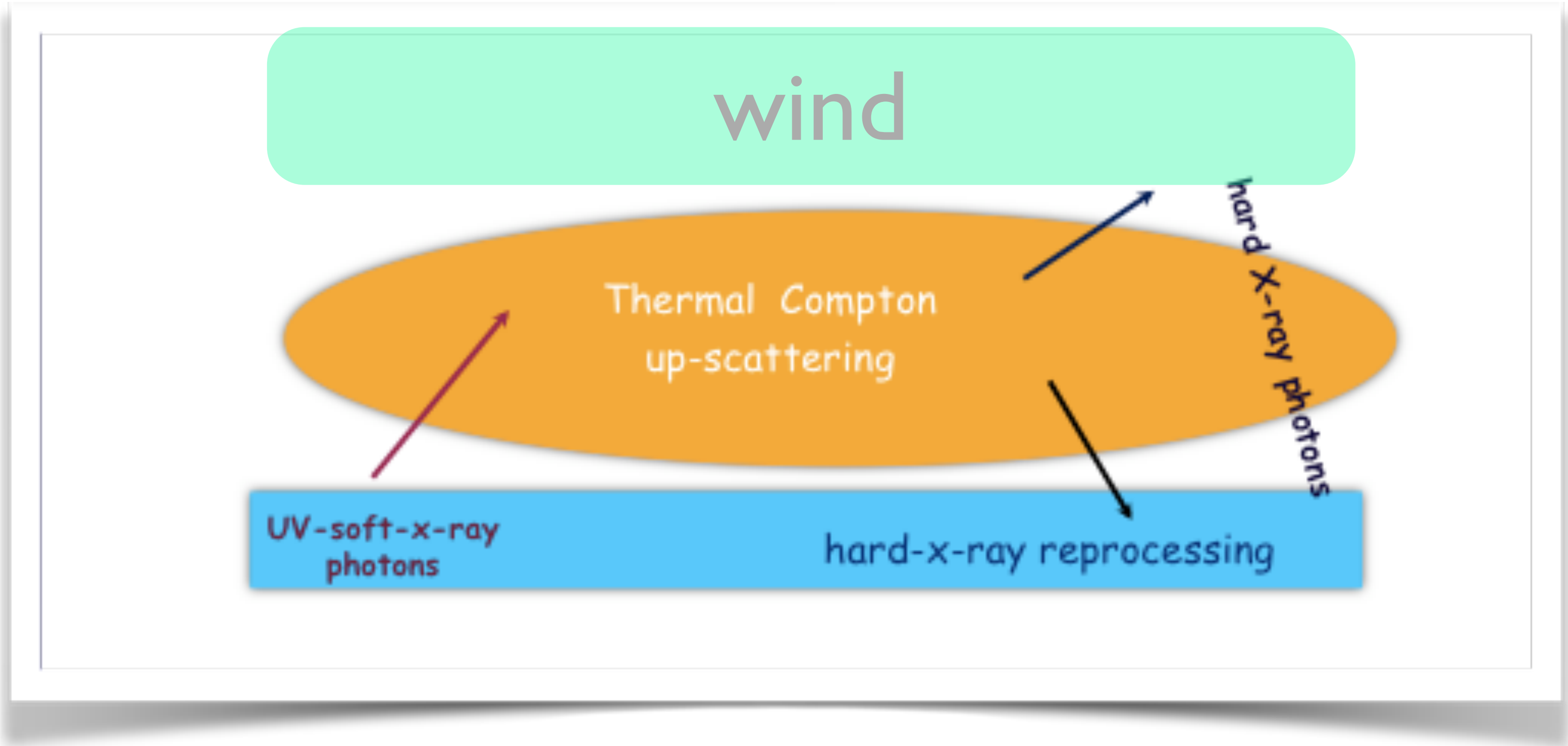

- Thermal Comptonization
- Hard X-ray reprocessing

Iron line

Compton hump

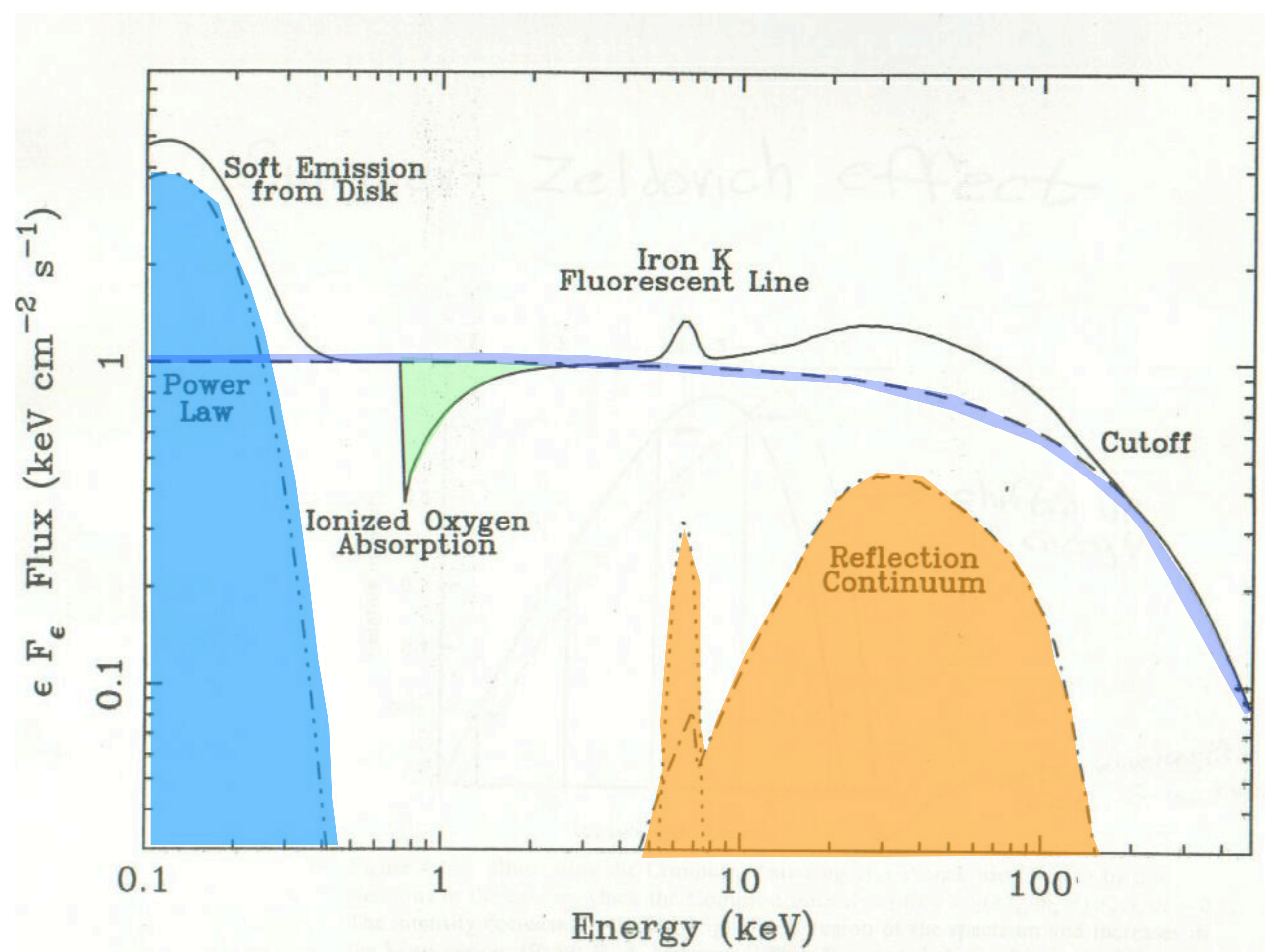

BROAD LINE

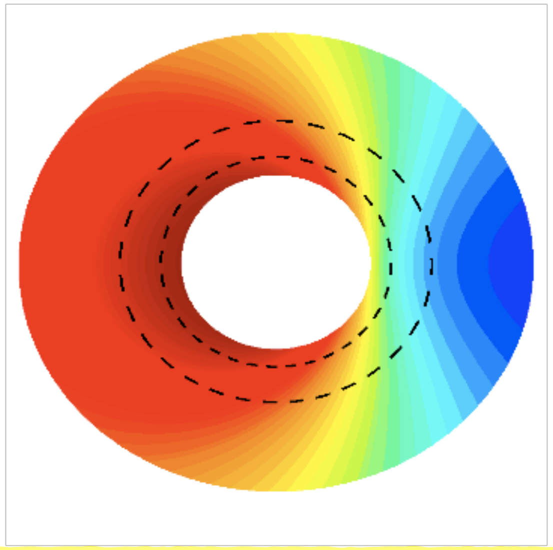

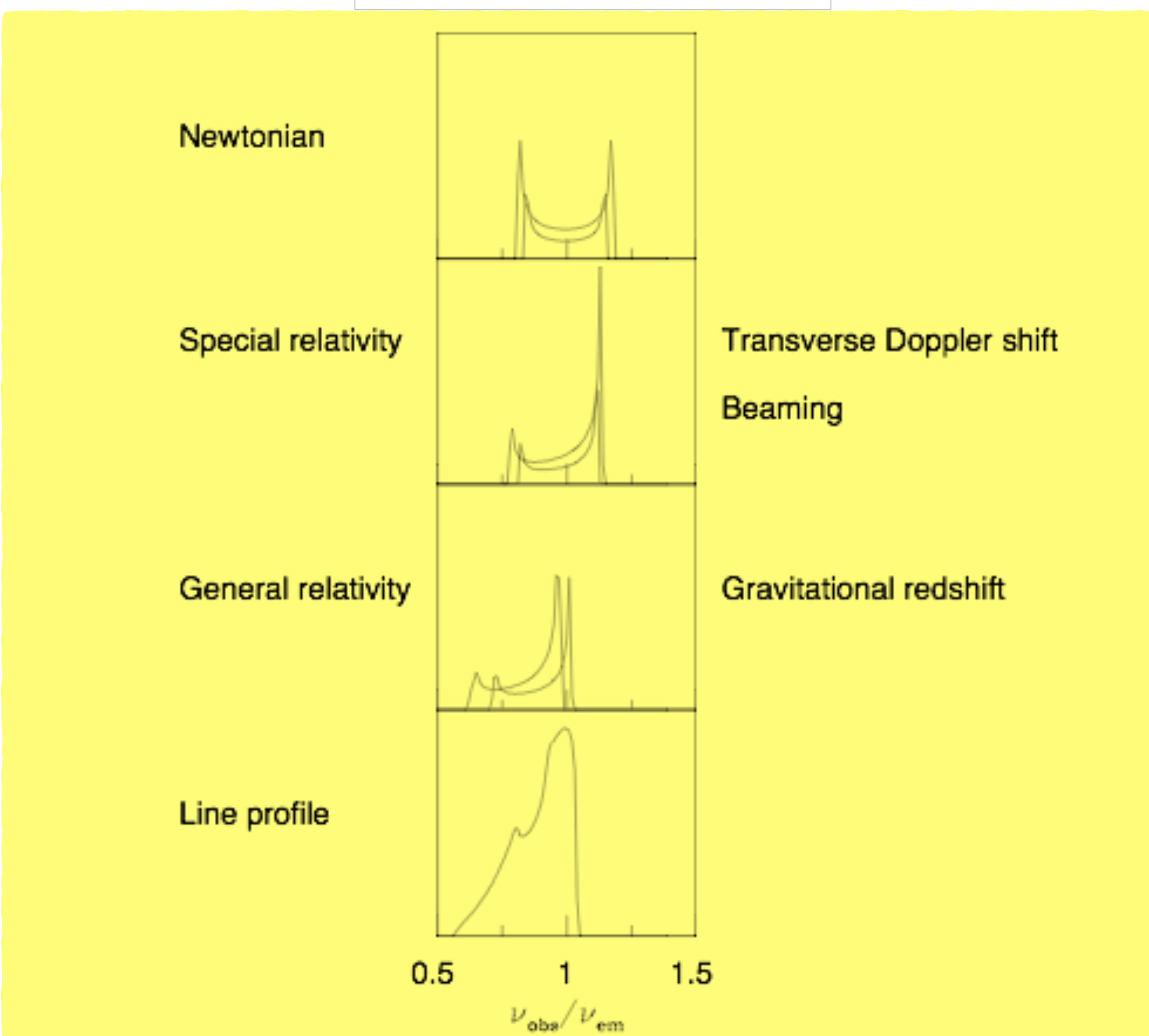
Newtonian
Special relativity
Transverse Doppler shift
Beaming
General relativity
Gravitational redshift
Line profile
0.5
1
1.5
ν_{obs}/ν_{em}

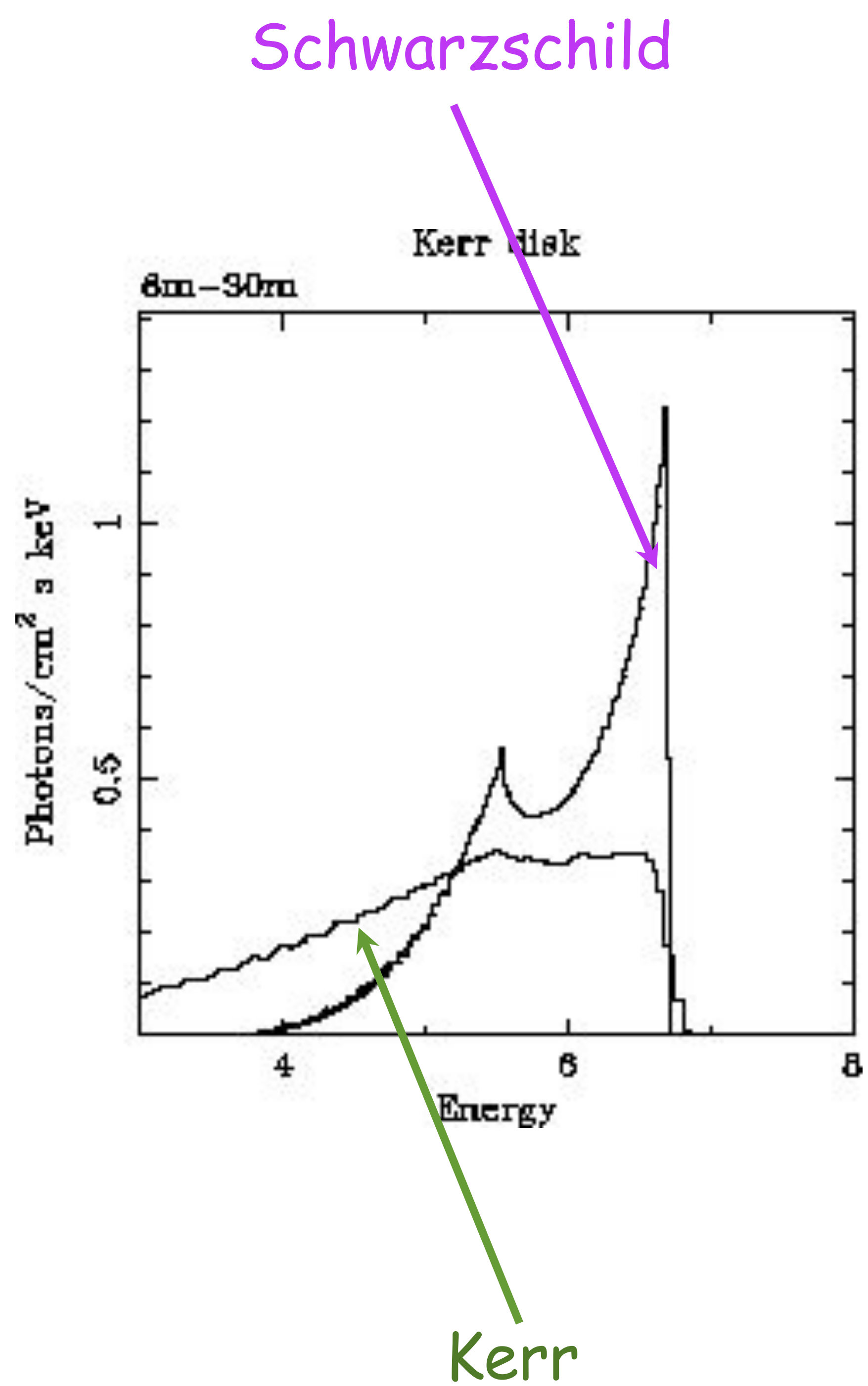
Schwarzschild
Kerr disk
6m–30m
Photons/cm^2 s keV
0.5
1
4
6
8
Energy
Kerr

Reflection

At low energies <10 keV the high-Z ions absorb the X-rays. A major part of the opacity above 7 keV is due to Fe K-edge opacity.

At high energies the Compton shift of the incident photons becomes important.

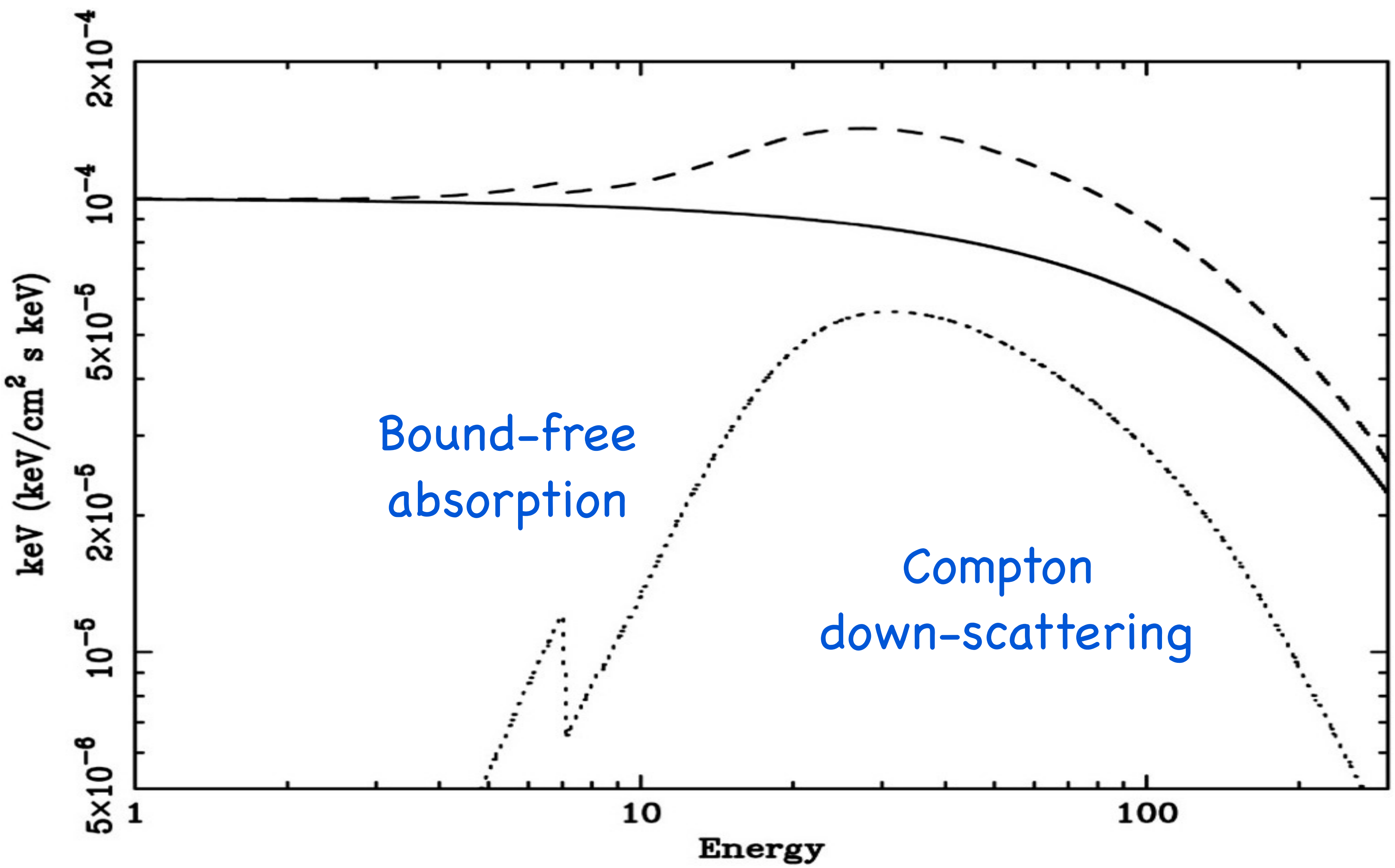

Inefficient Engine

Energy Equation

$$q^{+} = q^{-} + q^{adv}$$

Thin Accretion Disk

(Shakura & Sunyaev 1973;
Novikov & Thorne 1973;...)

Most of the viscous heat energy is radiated

$$q^{-} \approx q^{+} \gg q^{\rm adv}$$

$$L_{\rm rad} : \; 0.1\dot{M}c^{2}$$

Advection-Dominated Accretion Flow (ADAF)

(Ichimaru 1977; Narayan & Yi 1994, 1995; Abramowicz et al. 1995)

Most of the heat energy is retained in the gas

$$q^{-} \ll q^{+} \approx q^{\rm adv}$$

$$L_{\rm rad} \ll 0.1\dot{M}c^{2}$$

$$L_{\rm adv} : \; 0.1\dot{M}c^{2}$$

q+ is the energy generated by viscosity per unit volume
q- is the radiative cooling per unit volume
q_{adv} represents the advective transport of energy

$$L_{acc} = 2\eta GM\dot{M}/R = \eta\dot{M}c^{2}$$

ADAF

In this solution the accreting gas has a very low density and is unable to cool efficiently. The viscous energy is stored in the gas as thermal energy instead of being radiated and is advected onto the BH. Ions and electrons are thermally decoupled.

- Very Hot: Ti~ 10^{12}K (R_S/R), Te~ 10^{9-11}K (since ADAF loses very little heat).

- Geometrically thick: H~R (most of the viscosity generated energy is stored in the gas as internal energy rather than being radiated, the gas puffes up

- Optically thin (because of low density)

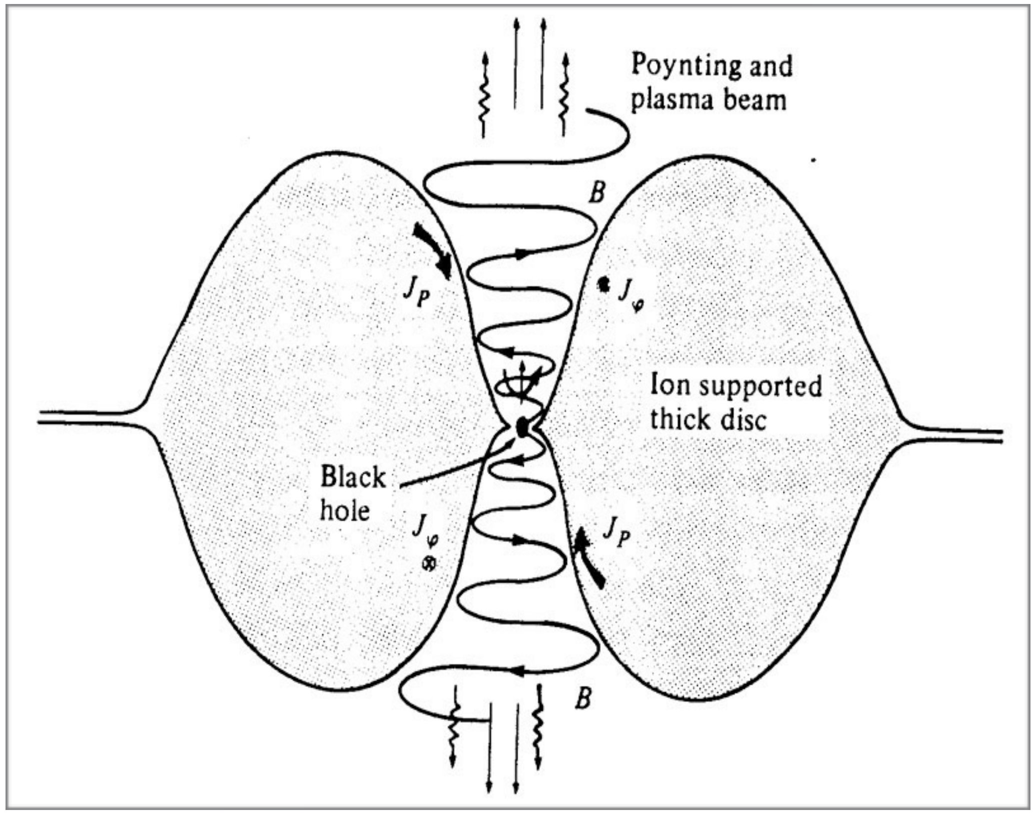

ADAF

Typical luminosities: **L <(0.01-0.1)L$_{Edd}$**

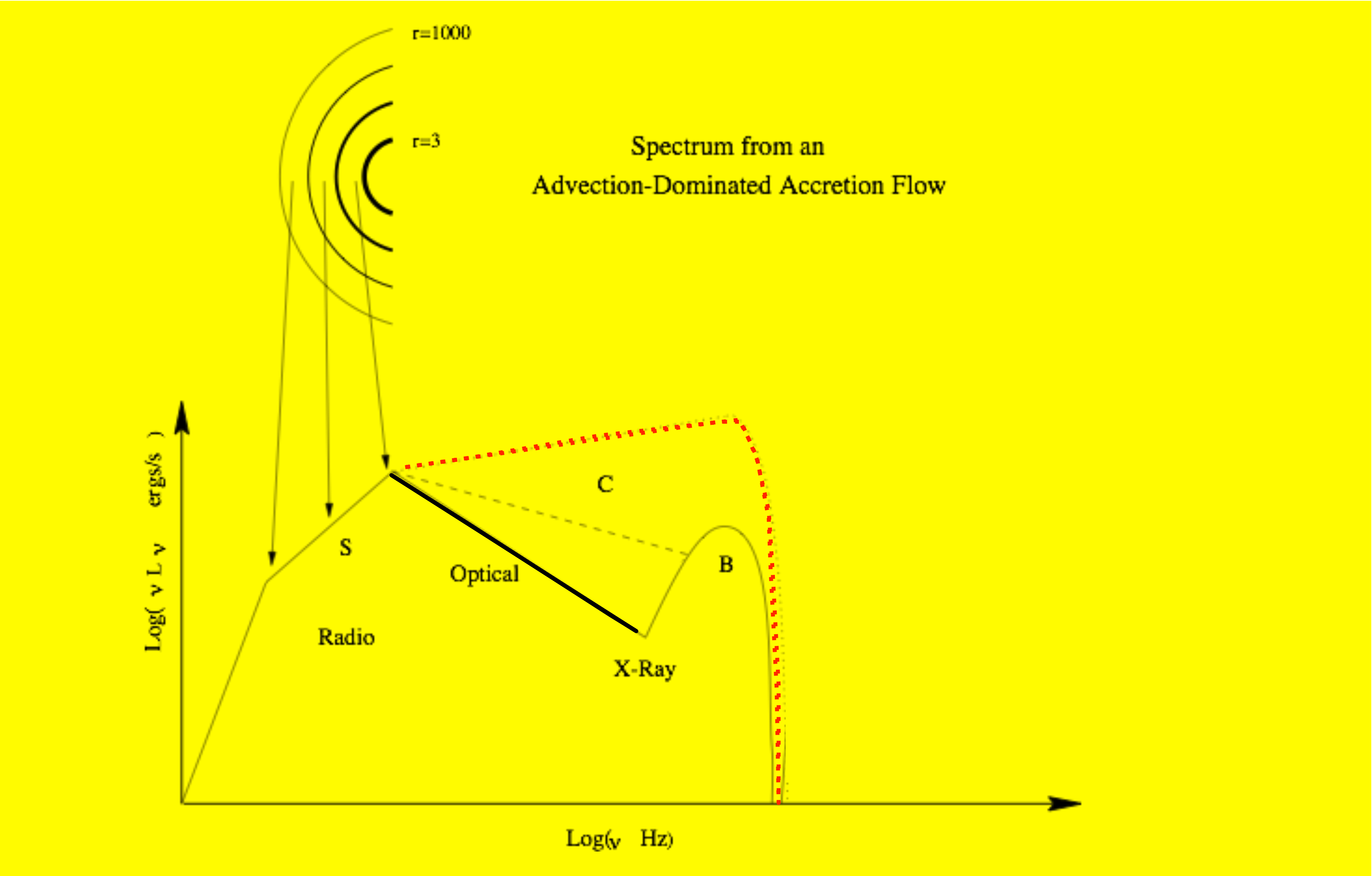

Schematic spectrum of an ADAF around a black hole. S, C, and B refer to electron emission by synchrotron radiation, inverse Compton scattering, and bremsstrahlung, respectively. The solid line corresponds to a low accretion, the dashed line to an intermediate accretion , and the dotted line to the highest (possible) accretion.


AGN radio loud more complex: JET

Jet can dominate all the electromagnetic spectrum

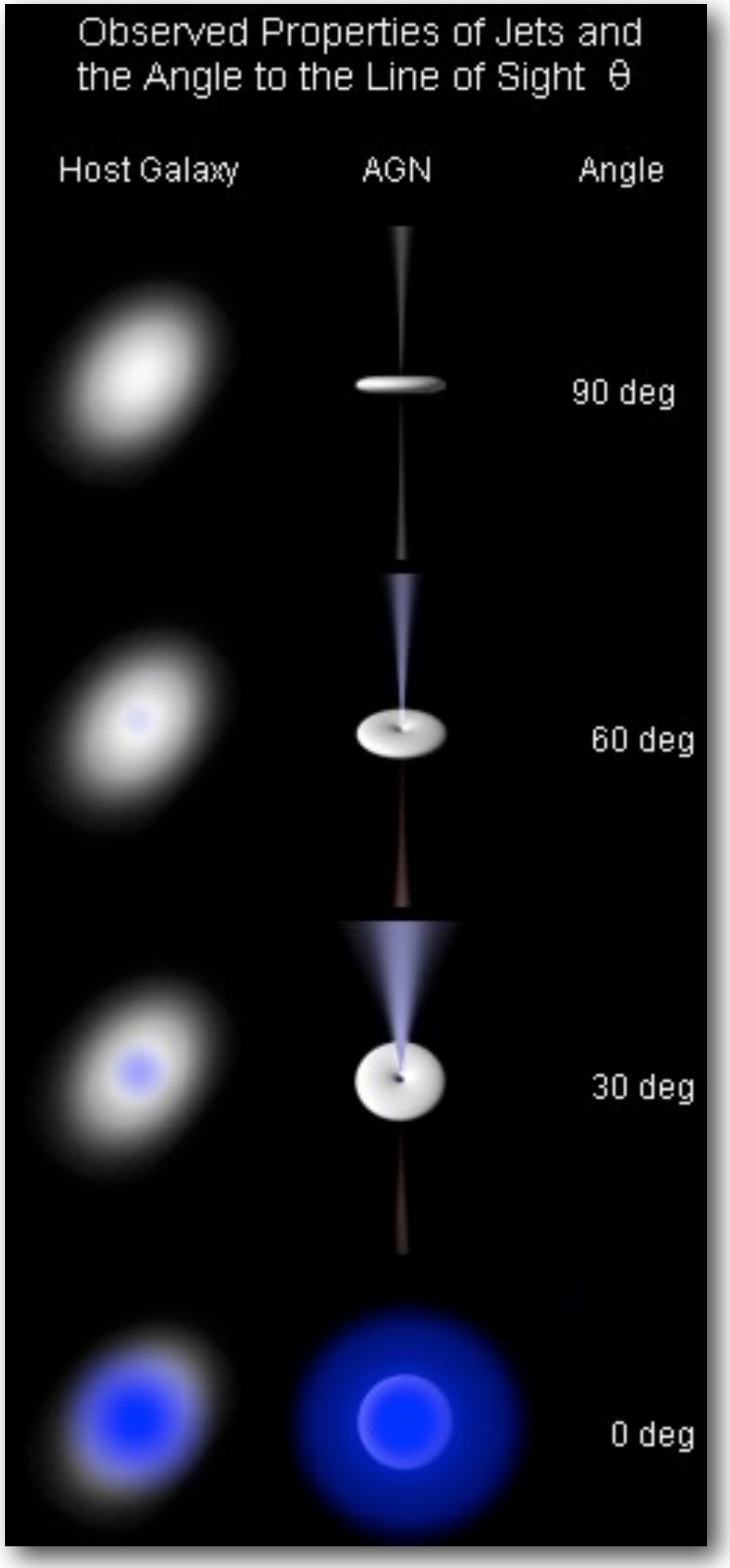

The jet emission is strongly Doppler boosted

The key parameter is the Doppler Factor $\delta(\beta, \theta)$

$$\delta = [\gamma(1 - \beta cos\theta)]^{-1}$$

Urry & Padovani 1995

$\gamma = \sqrt{(1-\beta^2)}$ Lorentz factor

β =v/c bulk velocity

θ angle between the jet axis and the line of sight

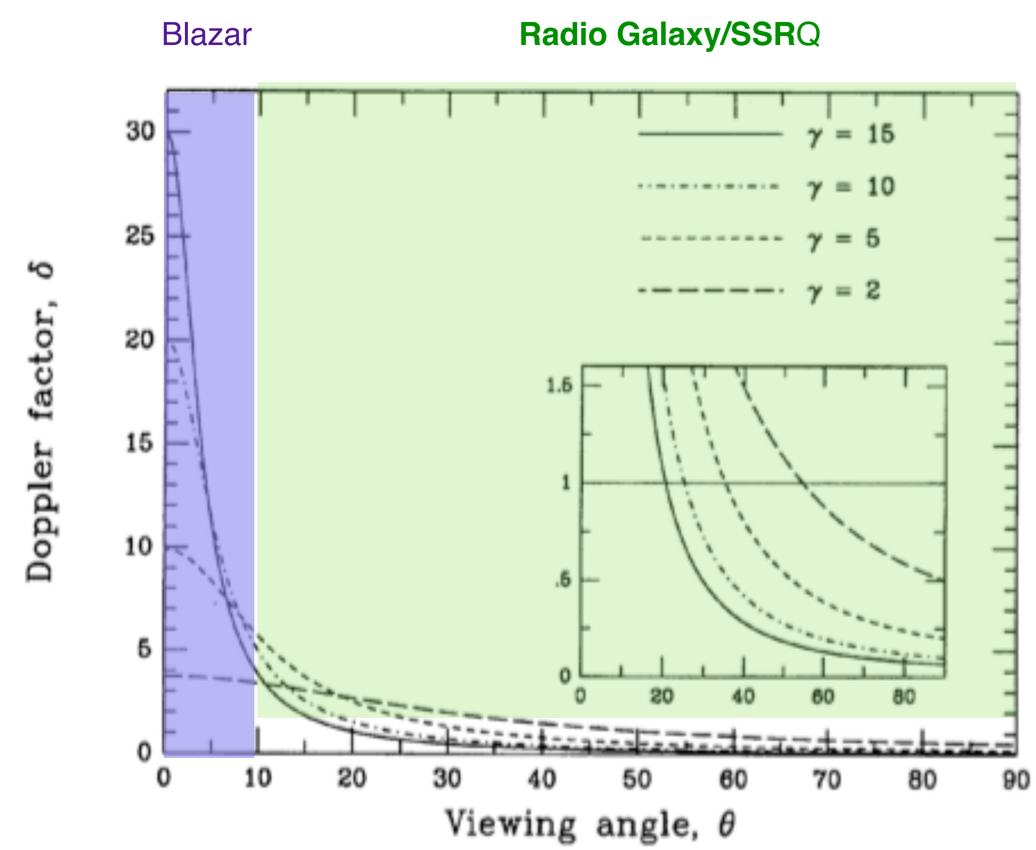

The Doppler factor relates intrinsic and observed flux for a moving source at relativistic speed v=β c.

For an **intrinsic** power law spectrum: $F'(\nu') = K (\nu')^{-\alpha}$
the **observed** flux density is

$$F_\nu(\nu) = \delta^{3+\alpha} F'_{\nu'}(\nu)$$

$$\Delta t = \Delta t' / \delta$$

When the jet is the dominant component: AGN are classified as BL LAC or Flat Spectrum Radio Quasars

LERG

HERG

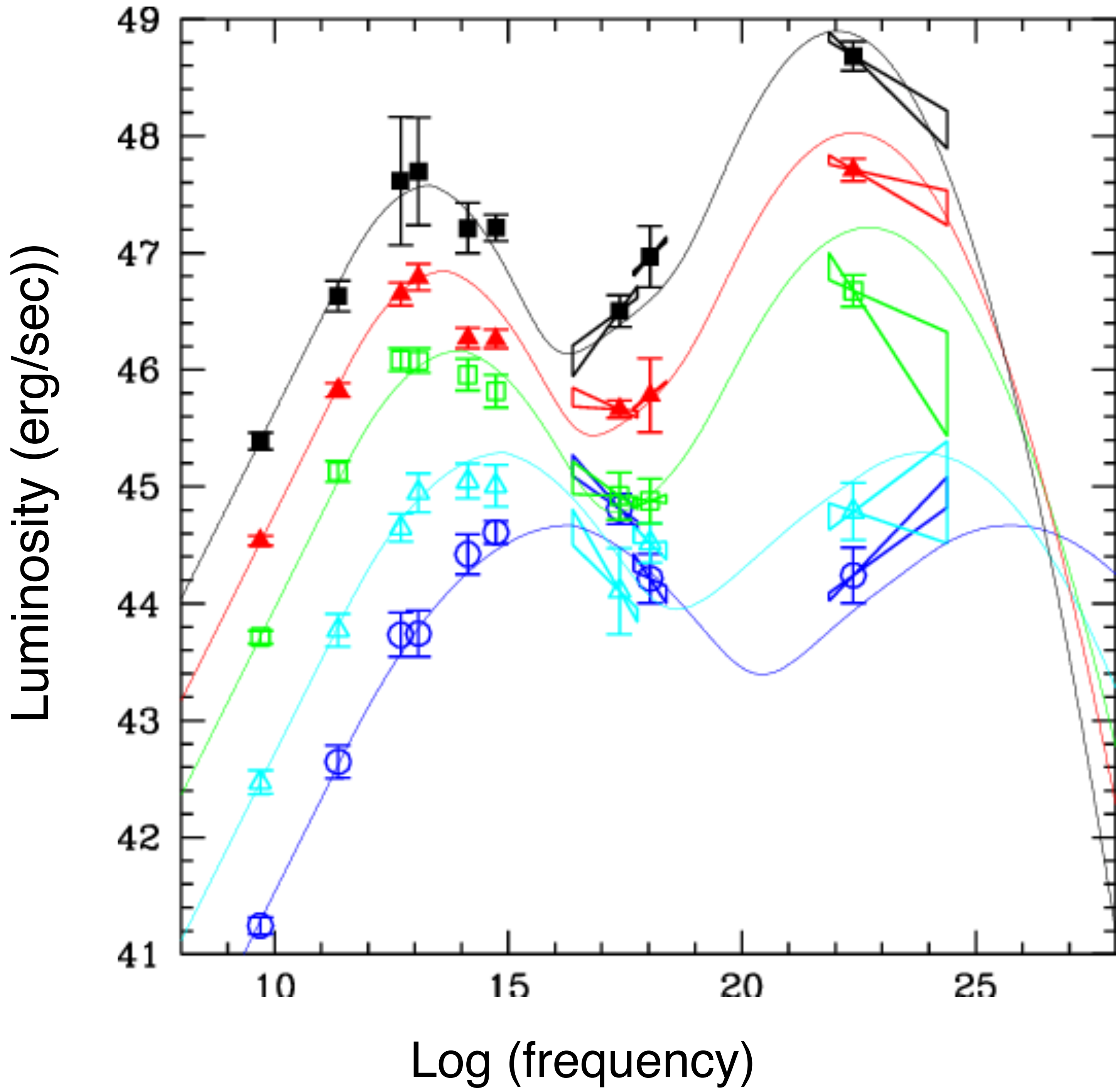

double peaked SED

(Fossati et al. 1998)

Blazars: BL Lacs (BL) and Flat Spectrum Radio Quasar (FSRQ)

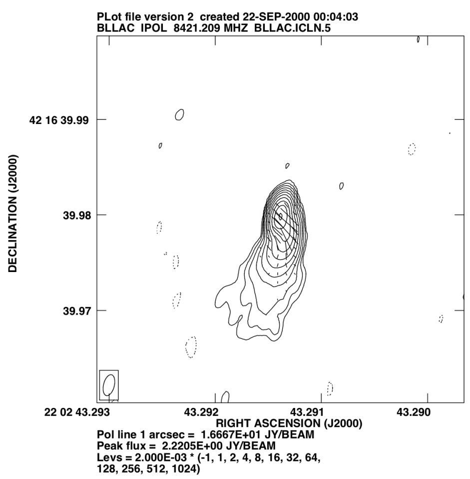

Compact in radio

Extremely variable

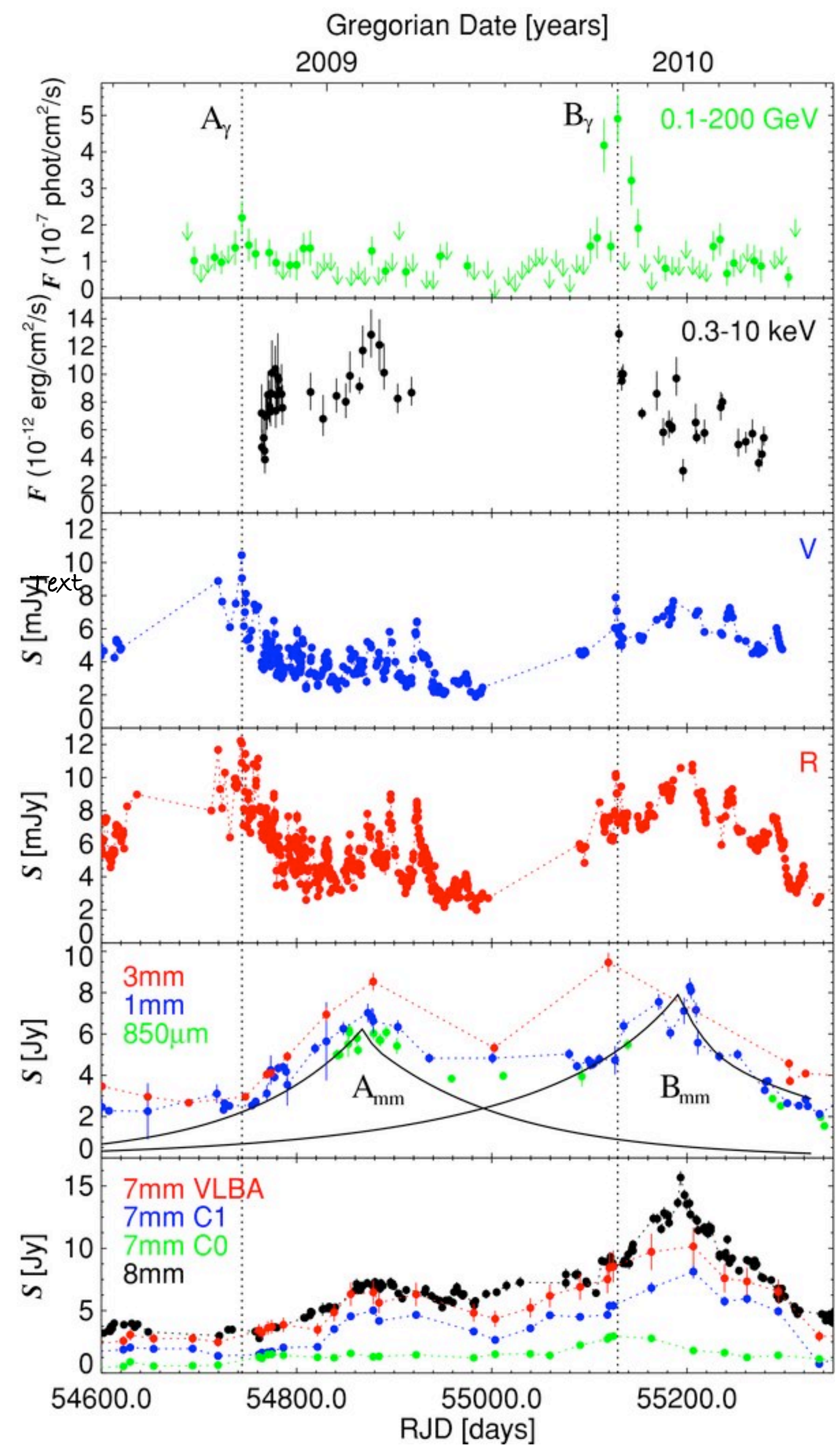

OJ 287 light curves from radio to gamma
Agudo et al. 2011ApJL 726, L13

BL are almost featureless in the optical band (FSRQ can show emission lines overimposed on a strong continuum)

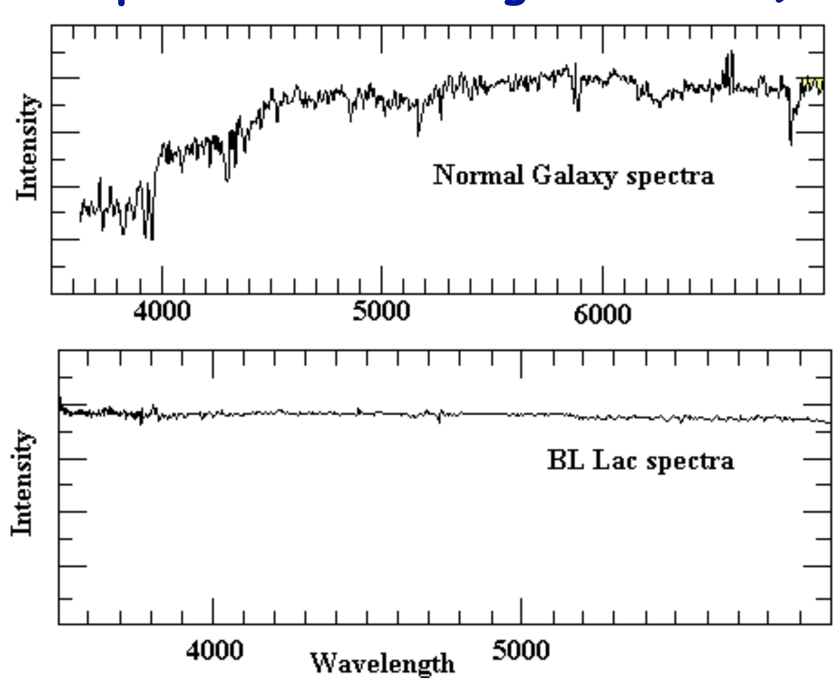

BLAZARS: double peaked SED

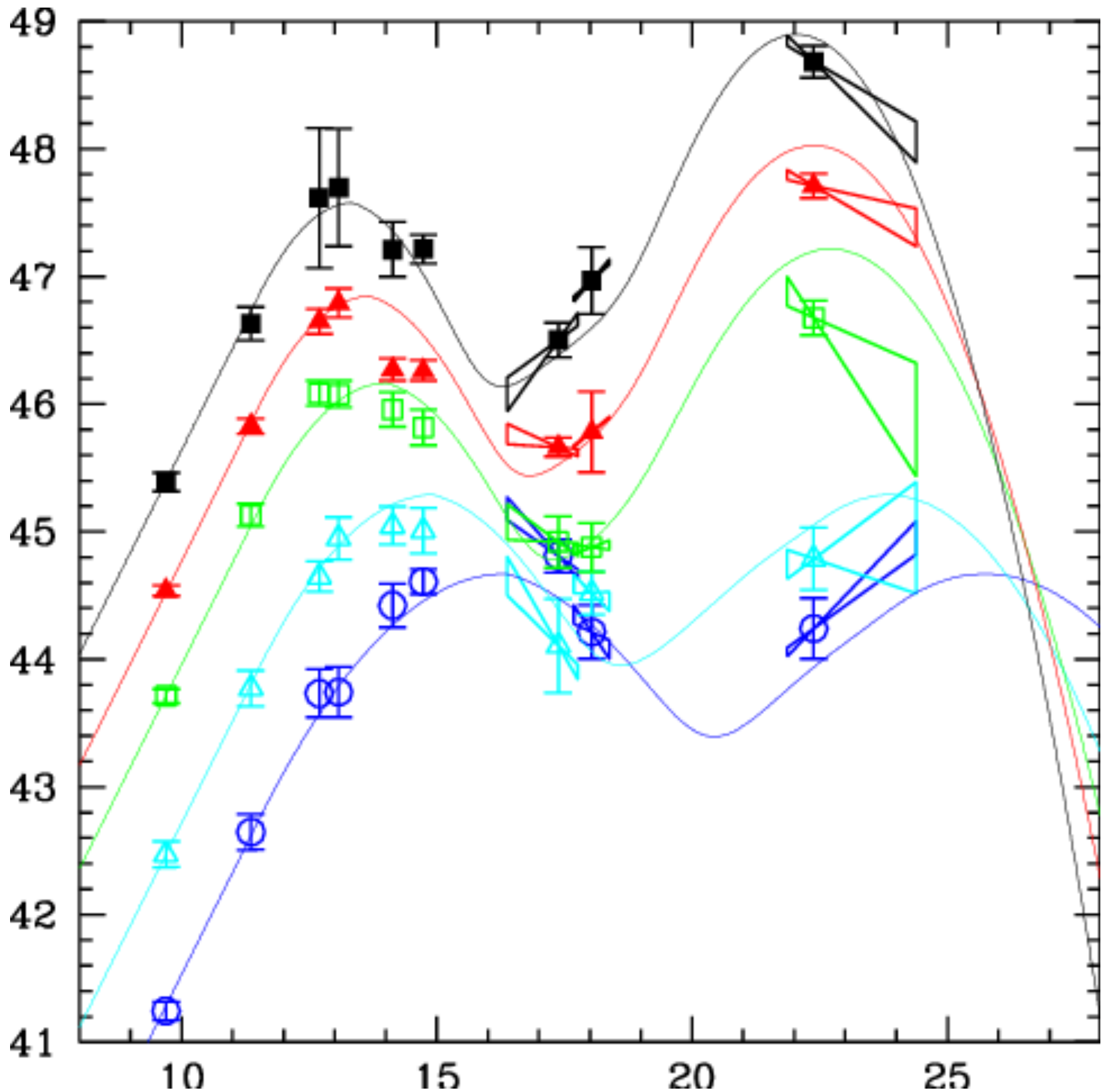

Synchrotron Radiation

Synchrotron radiation is due to the movement of an electron charge in a magnetic field. As a particle gyrates around a magnetic field, it will emit radiation at a frequency proportional to the strength of the magnetic field and its velocity.

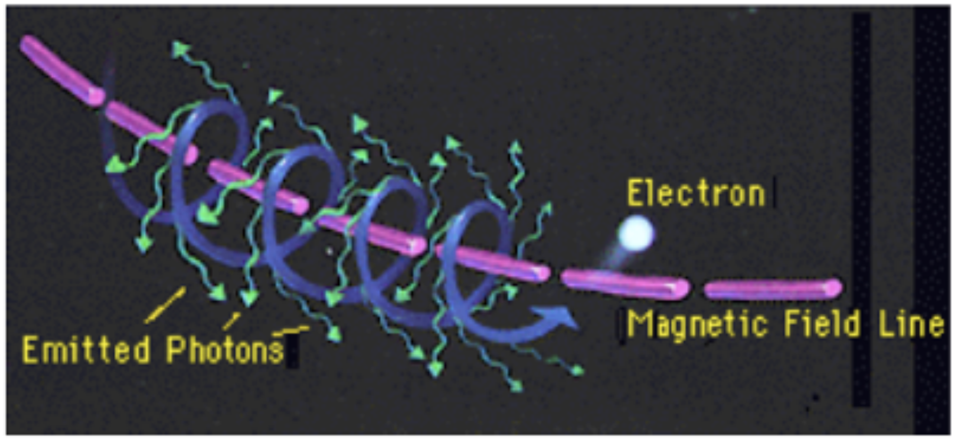

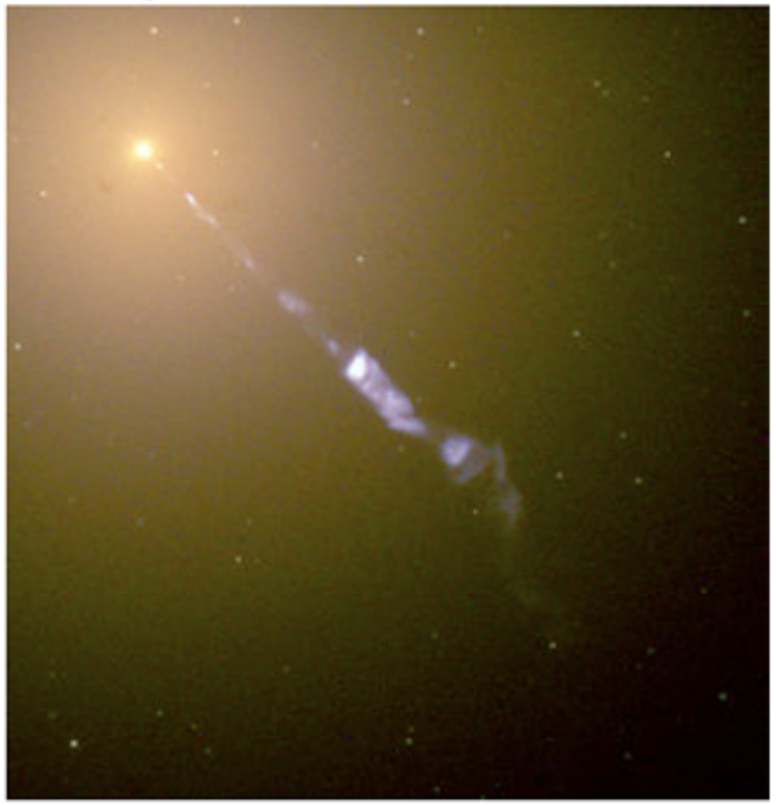

Synchrotron radiation is highly polarized and is seen at all wavelengths. At relativistic speeds, the radiation can also be beamed. It is very common in radio spectrum, but can be seen in x-rays. It is usually fit as a power law. For full details, see the review by Ginzburg & Syrovatskii (1969)

The synchrotron radiation of a power law distribution of electron energies

Synchrotron

$$N(\gamma_e) = K\gamma_e^{-p}, \quad \gamma_{min} < \gamma_e < \gamma_{max}, \; p = 1 + 2\alpha$$

$$\epsilon_{sin}(\nu) \propto K B^{\alpha+1} \nu^{-\alpha} \quad \text{erg cm}^{-3}\,\text{s}^{-1}\,\text{sr}^{-1}$$

Inverse Compton Radiation

The general result that the frequency of the scattered photons is $\nu \approx \gamma^2 \nu_0$ is of profound importance in high energy astrophysics. We know that there are electrons with Lorentz factors $\gamma \sim 100 - 1000$ in various types of astronomical source and consequently they scatter any low energy photons to very much higher energies. Consider the scattering of radio, infrared and optical photons scattered by electrons with $\gamma = 1000$.

Waveband	*Frequency (Hz)* ν_0	*Scattered Frequency (Hz) and Waveband*
Radio	10^9	$10^{15} =$ UV
Far-infrared	3×10^{12}	$3 \times 10^{18} =$ X-rays
Optical	4×10^{14}	$4 \times 10^{21} \equiv 1.6\text{MeV} = \gamma$-rays

Thus, inverse Compton scattering is a means of creating very high energy photons indeed. It also becomes an inevitable drain of energy for high energy electrons whenever they pass through a region in which there is a large energy density of photons.

Inverse Compton scattering

When the electron is not at rest, but has an energy greater that the typical photon energy, there can be a transfer of energy from the electron to the photon. This process is called Inverse Compton to distinguish it from the direct Compton scattering, in which the electron is at rest, and it is the photon to give part of its energy to the electron.

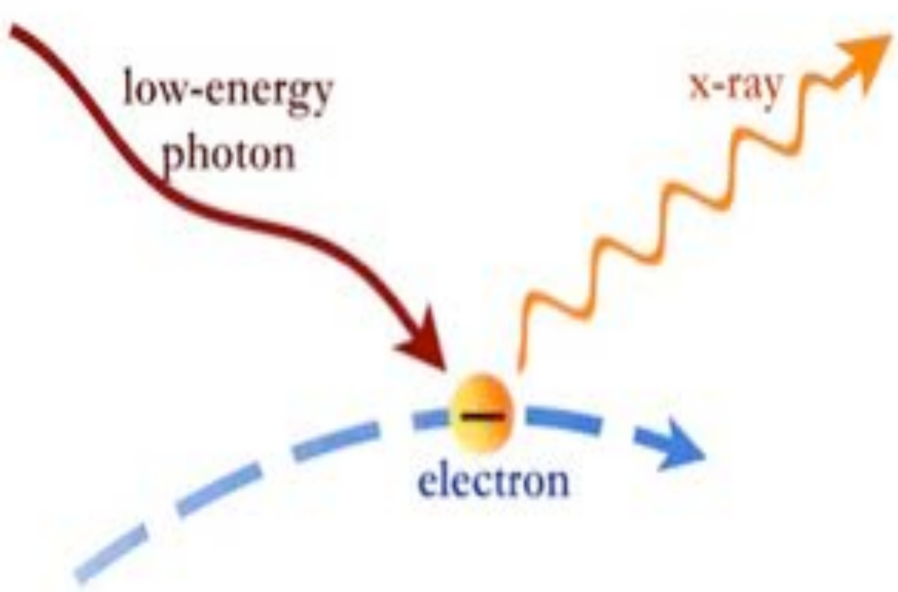

$$< \nu >= \frac{4}{3}\gamma^2\nu$$

Inverse Compton

For a power law distribution of electrons:

$$N(\gamma_e) = K\gamma_e^{-p}, \quad \gamma_{min} < \gamma_e < \gamma_{max}, \; p = 1 + 2\alpha$$

Inverse Compton

$$\epsilon_c(\nu_c) \propto K\nu_c^{-\alpha} \int \frac{Ur(\nu)\nu^{\alpha}}{\nu} d\nu$$ erg cm^{-3} s^{-1} sr^{-1}

U_r is the radiation energy density

$$U_r = \int n(\epsilon)\epsilon d\epsilon$$

- Synchrotron photons in the jet
- Environment photons from Accretion Flow, BLR, NLR, Torus
- Cosmic Microwave Background (CMB) photons

Synchrotron Self–Compton

Consider a population of relativistic electrons in a magnetized region. They will produce synchrotron radiation, and therefore they will fill the region with photons. These synchrotron photons will have some probability to interact again with the electrons, by the Inverse Compton process. Since the electron "work twice" (first making synchrotron radiation, then scattering it at higher energies) this particular kind of process is called synchrotron self-Compton, or SSC for short.

External Compton

The population of relativistic electrons in a magnetized region can also interact with photons externa to the jet produced in the accretion disk, in the broad/narrow line regions in the torus. This particular kind of process is called External Compton, or EC for short.

- Self Synchrotron Model

U(r) are synchrotron photons in the jet.

- Synchrotron photons in the jet
- Environment photons from Accretion Flow, BLR, NLR, Torus

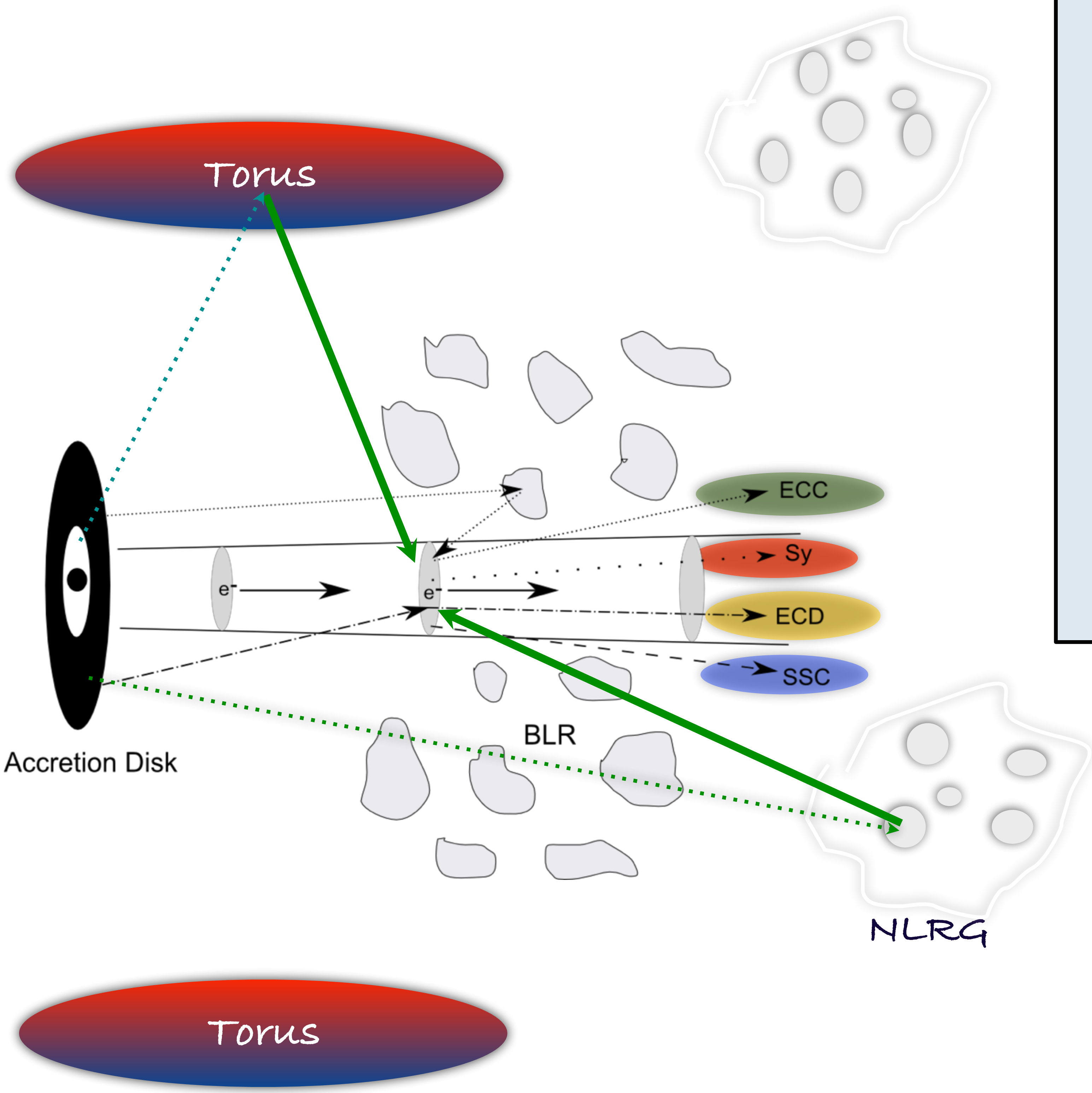

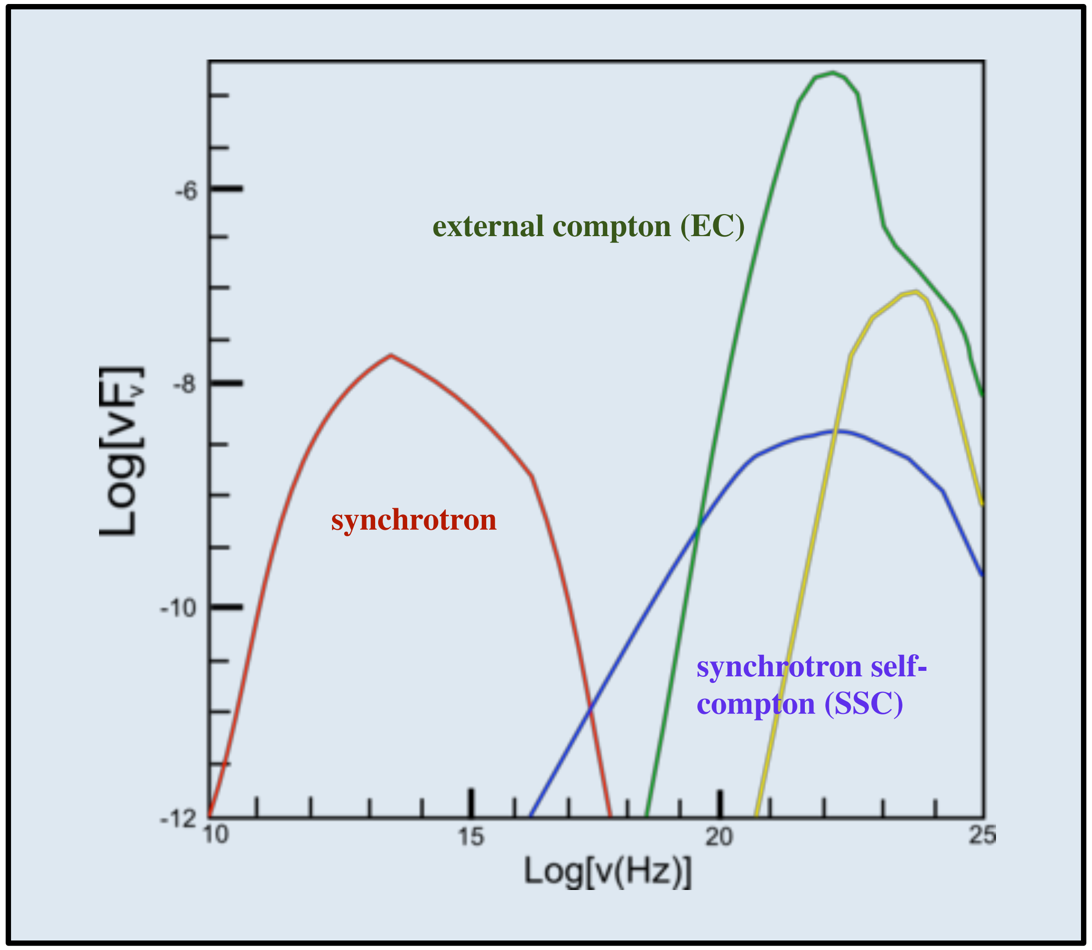

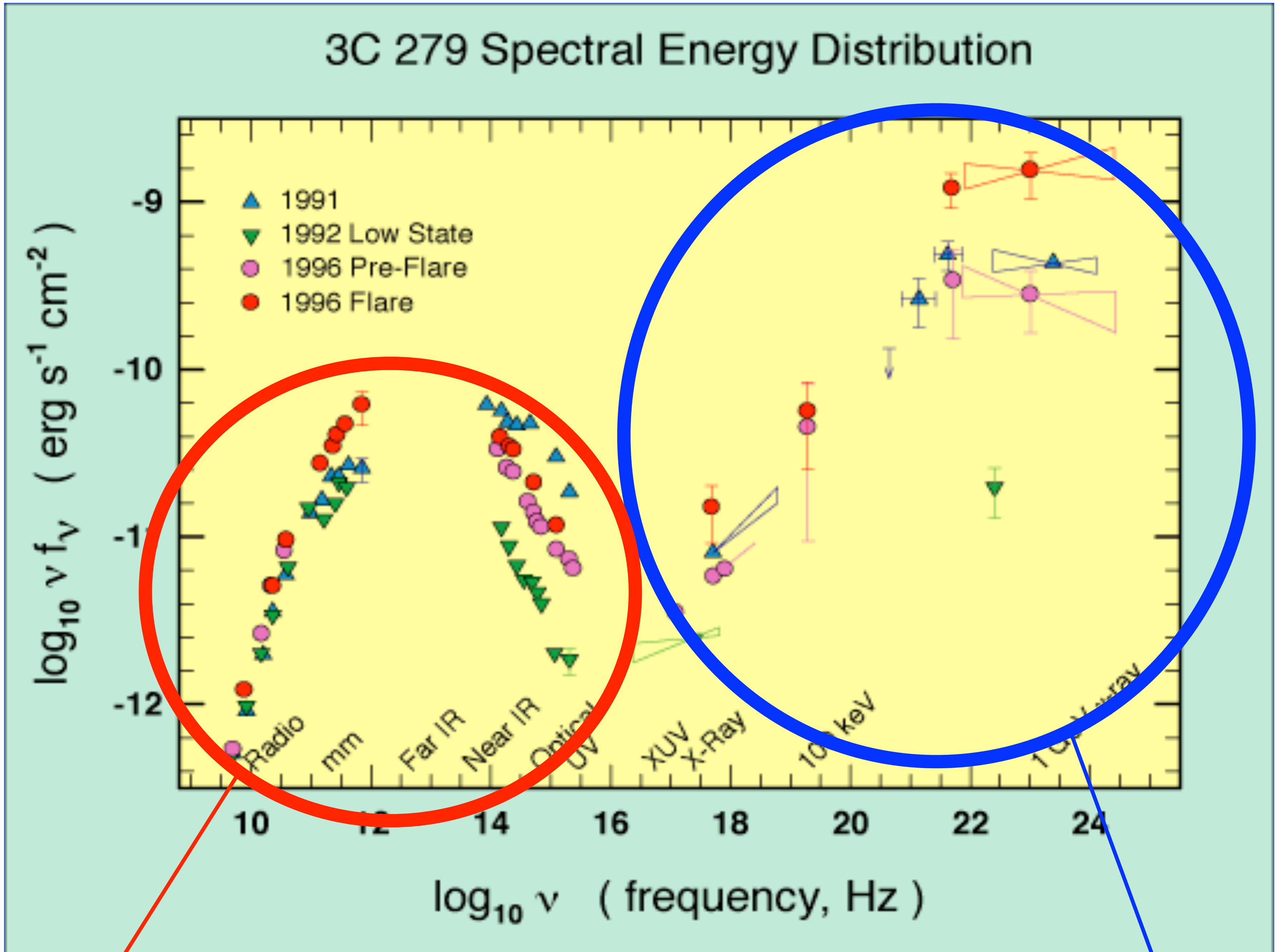

Synchrotron

Inverse Compton

Revised AGN Unified Model

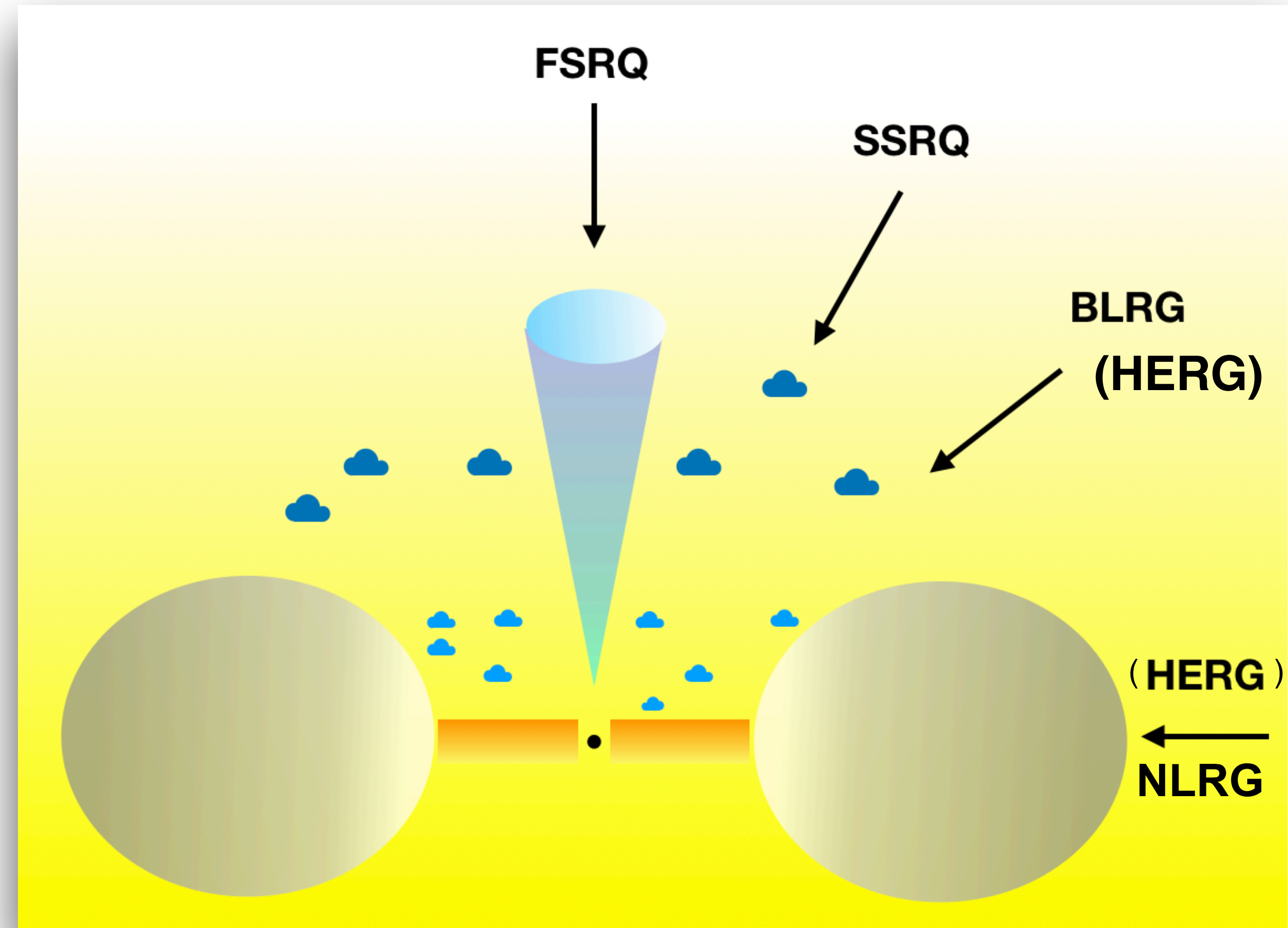

Efficient Accretion
DISK

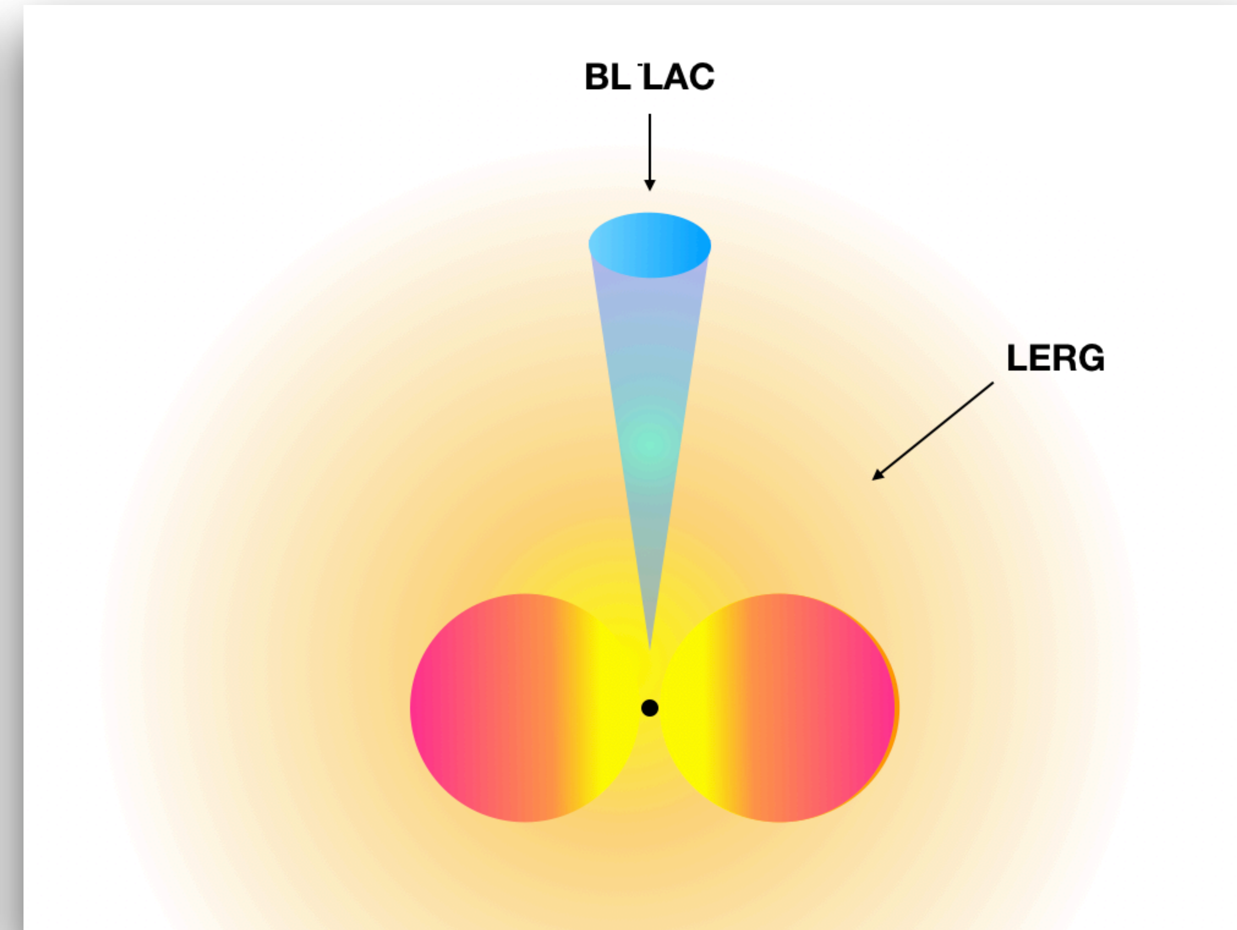

Inefficient flow
ADAF

Radio Loud AGN in the X-ray band

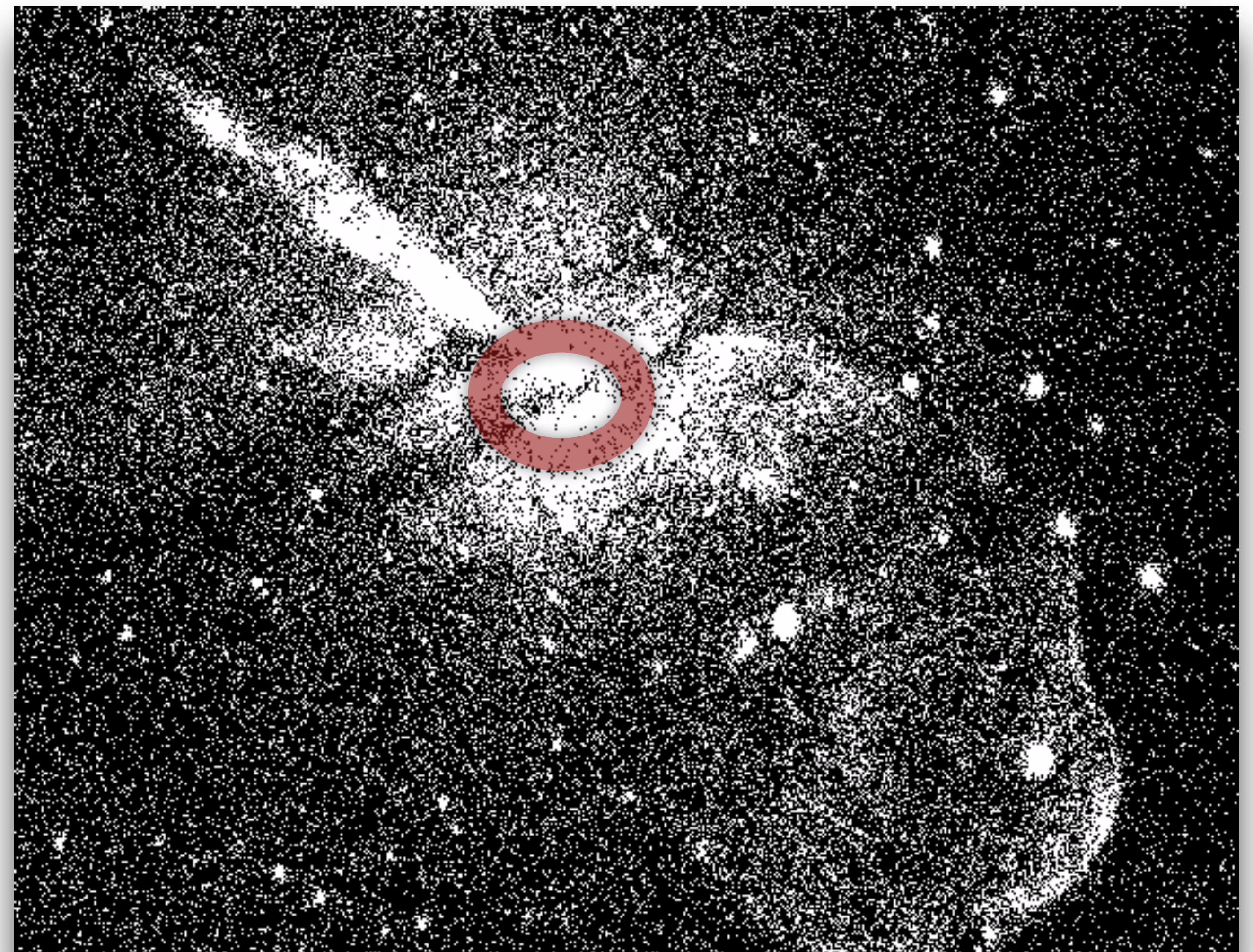

CORE

While in LERG jet is always the dominant component, in HERG jet and disk emission are in competition

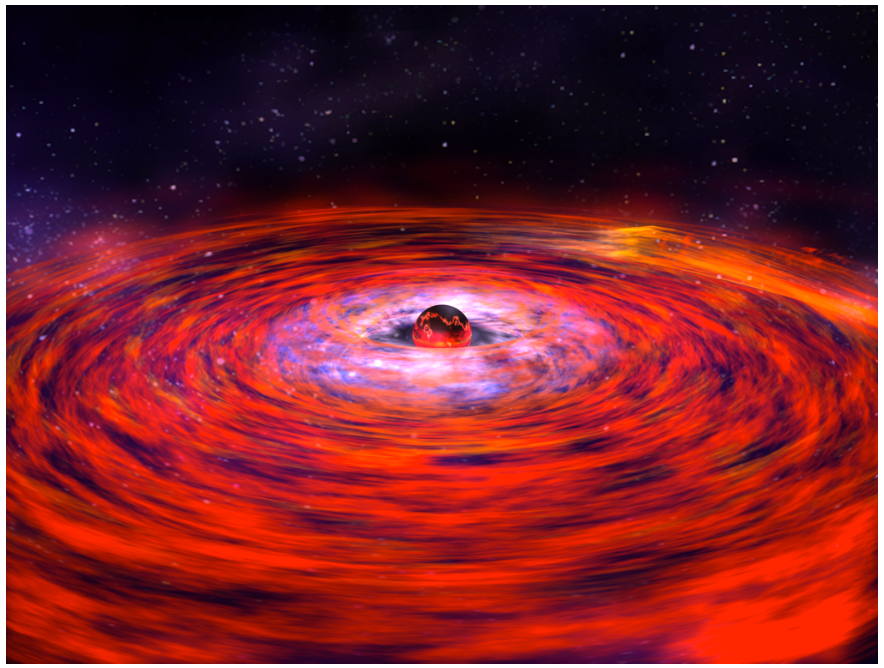

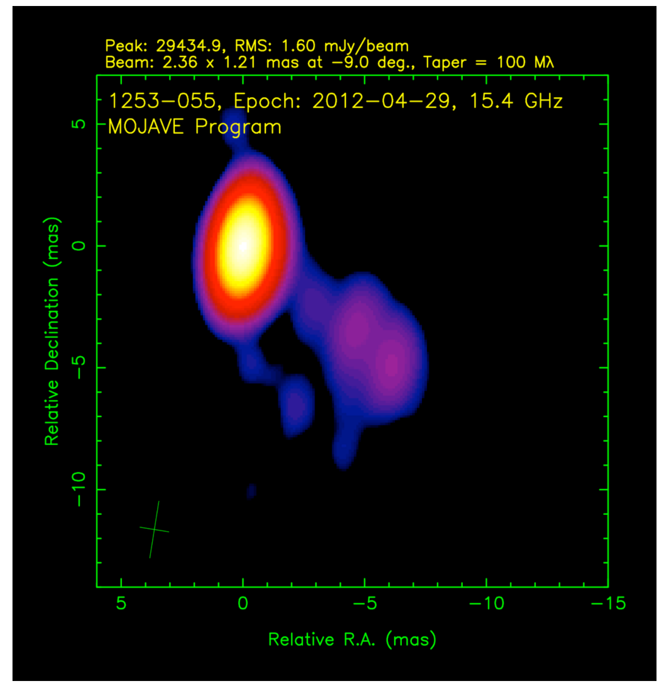

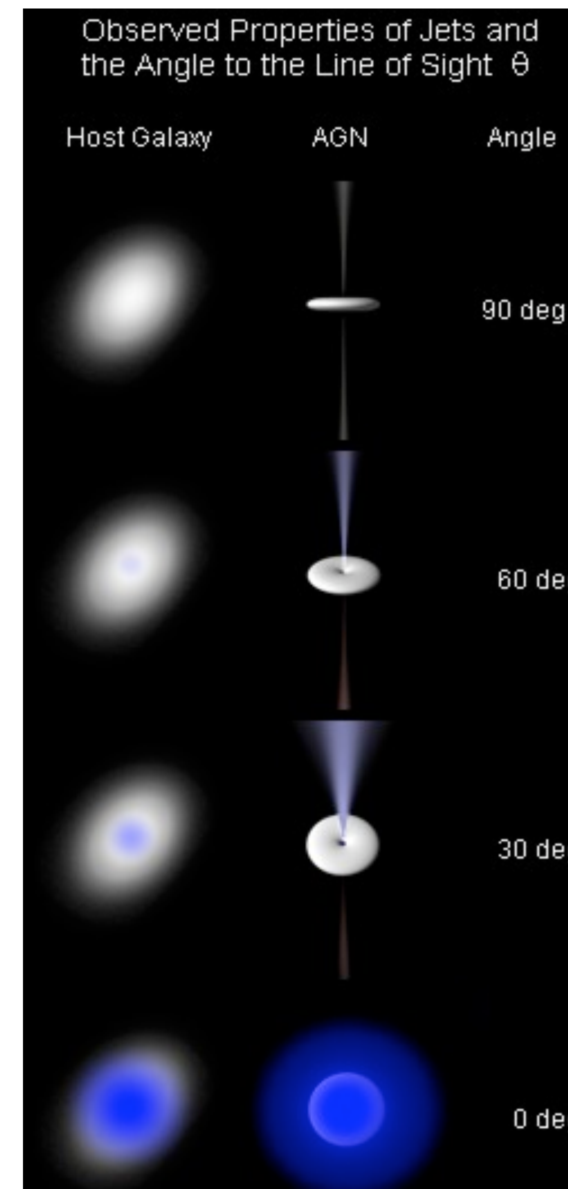

X-ray Spectra:Accretion Disk and pc-scale Jet emission are in competion:

Angle of sight = 0° ==> Jet radiation dominates

Angle of sight = 90° ==> Accretion disk dominates

Jet is the dominant component:
Only a power law

Accretion is dominant
and iron line emerges

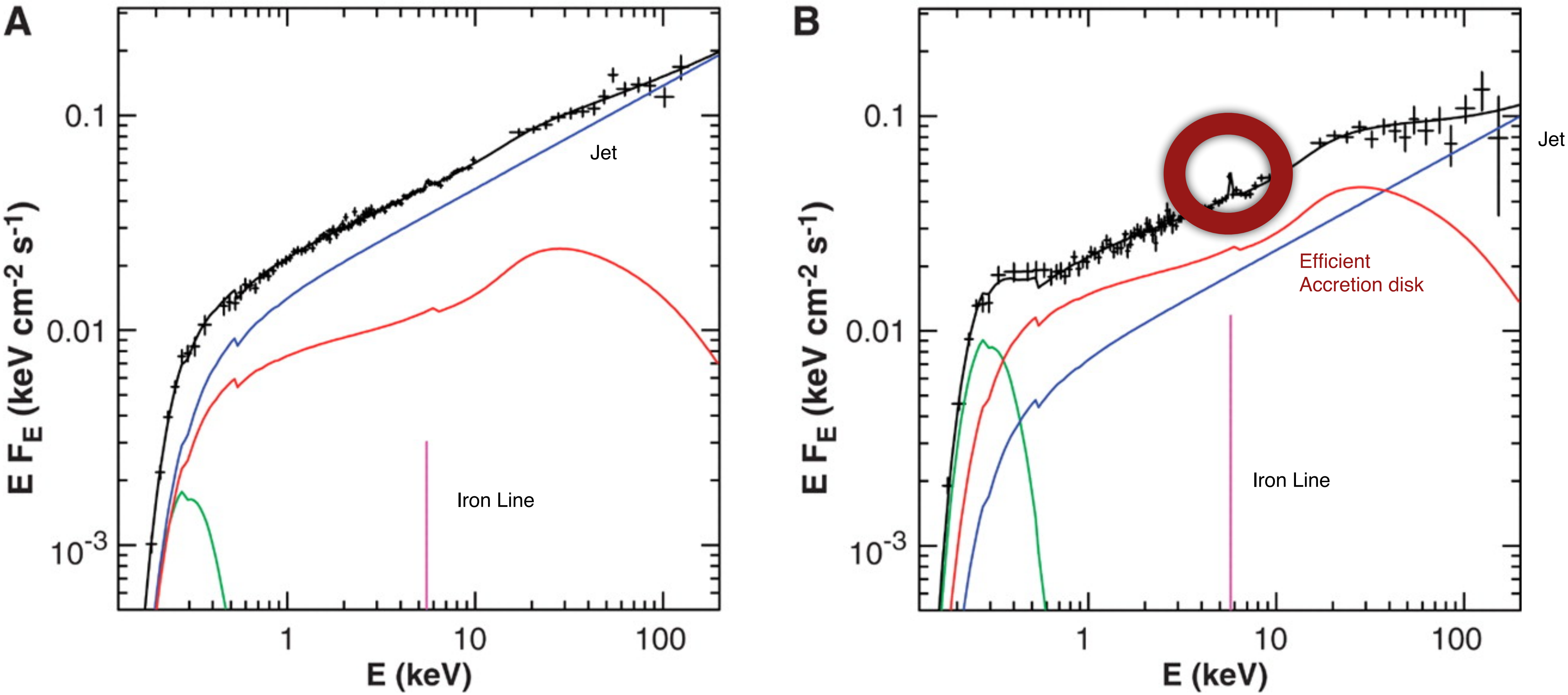

The case of 3C273

In radio galaxies the jet is pointed away from the observer, extended structure can be observed

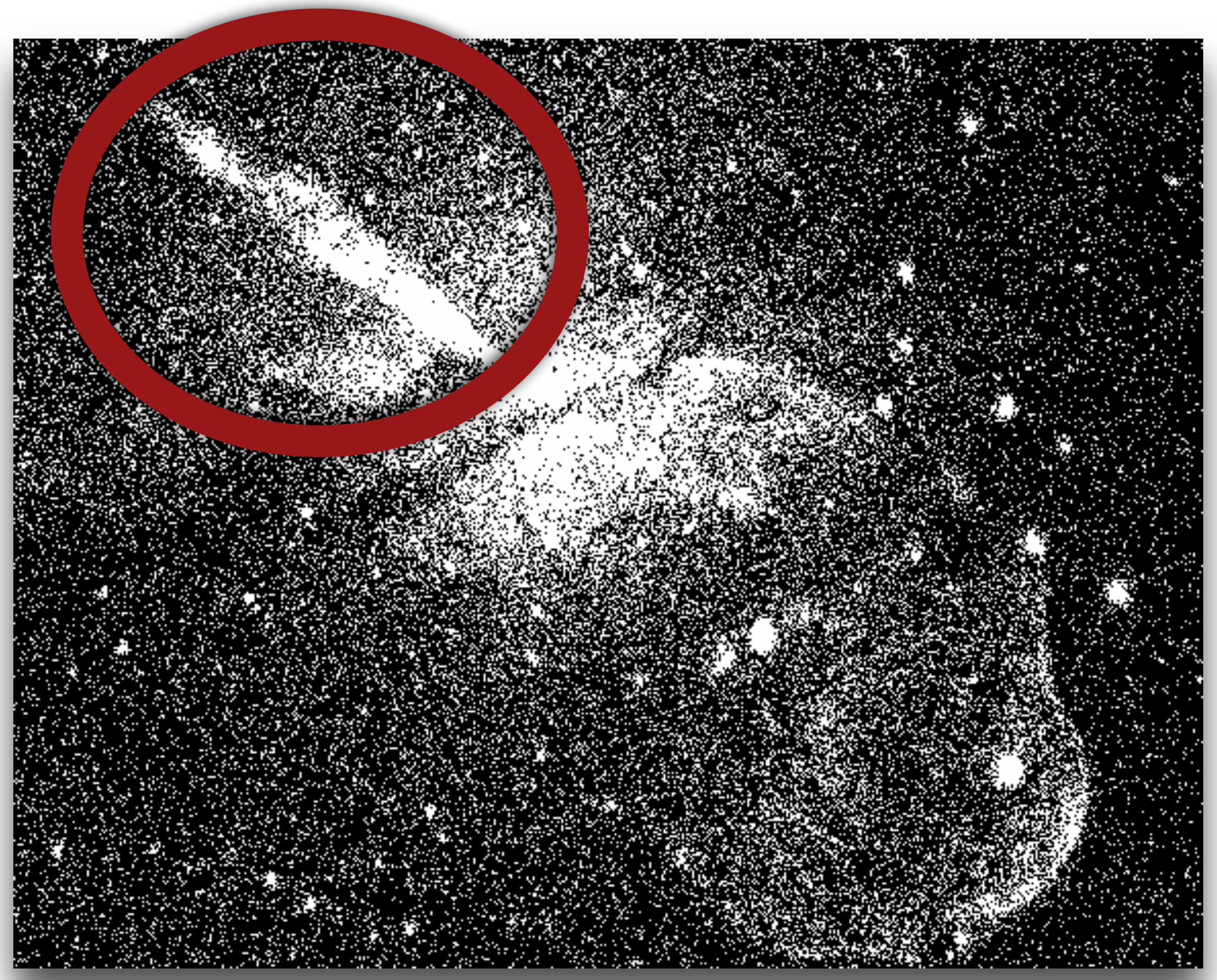

Jet at kpc scales

Kpc Jet

Synchrotron process

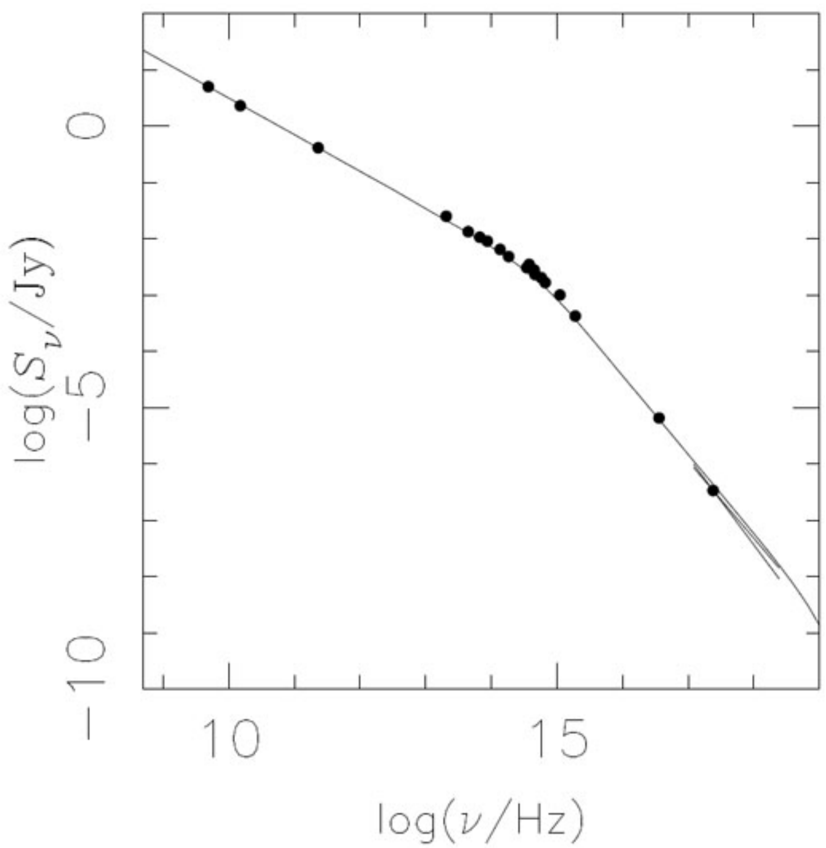

FRI-LERG

For low-luminosity (FRI) radio sources, there is strong support for the synchrotron process as the dominant emission mechanism for the X-rays, optical, and radio emissions

FRII sources require multi-zone synchrotron models, or synchrotron and IC models (seed photons: CMB). (Harris & Krawczynski, 2002)

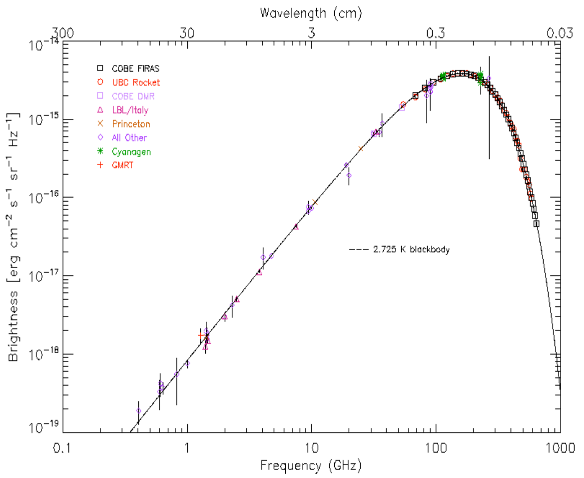

FRI-LERG

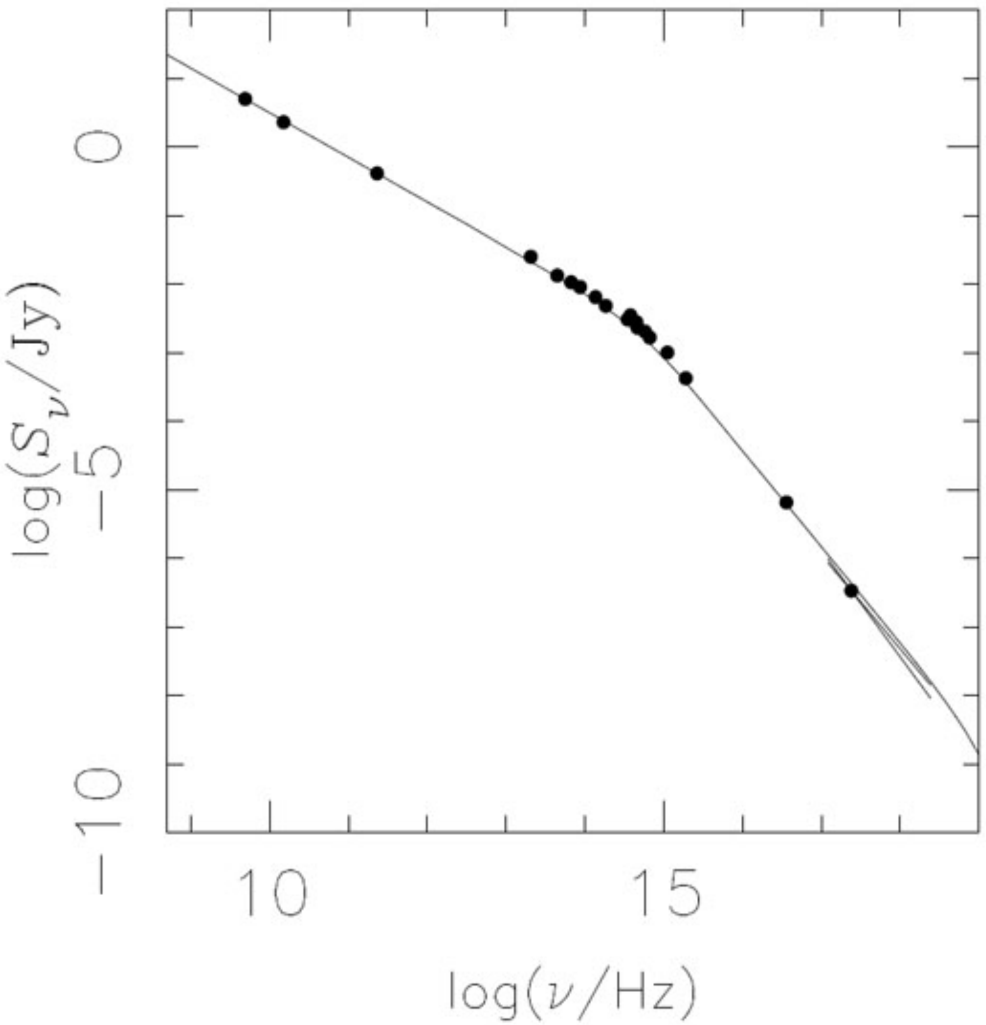

FRII-HERG

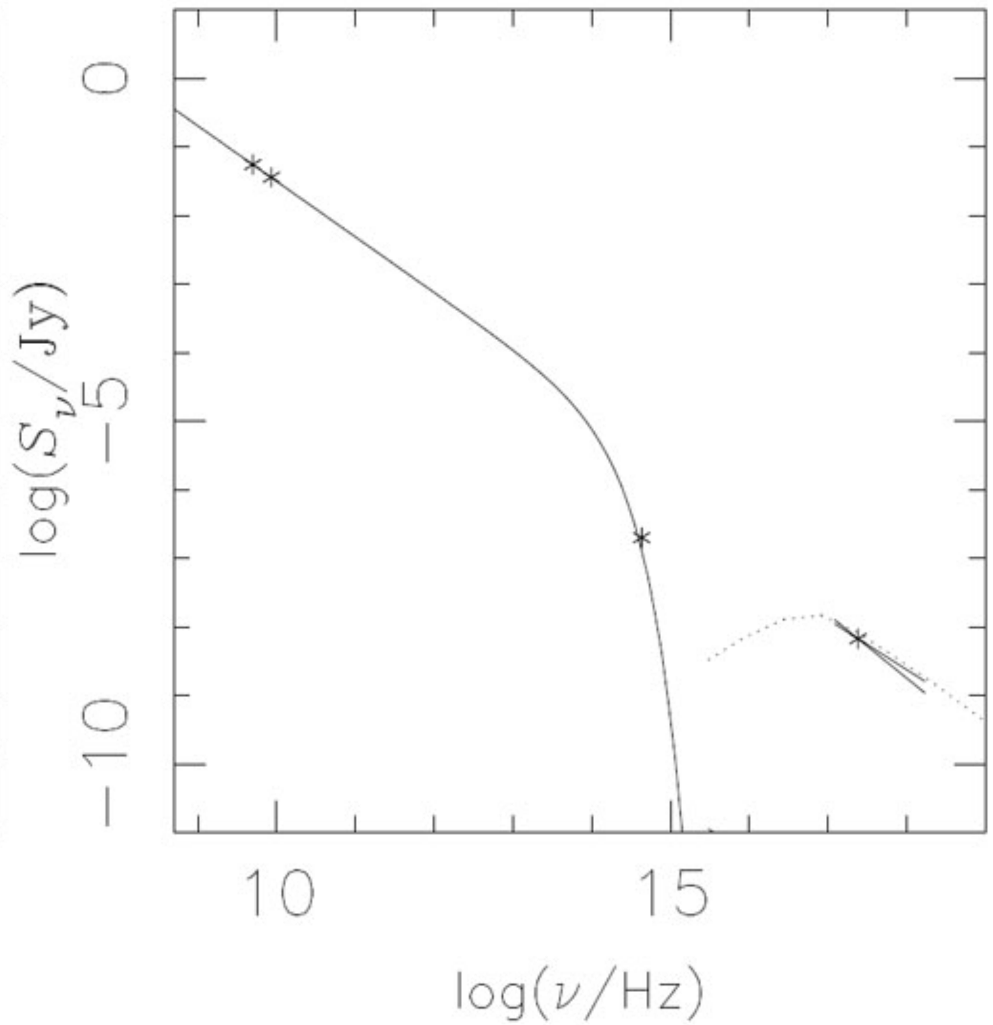

In radio galaxies the jet is pointed away from the observer, extended structure can be observed

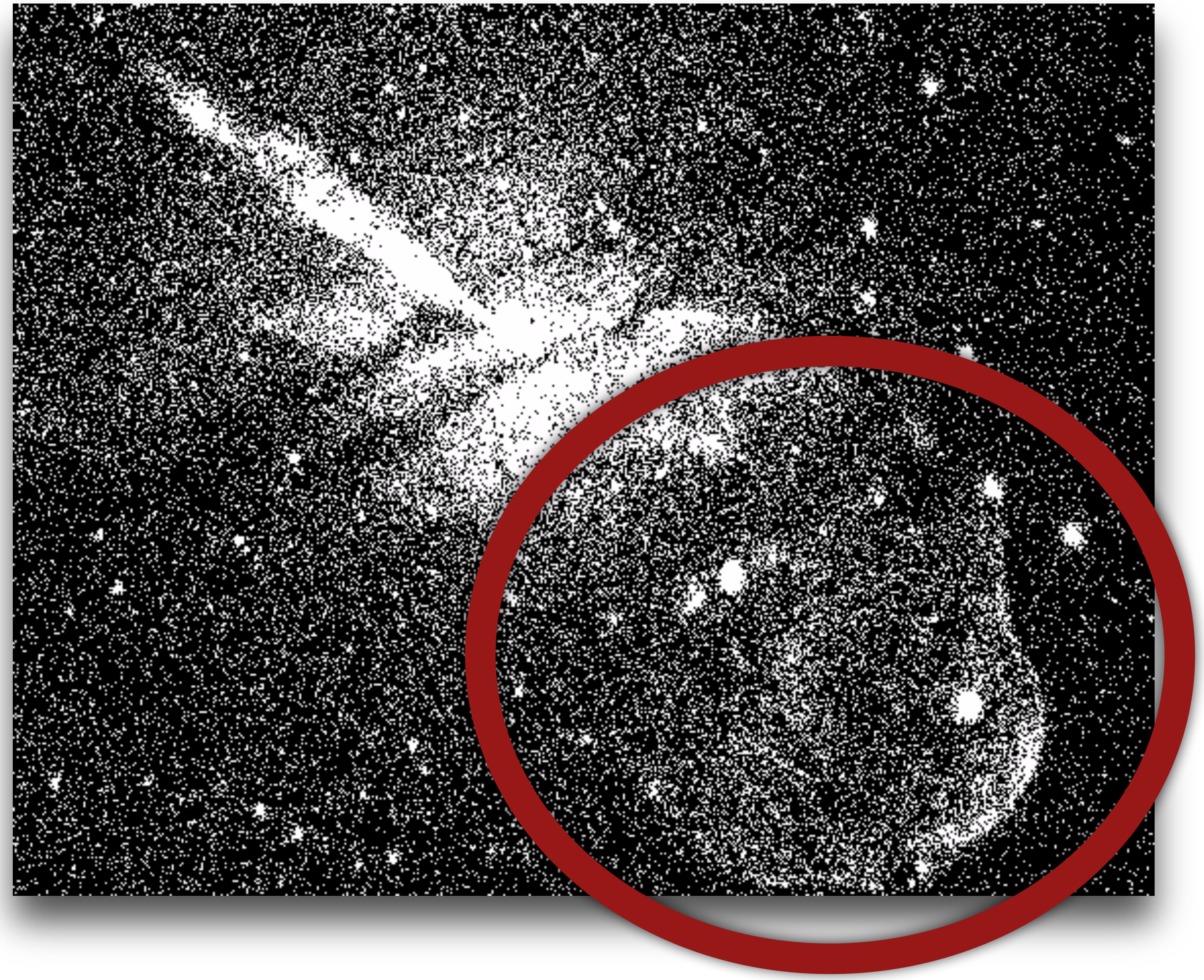

Lobes

Lobes

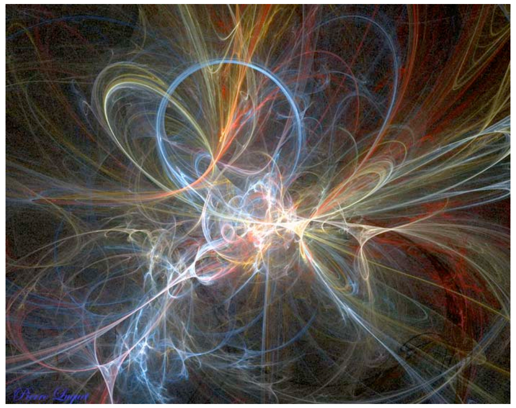

relativistic electrons

+

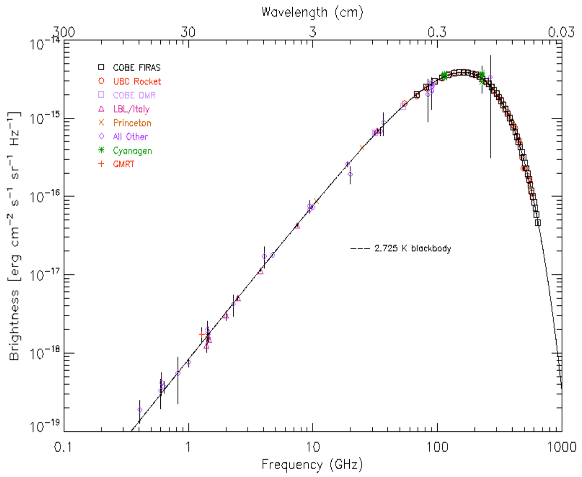

CMB

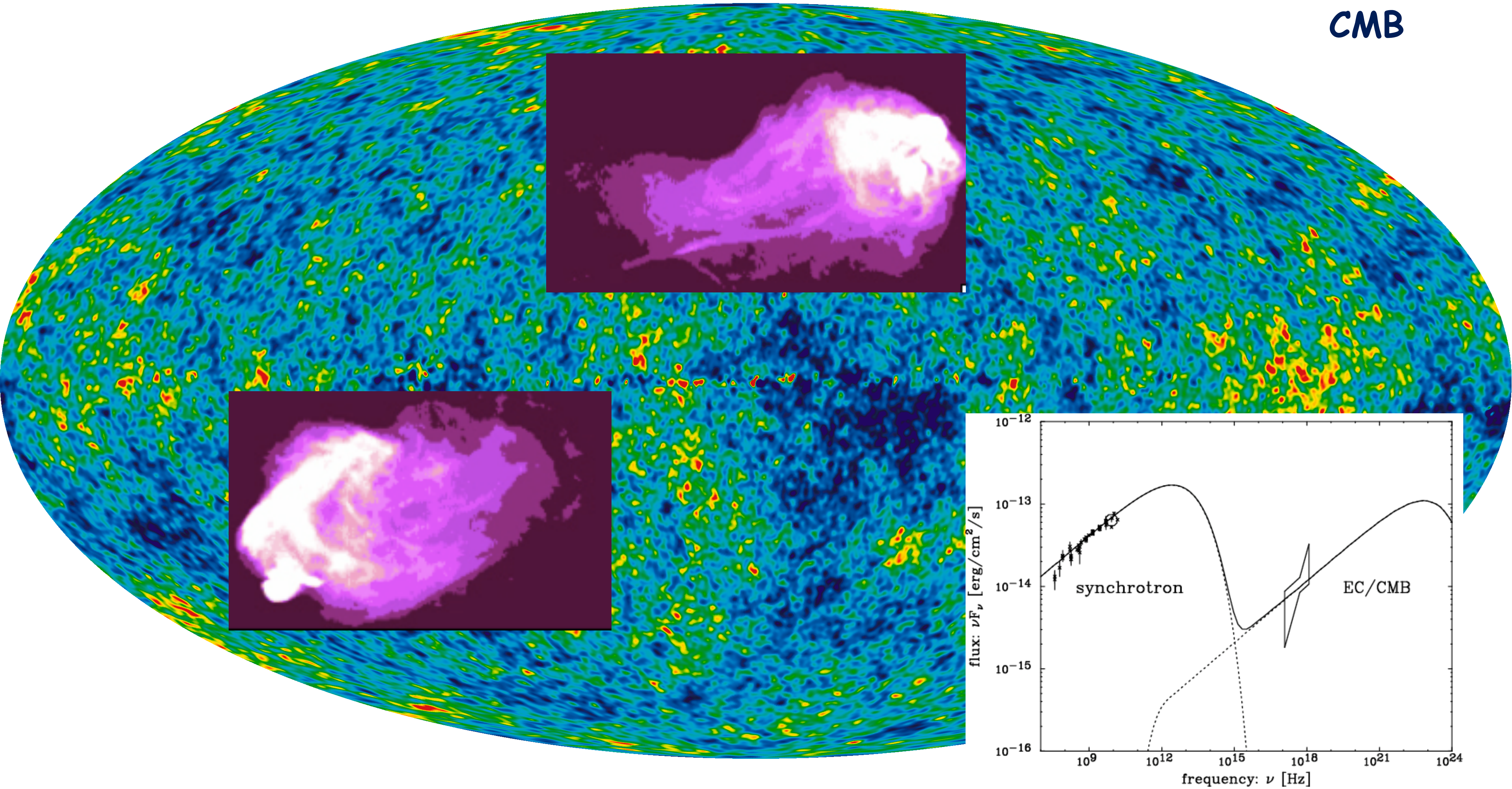

Calcolo del Campo Magnetico

Equipartition

$$W_{\text{total}} = G(\alpha)\eta L_\nu B^{-3/2} + V\frac{B^2}{2\mu_0}.$$

$$W_{\text{particles}} = G(\alpha)\eta L_\nu B^{-3/2},$$

Minimum Energy Requirements

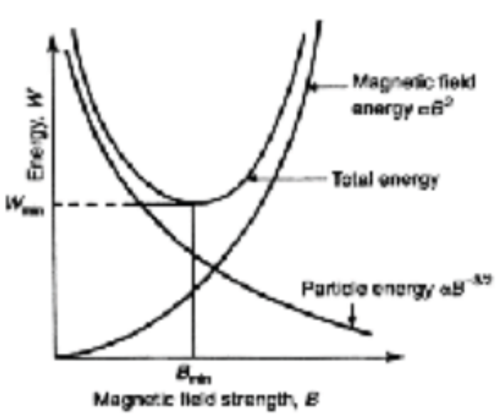

The diagram shows the variation of the energies in particles and magnetic field as a function of B. There is a minimum total energy,

$$B_{\text{min}} = \left[\frac{3\mu_0}{2}\frac{G(\alpha)\eta L_\nu}{V}\right]^{2/7}.$$

This magnetic field strength B_{min} corresponds to approximate equality of the energies in the relativistic particles and magnetic field.

we find

$$W_{\text{mag}} = V\frac{B^2_{\text{min}}}{2\mu_0} = \frac{3}{4}W_{\text{partic}}$$

Thus, the condition for minimum energy requirements corresponds closely to the condition that there are equal energies in the relativistic particles and the magnetic field.

X-ray - Radio Lobe Emission

Radio flux:

$$L_{\sin} = Vk_e C_{\sin} B^{\frac{p+1}{2}} \nu^{\frac{-(p-1)}{2}}$$

X-ray flux:

$$L_{IC} = Vk_e C_{IC} \nu^{\frac{-(p-1)}{2}}$$

$$B_{IC} = \left[\frac{F_{\sin}}{F_{IC}}\frac{C_{IC}(1+z)^{\alpha+3}}{C_{\sin}}\right]^{\frac{1}{\alpha+1}} \left(\frac{\nu_{\sin}}{\nu_{IC}}\right)^{\frac{\alpha}{\alpha+1}}$$

$\alpha = \alpha_r = \alpha_x$, V= volume

$N(\gamma) = Ke\,\gamma^{-(2\alpha+1)}$

In radio galaxies the jet is pointed away from the observer, extended structure can be observed

Hot spot

Hot Spots

Terminal hotspots, like knots, are thought to be localized volumes of high emissivity which are produced by strong shocks or a system of shocks. Hot spot spectra are generally consistent with SSC predictions but a significant number appeared to have a larger X-ray intensity than predicted. This excess could be attributed to a field strength well below equipartition, IC emission from the decelerating jet 'seeing' Doppler boosted hotspot emission or an additional synchrotron component, ecc